2019-04-01

Antibacterial and Antifungal Activity of Ceragenins, Mimics of Endogenous Antimicrobial Peptides

Marjan Mohammadihashemi
Brigham Young University

Antibacterial and Antifungal Activity of Ceragenins, Mimics of Endogenous Antimicrobial Peptides

Marjan Mohammadihashemi

A dissertation submitted to the faculty of
Brigham Young University
in partial fulfillment of the requirements for the degree of

Doctor of Philosophy

Paul Bennett Savage, Chair
Joshua Andersen
Steven William Graves
David John Michaelis
Joshua L. Price

Department of Chemistry and Biochemistry

Brigham Young University

ABSTRACT

Antibacterial and Antifungal Activity of Ceragenins, Mimics of Endogenous Antimicrobial Peptides

Marjan Mohammadihashemi
Department of Chemistry and Biochemistry, BYU
Doctor of Philosophy

The continuous emergence of drug-resistance pathogens is a global concern. As a result, substantial effort is being expended to develop new therapeutics and mechanisms for controlling microbial growth to avoid entering a "post-antibiotic" era in which commonly used antibiotics are no longer effective in treating infections. In this work, we investigate the efficacy and application of ceragenins as non-peptide mimics of antimicrobial peptides (AMPs).

First, this work examines the susceptibility of drug-resistant Gram-negative bacteria. The susceptibility of colistin-resistant clinical isolates of *Klebsiella pneumoniae* to ceragenins and AMPs suggests that there is little to no cross-resistance between colistin and ceragenins/AMPs. Furthermore, Lipid A modifications are found in bacteria with modest changes in susceptibility to ceragenins and with high levels of resistance to colistin. Next, we investigated the potential for cross resistance between chlorhexidine, colistin, AMPs and ceragenins as repeated exposure of bacteria to chlorhexidine might result in cross resistance with colistin, AMPs or ceragenins. Furthermore, a proteomics study on the chlorhexidine-resistant strains showed that chlorhexidine resistance is associated with upregulation of proteins involved in the assembly of LPS for outer membrane biogenesis and virulence factors in *Pseudomonas aeruginosa*.

Second, this dissertation describes the antifungal activity of ceragenins against an emerging multidrug-resistant fungus, *Candida auris*. We found that lead ceragenins displayed activities comparable to known antifungal agents against *C. auris* isolates. We also found that fungal cell morphology was altered in response to ceragenin treatment, that ceragenins exhibited activity against sessile organisms in biofilms, and that gel and cream formulations including CSA-44 and CSA-131 resulted in a significant log reduction against established fungal infections in *ex vivo* mucosal tissues.

Finally, a hydrogel film containing CSA-131 was generated on endotracheal tubes (ETTs). ETTs provide an abiotic surface on which bacteria and fungi form biofilms that cause serious infections. In this study, the eluting ceragenin prevented fungal and bacterial colonization of coated ETTs for extended periods while uncoated tubes were colonized by bacteria and fungi. Coated tubes were well tolerated in intubated pigs. The ability of ceragenins to eradicate established biofilms make them attractive potential therapeutics for persistent infections in the lung, including those associated with cystic fibrosis. In *ex vivo* studies, we initially found that this ceragenin, at concentrations necessary to eradicate established biofilms, also causes loss of cilia function. However, by formulating CSA-131 in poloxamer micelles, cilia damage was eliminated and antimicrobial activity was unaffected. These findings suggest that CSA-131, formulated in micelles, may act as a potential therapeutic for polymicrobial and biofilm-related infections in the lung and trachea.

Keywords: antimicrobial peptides, ceragenins, CSA-131, CSA-44, antimicrobial activity, antifungal activity, endotracheal tube, colistin-resistant bacteria, drug-resistant, *Candida auris*, cilia

ACKNOWLEDGEMENTS

I would like to express my sincere appreciation and gratitude to all those who helped me to finish this work and write this dissertation at Brigham Young University.

I am indebted to my husband, Mehdi Forouzan, for his love and support without which I could not have moved through this tortuous path. I would like to thank my parents for their prayers and warm support.

Particular thanks to Prof. Paul B. Savage for his guidance during my research. Prof. Savage helped me to think independently and be a better writer and researcher. The energy, enthusiasm, and encouragement I received from him have been key factors in my success.

I would also like to thank all the committee members, Dr. Josh L. Andersen, Steven W. Graves, Joshua L. Price and David J. Michaelis for their support and inspiring suggestions and comments through my dissertation, proposal, and annual evaluations.

I am very grateful to all the students, technicians, and Professors including Joseph Reiley, Brett Holden, John Rovig, Christopher Lew, Michael Standing, Scott Weber, Brian Hilton, Jordan Coburn, John Wilson, Maddison Taylor, Ryan Moore, Aaron Zaugg, Lindsy Meservey, Thomas Knapp, Tania Nance, Shawn Gubler, Darius Baradaran, Elliot Sherren, Samuel Ellis, Chanica Sintima, Sara Mata Guzman, Colten McEwan, Richard Carson, Monique Speirs, Shenglou Deng, Dr. John C. Price and Dr. Scott R. Burt who provided assistance during my research.

This work was mainly supported by the N8 Medical Device, NIH and Brigham Young University.

TABLE OF CONTENTS

LIST OF TABLES

LIST OF FIGURES

Chapter 1 Introduction

1.1 The antimicrobial resistance crisis

The discovery of antibiotics was one of the most important advances in medicine. These drugs were heralded for their effectiveness and, as a result, began to be prescribed across the world [1]. However, widespread use of antibiotics has resulted in the generation of mutational resistance in bacteria as well as adaptational resistance mechanisms. These have led to the rise of hyper-resistant bacteria, often called superbugs. Today, the phenomenon of antibiotic resistance has become a global public health concern, with 700,000 global deaths annually attributed to antimicrobial resistance (AMR). This count is expected to reach 10 million by 2050 as the decreasing effectiveness of available market drugs continues to compound this problem [2]. There are two ways to combat this problem. First, novel antimicrobials must be researched whose mechanisms of action are new and unique—to which superbugs are not already resistant. Second, the advancement of AMR worldwide must be curtailed by monitoring the use of antimicrobials [3].

Currently, market conditions fail to adequately incentivize research and development of novel antimicrobials. Newly developed drugs are used sparingly to prevent the development of resistance in pathogens, causing novel drugs to be bought in low quantities and turn an underwhelming profit margin [4]. Without sufficient incentivization large-scale drug companies have left for more lucrative fields. The remaining small-scale companies lack the funding necessary to develop truly novel medicine, and often modify or improve upon existing medications, instead. Therefore, the majority of new antimicrobials hitting the market do not operate through an original mechanism of action and are not effective against resistant organisms. As a result, the

current production of novel antimicrobials is markedly insufficient for preventing the global AMR crises [5].

To stem the threat of AMR, international efforts have already been launched to bolster the research and development of new antimicrobials. Programs include the Joint Programming Initiative on Antimicrobial Resistance and the Biomedical Advanced Research and Development Authority's Broad Spectrum Antimicrobials Program among others. While these programs are an encouraging step in the right direction, their effectiveness has nonetheless been called into question. For example, many of these programs focus heavily on funding early-stage research for new drugs but lack funding for late-stage development to see these projects through to completion. Additionally, private investment in development is poorly incentivized and the many initiatives that have been launched are not well coordinated with each other. A possible solution to this problem is for a global governing body such as the World Health Organization (WHO) to create a worldwide, legally binding initiative that requires strong action to curb AMR and to incentivize research and development of fully novel antimicrobials [6].

In this dissertation we focused on a novel class of antibiotic termed ceragenins. The previous studies on ceragenins revealed the broad-spectrum activity of ceragenins on different organisms, including Gram-positive and Gram-negative bacteria and fungi. The overall goal of this research was to investigate of the efficacy of ceragenins against multi-drug resistant bacteria or fungi and clinical application of them in medical devices.

Our studies highlighted that ceragenins retain their activity against multi-drug resistant clinical isolates of bacteria and fungi. Moreover, application of ceragenins in endotracheal tubes (ETTs) and cream formulation demonstrate that they have wide potential application in intubated patients, topical infection treatment, and cystic fibrosis patients. Overall, our studies will facilitate

transition of ceragenins and ceragenin containing products from early clinical phases to commercialization.

Chapter 2 Literature review

2.1 Introduction

Antimicrobial peptides (AMPs) are evolutionarily conserved molecules that exist in organisms ranging from prokaryotes to humans as a first line of defense [7,8]. They are naturally found in the skin, airways, gastrointestinal tract, and urinary and reproductive tracts with the highest concentrations of AMPs being found in the tissues that are exposed to pathogens [9,10]. They display broad-spectrum activity against bacteria, fungi, lipid-enveloped viruses and parasites. In higher organisms, AMPs exert additional immunomodulatory activities such as anti-inflammatory properties, through sequestration of bacterial endotoxins, and acceleration of wound healing by promotion of cell migration into wound beds and neovascularization. Common features of AMPs are juxtaposed cationic amino acids and hydrophobic residues on opposing faces of helices or sheets. This morphology provides them with a unique amphiphilic structure that selectively associates with microbial membranes, disrupts membrane integrity, and leads to cell death.

AMPs have existed for eons and have played a central role in nearly all organisms in controlling the growth of pathogens. Even though most common pathogens have been exposed to AMPs for extended periods, most remain susceptible to AMPs, while pathogens have developed high levels of resistance to most other clinically-used antibiotics [11]. The cause of the enduring activity of AMPs may be due to a variety of factors: First, AMPs have co-evolved with the pathogens they are fighting, and through natural selection AMPs with optimized properties are selected for as they increase the fitness of their host. Second, while some AMPs are constitutively expressed, some are only released or have their expression substantially up-regulated with infection or inflammation. This non-constitutive and localized expression may also hinder a

pathogen's ability to form resistance as it never is allowed to adapt to an environment that contains sub-therapeutic levels of AMP [12]. Finally, AMPs target the membranes of microorganisms rather than specific enzymatic pathways. Consequently, resistance to AMPs requires modification to a gross structural component of microorganisms, a process that may come with a metabolic cost or substantial changes in interactions of the microorganisms with their environment [13].

Despite the broad-spectrum antimicrobial activities of AMPs and the belief that microorganisms are unlikely to become resistant to AMPs, their clinical application is limited due to the high cost of production and their degradation by bacterial proteases. In order to overcome these clinical challenges, ceragenins were developed as non-peptide mimics of AMPs. They are based on a common bile acid and mimic the amphiphilic morphology of AMPs with a similar spectrum of activity against bacteria, fungi and lipid-enveloped viruses.[14] Straightforward preparation of ceragenins and their stability in the presence of proteases paves the way for large-scale production and clinical application. This chapter will discuss the development of ceragenins, their breadth of antimicrobial activities, impacts on innate immune functions and wound healing, and specific applications of ceragenins as stand-alone antimicrobial agents and in medical applications.

2.2 Antimicrobial peptides: source and history

The first human AMP described, lysozyme, was discovered in 1922 by Alexander Fleming from his own nasal mucus. Further investigation demonstrated that lysozyme targets bacteria by hydrolyzing the linkage of peptidoglycan of the cell wall in Gram-positive bacteria [15-18]. However, antimicrobial use of lysozyme was overshadowed by the discovery of penicillin in 1928, also by Fleming [19]. The emergence of drug-resistant pathogens in the 1960s brought the potential of

therapeutic use of AMPs again to the attention of scientists. Pioneering work in 1956 resulted in discovery of defensins, the first animal-originated AMPs, isolated from rabbit leukocytes [20]. This was followed by the report of lactoferrin from milk in the 1960s [21]. Cecropin, first isolated from the Cecropia silk moth *Hyalophora cecropia* in 1981, was the first helical AMP reported [22,23]. Zasloff and colleagues isolated magainins from the skin of the African clawed frog *Xenopus laevis* in 1987 and found that it displayed broad spectrum antimicrobial activity [24]. It is also worth noting that prokaryotes produce and release AMPs to fight other microorganisms in their environment; however, these AMPs mostly have cyclic or branched structures. These AMPs are often synthesized by a non-ribosomal peptide synthase through a specialized metabolic pathway, unlike eukaryotic AMPs which are synthesized by the ribosome. To date, over 250 of these bacteriocins have been identified from bacteria [19]. Of particular interest are the commercial antibiotics polymyxin B (cationic) and vancomycin (non-cationic), which are isolated from *Bacillus polymyxa* and *Amycolatopsis orientalis*, respectively. Polymyxin B displays potent antibacterial activity against Gram-negative bacteria and vancomycin against Gram-positive bacteria [25,26].

2.3 Structure and mechanism of action of AMPs

AMPs mainly fall into three classes: α-helical, β-sheet, and extended, depending on their secondary structures [27,28]. Magainins and the human cathelicidin LL37 (hereafter LL-37) are prominent examples of AMPs with substantial α-helical structure [29,30]. β-sheet AMPs include defensins and feature disulfide bond that stabilize their structure [31]. AMPs derived predominantly from one type of amino acid are categorized as extended AMPs and include human histatins, which are rich in histidine, and bovine indolicidin, which is rich in tryptophan and arginine [32].

Nearly all AMPs are amphipathic, meaning they have both cationic and hydrophobic character. However, unlike typical surfactants, with polar head groups and hydrophobic tails, AMPs display polar, cationic functionality on one face of the molecule with hydrophobic groups juxtaposed on the opposite face [33]. Defensins and cathelicidins constitute the major families of membrane-active AMPs in vertebrates [34]. With these AMPs, an initial, selective electrostatic interaction between the positive charges on one face of the AMPs and negative charges of membranes occurs. Due to their facial amphiphilicity, the hydrophobic domains of AMPs cannot stably insert into intact membranes, and at sufficient local concentrations, AMPs cause membrane perturbation leading to a loss of polarization, resulting in cell death. Membrane composition allowing selective association of AMPs with microbial membranes plays a key role in cell selectivity [35]. For example, magainins show higher affinity for anionic phospholipids, which are highly represented in bacterial membranes. Cell membranes of higher organisms, however, feature neutral phospholipids and cholesterol, which diminish AMP interactions [36,37]. For this reason, much higher concentrations of AMPs are required to kill cells from higher organisms as compared to microbial cells. Targeting of the cell membranes by AMPs gives rise to their breadth of spectrum of activity: bactericidal activity against Gram-negative and positive bacteria, antifungal activity and even activity against lipid-enveloped viruses. This breadth of activity may offer advantages over antibiotics that target specific cellular processes, such as DNA and protein synthesis, leading to narrow spectra of activity. Membrane-targeting properties of AMPs contribute to the rapid antimicrobial activity, with some AMPs able to kill microorganisms with only seconds of exposure [23,38].

In higher eukaryotic organisms, AMPs display immunomodulatory activities [39], including anti-inflammatory properties through the sequestration of bacterial endotoxins such as lipopolysaccharide (LPS). In addition, multiple studies support the idea that human AMPs improve

wound healing *via* promotion of cell migration into wound beds, clearance of bacteria from the wound bed, reduction of local inflammation and facilitation of wound restructuring through angiogenesis, and neovascularization [40,41].

AMPs are generally constitutively expressed in healthy epithelium, and their production is upregulated in response to injury or infection to moderate microbial proliferation and signal host cells to activate secondary immunomodulatory roles [42]. For example, a study with a human skin wound healing model, LL-37 was expressed acutely post-injury, whereas its concentration was reduced in chronic ulcer epithelium where re-epithelization is impaired, suggesting that LL-37 plays a prominent role in wound closure [43].

Despite the broad-spectrum antimicrobial activities of AMPs and their wound-healing and immunomodulatory properties, there are factors that limit their clinical applications. These include their susceptibility to proteases released by bacteria, the high cost of producing them on a large scale, decreased activity when immobilized, and folding problems in the production of some large AMPs [23].

We developed ceragenins as non-peptide mimics of AMPs [44]. They are synthesized from cholic acid, a common bile acid, in few synthetic steps (Figure 2-1) [45-47]. Due to the fact that they are not peptide-based, they are not substrates for ubiquitous proteases. Preparation and purification of ceragenins on a large scale is relatively straightforward, they are stable under physiological conditions and even long-term storage in solution does not reduce their antibiotic activities[14,48]. As ceragenins follow the amphiphilic structure of AMPs they display a similar spectrum of activity against bacterial, fungi and lipid-enveloped viruses [49].

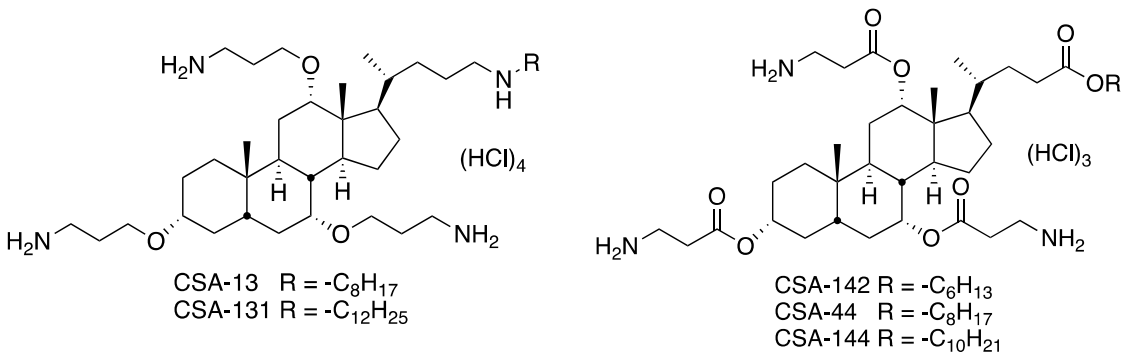

Figure 2-1: Structures of selected ceragenins CSA-13, CSA-131, CSA-142, CSA-44 and CSA-144

2.4 Design of ceragenins

Preliminary design of the ceragenins (examples in Figure 2-1) was based on the presumed lipid A binding domain of polymyxin B. The primary amines from diaminobutyric acid groups in polymyxin B are oriented on one face of the molecule, and to mimic this arrangement, three primary amines were tethered to cholic acid to generate similar amine spacing in ceragenins. Tether lengths were incrementally varied to determine the optimal spacing between the steroid backbone and the amine groups [50-53]. These initial attempts to mimic the structure of polymyxin B resulted in preparation of ceragenins with activity against *Escherichia coli* [minimal inhibitory concentration (MIC) range 2.0–46 μg mL^{-1}]. A truncated form of polymyxin B, polymyxin B nonapeptide, permeabilizes the outer membranes of Gram-negative bacteria, sensitizing them to hydrophobic antibiotics. With the initial series of ceragenins, this type of sensitization was observed with erythromycin against *E. coli*; concentrations of CSA-8 as low as 1 μg mL^{-1} lowered the MIC of erythromycin from 70 to 1 μg mL^{-1} [54]. Further structure-activity studies demonstrated that the chain extending from the D ring of the bile acid played a central role in controlling direct antibacterial activity vs. sensitizing activity of Gram-negative bacteria. With lipophilic groups attached to this chain, the resulting ceragenins displayed broad-spectrum antibacterial activity

(Gram-negative and -positive). For example, CSA-13 gave an MIC of 3.0 μg mL^{-1} against *E. coli* (Gram-negative) and 0.40 μg mL^{-1} against *Staphylococcus aureus* (Gram-positive). Ceragenins lacking lipophilic groups on the D-ring retained antibacterial activity against Gram-positive bacteria but lost substantial activity against Gram-negative bacteria. For example, CSA-8, without an extensive lipid chain, gave an MIC of 36 μg/mL against *E. coli*, and an MIC of 2.0 μg/mL against *S. aureus*. Nevertheless, ceragenins lacking lipophilic groups extending from the D ring retained the ability to sensitize Gram-negative bacteria to hydrophobic antibiotics [55].

From these results, we postulated that lipid chains extending from the D ring enabled ceragenins to traverse the outer membrane and exert antibacterial activity through interactions with the cytoplasmic membrane. Gram-positive bacteria lack an outer membrane, and they are susceptible to ceragenins with and without a lipid chain. Ceragenins lacking a lipid chain extending from the D ring remain on the outer surface of the outer membrane, and association of these ceragenins with the lipid A component of the membrane causes perturbations in the membrane that allow hydrophobic antibiotics to traverse the membrane [47,50,56].

Further structure activity studies involved replacement of the ether bonds tethering the amines to the bile acid with amide and ester groups. To use amide groups in the tethers, it was necessary to synthesize a tri-amino version of cholic acid [57]. These amines were functionalized with amino acids, generating amides. The resulting ceragenins displayed antibacterial activity, but less than that of the ceragenins with ether bonds for the tethers. By differentially protecting the three amines in the tri-amino version of cholic acid, it was possible to sequentially incorporate different amino acids at each amine. Although this method of preparing ceragenins resulted in the production of large numbers of compounds, none were as active as ether-based compounds. The ester-based compounds (*e.g.*, CSA-44) were prepared from cholic acid, and some of the resulting compounds

showed activity that rivaled that of the ether-based compounds. A feature of the ester-based compounds is that the ester groups spontaneously hydrolyzed in water (half-life of 37 days at pH 7). Hydrolysis of all of the esters gave cholic acid, an amino acid and a waxy alcohol [58-60].

2.5 Mechanism of action of ceragenins

A primary mode of antimicrobial activity of AMPs involves selective association with microbial membranes, and this association is mediated by ion pairing of positively charged AMPs with negatively charged microbial membranes [61]. Similarly, ceragenins selectively associate with negatively charged components of bacterial cell membranes, and ceragenins have been shown to sequester bacterial endotoxins (*e.g.*, LPS and lipoteichoic acid), which make up membranes of Gram-negative and positive bacteria [62,63]. This affinity for bacterial membrane components translates into cell selectivity; in studies with intact cells, ceragenins were shown to selectively associate with prokaryotes over mammalian cells, and this selective affinity is likely due to the higher net negative charge present on prokaryotic membranes [35].

As a consequence of the interactions of AMPs with the outer membranes of Gram-negative bacteria, blebs form on the surface [64-66], and similar morphological changes occur with ceragenin-treated, Gram-negative bacteria [56]. This observation, along with measurement of affinity of ceragenins for the lipid A portion of lysophosphatidic acid (LPA) and the cell selectivity described above, attest to the interactions between ceragenins and the outer membranes of Gram-negative bacteria. However, perturbation of the outer membrane is insufficient for cell death, and the ultimate target must be the cytoplasmic membrane [67,68]. As described above, a lipid chain extending from C24 is required for ceragenins to traverse the outer membrane of Gram-negative bacteria and gain access to the cytoplasmic membrane. A ML-35p mutant strain of *E. coli* was

used to show that ceragenins containing such a lipid chain traverse the outer membranes of Gram-negative bacteria and to gain access to the cytoplasmic membrane [69]. Association of ceragenins with the cytoplasmic membranes of bacteria, in sufficient concentrations, leads to formation of transient membrane defects, membrane depolarization and cell death. This mechanism of action is best described by the carpet model proposed for the activity of AMPs with bacteria [35]. Although antiviral and antifungal mechanisms of action of ceragenins are not completely understood, electron micrographs of ceragenin-treated *vaccinia* virus exhibited considerable morphological changes in the viral lipid envelope, and ceragenin-treated fungal cells displayed changes in cell shape, similar to that observed with AMPs [70].

2.6 Antimicrobial spectrum of activity of ceragenins

2.6.1 Antibacterial activity

The antimicrobial activities of ceragenins have been studied more with bacteria than with other organisms (*e.g.*, fungi and viruses). While they display activity against both Gram-positive and Gram-negative bacteria, ceragenins tend to be active at lower concentrations against Gram-positive bacteria, possibly due to the permeability barrier of the outer membranes of Gram-negative bacteria. Ceragenins have shown activity against a wide array of clinical isolates and drug-resistant bacteria, supporting their potential for clinical use as the threat of antibiotic-resistant bacteria grows[55,71,72]. To highlight the broad-spectrum antibacterial activities of ceragenins, their abilities to eliminate drug-resistant organisms are highlighted below.

Susceptibility experiments of CSA-13 with four clinical isolates of vancomycin-resistant *S. aureus* and 50 clinical isolates of glycopeptide-intermediate and heterogeneous glycopeptide-

intermediate *S. aureus* showed that the MIC_{50}, MIC_{90} and MBC of all isolates was 1 μg mL^{-1} [73]. These results demonstrate that there is no cross reactivity between glycopeptides and ceragenins. A more pressing concern may be with multi-drug resistant Gram-negative pathogens. In a study with 60 carbapenem-resistant *Acinetobacter baumannii* strains isolated from blood specimens of bacteremia patients, CSA-13 gave MIC_{50} and MIC_{90} of 2 and 8 μg mL^{-1}, respectively. Similar results were observed with 50 strains of *Pseudomonas aeruginosa* isolated from cystic fibrosis patients [74].

Ceragenins have also shown activity against cariogenic and periodontopathic bacteria[48]. Susceptibilities of broad-spectrum pathogens associated with oral and upper respiratory tract infections including *Streptococcus mutans* (the leading etiological agent of dental caries) and *S. aureus* (which often colonizes the nasopharynx) were determined with ceragenins CSA-13, CSA-90 and CSA-92 and compared to LL-37. As shown in Table 2-1, all tested ceragenins revealed significantly potent antibacterial activity when compared to LL-37 [75]. Interestingly, *Lactobacillus casei*, considered a beneficial member of the gut microfluora, was much less susceptible to ceragenins and LL-37 than other organisms, indicating a possible adaptation of this strain to become tolerate to LL-37 and probably ceragenins.

Table 2-1: MIC [MBC] μg/mL of LL-37, CSA-13, CSA-90, CSA-92 against tested strains associated with oral infections.

Strains	LL-37	CSA-13	CSA-90	CSA-92
Staphylococcus aureus ATCC 29213	14 [28]	0.7 [1.4]	0.7 [2.8]	0.75 [0.75]
Streptococcus salivarius ATCC 13419	14 [28]	0.7 [1.4]	0.7 [1.4]	1.5 [3.0]
Streptococcus sanguinis ATCC 10556	14 [28]	0.7 [0.7]	1.6 [1.4]	1.5 [3.0]
Streptococcus mutants ATCC 35668	28 [28]	0.7 [1.4]	0.7 [1.4]	0.75 [1.5]
Enterococcus faecalis ATCC 29212	28 [56]	2.8 [2.8]	1.4 [2.8]	8.0 [3.0]
Moraxella catarrhalis ATCC 23246	28 [28]	1.4 [1.4]	0.7 [1.4]	0.35 [1.5]
Peptostreptococcus anaerobius ATCC 27337	224 [224]	5.6 [5.6]	22.4 [22.4]	5.8 [11.7]
Lactobacillus casei ATCC 393	224 [224]	22.4 [44.8]	44.8 [44.8]	46.8 [46.8]
Fusobacterium nucleatum ATCC 25586	224 [224]	11.2 [22.4]	11.2 [11.2]	11.7 [23.4]

The permeability barrier of the outer membranes of Gram-negative bacteria and the action of efflux pumps in these membranes contribute to resistance profiles of bacteria [76]. Association of ceragenins with the outer membranes decreases the permeability barrier resulting in synergy between ceragenins and other antibiotics [77]. For example, synergistic activities of CSA-13 were reported with colistin, tobramycin, and ciprofloxacin against *P. aeruginosa* strains isolated from cystic fibrosis patients. The synergistic effect of CSA-13 was stronger with colistin (54 % of tested strains) compared to tobramycin (25 % of tested strains) [78]. Further investigation showed that CSA-13 also displays synergistic activity with cefepime or ciprofloxacin against clinical isolates of *P. aeruginosa*, including multidrug-resistant *P. aeruginosa* [79]. In related studies, the synergistic effects of ceragenins with AMPs were studied; combinations of CSA-13 with selected AMPs LL-37, lysozyme, lactoferin, or secretory phospholipase A were evaluated against bacteria causing

topical infections. As expected, CSA-13 exhibited more potent antibacterial activity in the presence of all tested AMPs [80].

2.6.2 Antifungal activity

The continued emergence of drug-resistant fungal pathogens has highlighted the urgent need for novel antifungal agents [81]. AMPs display antifungal activity [23] and this observation led to the question of whether ceragenins, as mimics of AMPs, would also display antifungal activity. Fungicidal activity of ceragenins CSA-13, CSA-131 and CSA-192 was evaluated against four fluconazole–resistant *Candida* strains [82]. Interestingly, these ceragenins showed higher antifungal activity against these strains than LL-37 and omiganan, a synthetic AMP designed for antifungal activity. In addition to *Candida* spp., CSA-131 and CSA-192 were also found to be active against a broad array of fungal strains including *Cryptococcus*, *Aspergillus*, *Scedosporium*, *Rhizopus* and *Blastomyces*.

The primary antifungal mechanism of action of AMPs is proposed to involve interactions and potentially disruption of the fungal membrane. Apoptosis as a result of increased reactive oxygen species (ROS) and decreased mitochondrial function have been also observed [83-86]. In a recent study, LL-37 or CSA-13 immobilized on magnetic nanoparticles were to shown to increase ROS generation in fungal cells, suggesting an additional pathway of antifungal activity with *Candida* spp. (Figure 2-2) [87]. Nevertheless, additional information is still required to fully understand how ceragenins target and kill fungal cells.

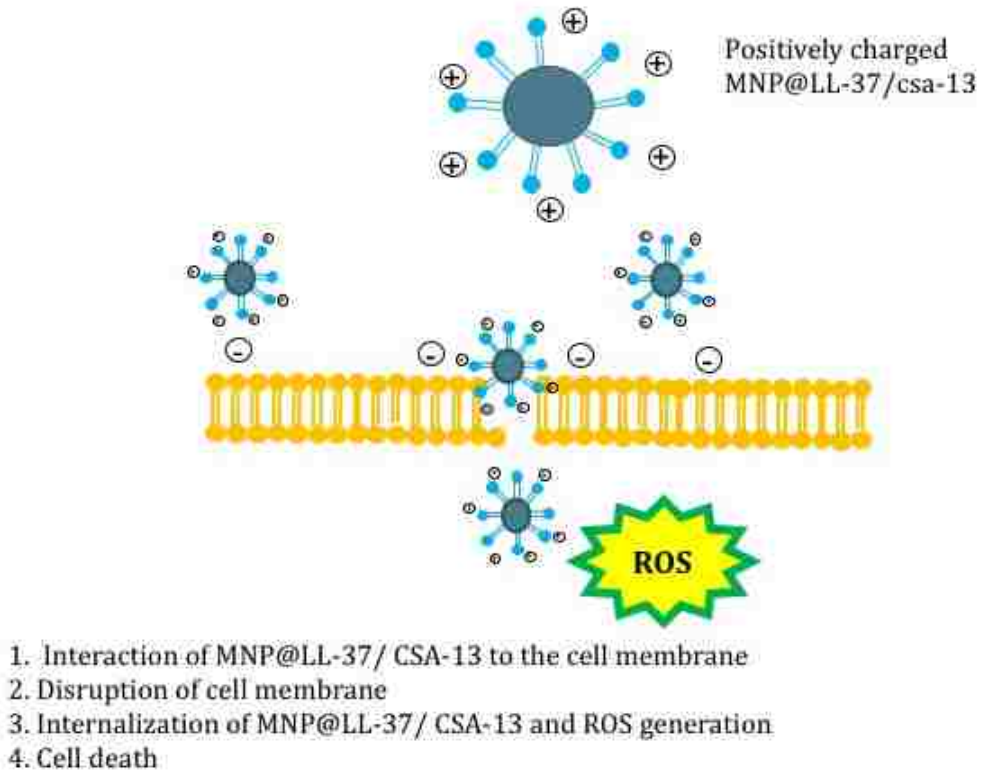

Figure 2-2: Proposed mechanism of positively charged coated magnetic 398 nanoparticles with LL-37 or CSA-13 against fungal cells membrane and contribution of LL-37/CSA-13 to generation of ROS.

2.6.3 Antibiofilm activity

Bacteria and fungi naturally exist in planktonic and biofilm forms. Planktonic cells are single, free-growing microorganisms, while biofilms form from groups of cells that aggregate through a protective extracellular polymeric matrix [88]. Biofilms are now thought to be involved in most infections, including chronic wounds, medical device-related infections, and cystic fibrosis-associated pneumonia. Eradication of biofilms can be a particularly daunting task due to the protective environment provided by the extracellular matrix and because cells within the biofilm are slow-growing and have low metabolic activity and therefore do not respond to antibiotics that target and inhibit cells that are rapidly growing and reproducing [89]. These factors lead to a 100–1,000-fold increase in the ability of the bacteria or fungi to resist antibiotic treatment, compared to

planktonic cells [23]. For example, β-lactam antibiotics inhibit the synthesis of the peptidoglycan layer of the bacterial cell wall and while their effect is considered bactericidal, it is most effective against cells that are growing and preparing to divide, as they require more peptidoglycan [90]. Consequently, β-lactams lose activity as bacteria transition from planktonic to sessile forms found in biofilms. Ceragenins and AMPs, on the other hand, target the bacterial membrane, and are able to kill bacterial and fungal cells regardless of whether they are rapidly growing, dividing, or sessile [42]. In addition, the relatively small size of ceragenins allows them to penetrate the extracellular matrix of biofilms and gain access to the cells within [14]. A comparative study of ceragenins with ciprofloxacin indicated that a much lower concentration of CSA-13 was required to eradicate an established biofilm consisting of a meticillin-resistant strain of *S. aureus* in comparison with ciprofloxacin. While treatment with CSA-13 caused a complete eradication of biofilm at a concentration between 16 and 32 μg mL^{-1}, treatment with ciprofloxacin resulted in an insignificant reduction of biofilm even at a concentration of 64 μg mL^{-1} [91]. In a similar study, it was observed that CSA-13 inhibits biofilm formation of both mucoid and nonmucoid phenotypes of *P. aeruginosa* at 1 μg mL^{-1} [92]. It was also noted that the rhlAB operon, which is controlled by quorum sensing and regulates rhamnolipid synthesis, was not an intracellular target of CSA-13 involved in the inhibition of biofilm formation. Further study with confocal laser scanning images of biofilms formed by *P. aeruginosa* revealed that bactericidal penetration of ceragenins into the biofilm matrix occurs within only 30 minutes of exposure of the ceragenin to the established biofilm [93].

2.6.4 Sporicidal activity

Some genera of bacteria such as *Bacillus* and *Clostridium* undergo a process of sporulation in response to unfavorable environmental conditions including depletion of nutrients [94]. Sporulation

enables bacteria to form inert, dormant spores, and this process involves formation of a multilayered structure different than vegetative cells [95]. Given the membrane-permeabilizing properties of ceragenins, activity of CSA-13 against the vegetative and spore forms of *B. subtilis* was assessed [96]. Treatment with CSA-13 significantly diminished the viability of vegetative cells and inhibited spore germination. Moreover, the surface electrical features of spores and vegetative cells measured through zeta potential provided evidence that the surfaces of spores exhibit a larger negative charge than vegetative cells. It was postulated that this charge density was the cause of the high affinity of CSA-13 for spore surfaces. Raman spectroscopy analysis further illustrated that ceragenin-treated spores release more calcium dipicolinic acid than untreated cells, implying that there is an increased permeability in the barriers of these spores, which increases their susceptibility to ceragenins.

2.6.5 Antiviral activity

AMPs exhibit antiviral activity through several mechanisms. First, by targeting the viral envelopes of lipid-enveloped viruses and disrupting membrane integrity, AMPs cause viruses to lose the ability to infect the host cells. Second, AMPs block viral receptors on the cell surface and prevent viruses from binding to host cells [23]. This can be seen in the interaction between θ defensins and viral glycoproteins of the Herpes simplex virus [97]. The antiviral activity of LL-37 against vaccinia virus has been established, and subsequently the antiviral activity of CSA-13 was studied against the same virus, which is a large double-stranded DNA virus that can infect a wide variety of mammalian cells as well as invertebrate cells [70]. CSA-13 showed potent antiviral activity through targeting the viral envelope. Additionally, topical application of CSA-13 in a murine model of vaccinia infection showed a substantial reduction in the number of satellite lesions that formed and in viral replication in the epidermis of infected mice.

2.6.6 Anti-parasite activity

The actions of a few AMPs have been studied with parasites, and anti-parasitic activities have been attributed to direct interactions with cell membranes. Magainins were reported as the first AMPs with anti-parasitic properties, displaying activity against *Paramecium caudatum* [24]. Cathelicidin is another example of an anti-parasite AMP, with activity against *Caernohabditis elegans* through pore formation on the cell membrane [98]. CSA-13 was also tested for anti-parasitic activity and showed an LD_{50} of *ca.* 9 and 5 μM with *Trypanosoma cruzi* and *Leishmania major*, respectively [99]. *Acanthamoeba castellanii* is a causative agent of corneal infections known as *acanthamoeba keratitis*. The parasite has two phases of life cycle, including cysts (the most resistant form) and trophozoites (the replicating stage) [100]. An *in vitro* evaluation of CSA-13 at concentrations of 25, 50, 75, and 100 mg mL^{-1} against both cyst and trophozoite forms of *A. castellanii* showed that CSA-13 inhibited trophozoite growth in a dose- and time-dependent manner. For example, within one hour of exposure to 100 mg mL^{-1} CSA-13, no viable trophozoites were detected [101]. Further study was performed using ceragenins CSA-13, CSA-44, CSA-131, and CSA-138 against metronidazole-susceptible and metronidazole-resistant strains of *Trichomonas vaginalis,* a parasitic protozoan transmitted *via* sexual intercourse and hosted only in humans. Overall, all tested ceragenins killed the tested *T. vaginalis* with a similar activity against metronidazole-susceptible and resistant strains, and CSA-13 was the most effective ceragenin in this study [102].

2.7 Effect of mucins, DNA and F-actin on the antimicrobial activities of ceragenins

The antimicrobial activities of AMPs and ceragenins may be influenced not only by modifications made by bacteria but also by production of specific molecules produced by the host. Because mucins, DNA and F-actin have been shown to deactivate AMPs, the question arose of

how these compounds would impact the activities of ceragenins. Comparative studies showed that these molecules had much less impact on the antibacterial activities of ceragenin CSA-13 than AMPs [63,103]. This observation is particularly important for potential applications of ceragenins in treating infections associated with cystic fibrosis. Mucins, DNA and F-actin are produced at relatively high concentrations in the lungs of those with cystic fibrosis. The smaller size of CSA-13 and lower positive charge, relative to endogenous AMPs, were proposed to be why the antibacterial activity of CSA-13 is less compromised by mucins, DNA and F-actin than AMPs. In a following study, the effects of selected depolymerizing factors (plasma gelsolin, DNase 1, and poly-asparate) on polyelectrolyte networks of F-actin and DNA in purulent body fluids were assessed in order to determine if they would improve the bactericidal activities of CSA-13, LL-37, tobramycin, colistin and polymyxin [104]. The depolymerizing compounds were found to enhance the activities of the tested antimicrobials, particularly CSA-13 and LL-37. Stronger antibacterial activity was observed with combination of DNase 1 and poly-aspartate as compared to the individual depolymerizing compounds [104]. These results provide strong evidence that because ceragenins possess potent antibacterial activity that is even sustained in the presence of complex anionic compounds, they offer excellent potential in treating chronic lung infections in cystic fibrosis patients, where the accumulation of polyanions creates major treatment obstacles.

2.8 Effect of poloxamer micelles on the antimicrobial activities and cytotoxicity of ceragenins

Clinical use of AMPs and ceragenins requires selective toxicity for microorganisms over host cells. One measure of cytotoxicity used to evaluate membrane-active compounds is measurement of concentrations of investigational antimicrobials that cause hemolytic activity. One such study showed that CSA-13 is not hemolytic at concentrations required for bactericidal activity and hemolysis was first observed at concentrations 10 times the bactericidal concentration [63]. Further

evaluation of hemoglobin release from human red blood cells showed that CSA-13 at a concentration of 10 mg mL^{-1} causes lysis in less than 10 % of erythrocytes while total hemolysis occurs at a concentration of 50 mg mL^{-1} [105]. These concentrations are higher than the concentrations required for bactericidal activity of ceragenins. In studies with HaCat cells, the toxicity profile of CSA-13 was similar to that of LL-37, without any toxicity at bactericidal concentrations [75].

Cytotoxicity was explored in a comparative study of ceragenins with bacterial cells and human umbilical vein endothelial cells. It was found that CSA-13 permeabilizes the plasma membrane of these eukaryotic cells in addition to the bacteria cells [106]. In an attempt to attenuate this effect of CSA-13 on eukaryotic cells, it was combined with the poloxamer Pluronic® F-127, a nonionic surfactant comprised of polyoxyethylene–polyoxypropylene copolymers (hereafter referred to as pluronic). The low toxicity of this poloxamer, great solubilizing capacity, and unique thermoreversible and drug releasing properties contribute to its applications in drug delivery as a pharmaceutical vehicle [107]. This poloxamer forms micelles that associate with hydrophobic and amphiphilic compounds. Formulation of ceragenins with pluronic resulted in well-defined micelles with lower toxicity toward eukaryotic cells, while antibacterial activity was not substantially impaired [80,108].

2.9 Nanoparticles as carriers of ceragenins

Metal-based nanoparticles provide a unique platform for the presentation of ceragenins in a pre-aggregated form. In addition, the distribution of magnetic nanoparticles can be controlled in tissues and silver-based nanoparticles display inherent antimicrobial activity. Multiple methods have proven effective in attaching ceragenins to nanoparticles. One method uses CSA-124, a

ceragenin formulated with a thiol group appendage. The thiol group can coordinate with thiophilic metals, such as silver, producing a monolayer on the surface of the nanoparticles [109]. Another method requires the generation of an aldehyde-containing surface on the nanoparticles. Ceragenins contain multiple amine groups, and these groups reversibly form Schiff bases with the aldehydes. On a surface with high aldehyde density, nanoparticles can then aggregate ceragenins in high concentrations [110].

Hoppens *et al.* [109] coated silver nanoparticles with CSA-124 and found that they were five times more bactericidal than silver alone. These nanoparticles displayed MICs of *ca.* 12 and 24 ppm against *S. aureus* and *E. coli*, respectively. Niemirowicz *et al.* [110] showed that magnetic nanoparticles coated with ceragenins retained their bactericidal activity. This association also increased the biocompatibility of ceragenins. Further testing also showed that even without direct conjugation of ceragenin to the nanoparticle, synergistic activity between nanoparticles and ceragenins occurred [111].

Durnás *et al.* [112] also evaluated magnetic nanoparticles for their activity against selected anaerobic bacteria often implicated in human disease. *In vitro* models testing CSA-13 and CSA-131 attached to nanoparticles showed comparable or stronger bactericidal activity against all of the tested strains, which included *Bacteroides fragilis*, *Propionibacterium acnes,* and a clinical isolate of *Clostridium difficile* (Table 2-2). Nanoprticles including CSA-131 also showed enhanced ability in preventing biofilm formation of *Bacteroides fragilis* and *Propionibacterium acnes. Neimirowicz et al.* [87] further studied the candidacidal activity of magnetic nanoparticles coated with CSA-13 and CSA-131. Their experiments confirmed that ceragenins attached to nanoparticles retained their highly potent fungicidal activity against multiple laboratory and clinical species of *C. albicans, C. glabrata, and C. tropicalis.*

Table 2-2: MIC [MBC] µg/mL of LL-37, CSA-13 and CSA-131 functionalized on nanoparticles against tested anaerobic strain.

Strains	LL-37	MNP@ LL-37	CSA-13	MNP@ CSA-13	CSA-131	MNP@ CSA-131	MNP
Bacteroides fragilis	128 [256]	128 [256]	4.0 [8.0]	2.0 [4.0]	8.0 [16]	4.0 [4.0]	>256 [>256]
Bacteroides thetaiotaomicron	128 [128]	128 [128]	8.0 [8.0]	2.0 [2.0]	8.0 [8.0]	16 [16]	>256 [>256]
Bacteroides stercoris	128 [128]	128 [256]	2.0 [2.0]	2.0 [2.0]	8.0 [16]	16 [32]	>256 [>256]
Prevotella melaninogenica	128 [128]	128 [128]	8.0 [8.0]	2.0 [2.0]	8.0 [8.0]	16 [16]	256 [256]
Prevotella oralis	8.0 [8.0]	16 [32]	0.5 [0.5]	1.0 [1.0]	4.0 [4.0]	16 [16]	256 [256]
Prevotella bivia	64 [64]	32 [32]	1.0 [1.0]	2.0 [2.0]	2.0 [4.0]	2.0 [4.0]	>256 [>256]
Prevotella disiens	16 [16]	16 [16]	1.0 [1.0]	1.0 [1.0]	2.0 [2.0]	4.0 [4.0]	>256 [>256]
Clostridium Perfringens	128 [256]	64 [128]	1.0 [1.0]	1.0 [1.0]	4.0 [4.0]	16 [16]	>256 [>256]
Peptostreptococcus spp.	8.0 [8.0]	16 [16]	0.5 [0.5]	0.5 [0.5]	4.0 [4.0]	8.0 [8.0]	>256 [>256]

2.10 Medical applications of ceragenins

2.10.1 Contact lenses

Contact lenses are abiotic surfaces on which pathogens can form biofilms and proliferate, potentially leading to microbial keratitis, a serious condition that affects up to 25,000 Americans each year. AMPs are present in conjunctival fluid and provide the surface of the eye an innate immune function that controls bacterial growth. Efforts have been made to provide contact lenses with a comparable innate immune function by attaching AMPs to lenses, and this combination reduced the ability of bacteria to colonize lenses [113]. However, the relatively high cost of AMPs and concerns over thermal stability (lenses are generally autoclaved in the final stages of production) complicate the use of AMPs in contact lenses. The relatively low cost of ceragenins

and the thermal stability of the ether-based compounds make them attractive alternatives to AMPs in providing an innate immune defense to contact lenses. In addition, ceragenins contain no chromophores (colorless), they are soluble in the polymers used to make lenses and they do not interfere with the polymerization processes involved in lens formation [114].

Two approaches were used in combining ceragenins and contact lenses. The first required appending a ceragenin with an acrylamide group, generating CSA-120 and allowing the ceragenin to participate in the radical polymerization steps that form lenses. The second involved formation of lenses in the presence of ceragenins, and in this approach ceragenins were able to elute from lenses.

Photo-initiated polymerization of acrylate groups is used to form hydrogel contact lenses. Acrylamide groups can participate in the polymerization process, and addition of CSA-120 to the reaction allowed covalent attachment of the ceragenin to the lens hydrogel. Up to 1.25 % CSA-120, relative to the dry mass of a lens, could be incorporated without causing phase separation in the hydrogel. When incorporated at this concentration in lenses, biofilm formation (*S. aureus*) was reduced by 3 logs after 24 h when tested in a 10 % bacterial growth medium. When 100 % medium was used, however, this inhibitory effect was lost, likely because the permanently bound ceragenin was covered by bacteria and bacterial debris.

To improve the duration of activity of ceragenins in contact lenses, a series of ceragenins were prepared in which the lengths of the lipid chain extending from bile acid were incrementally varied. The intent of these experiments was to match the hydrophobicity of the ceragenin to the hydrophobic domains in the lens hydrogel to limit elution of the ceragenin from the lens. With a shorter lipid chain, the ceragenin eluted too rapidly; however, with CSA-138, elution extended over weeks and provided antibacterial activity. At 1 % of the weight of dry lenses, CSA-138

inhibited the colonization of lenses by *S. aureus* for up to 30 days and by *P. aeruginosa* for up to 15 days (Figure 2-3) with daily inoculation with bacteria in fresh media. These results demonstrate that by tuning the properties of ceragenins to a hydrogel, the elution profile of the ceragenin can be controlled to provide long-lasting antimicrobial activity [114].

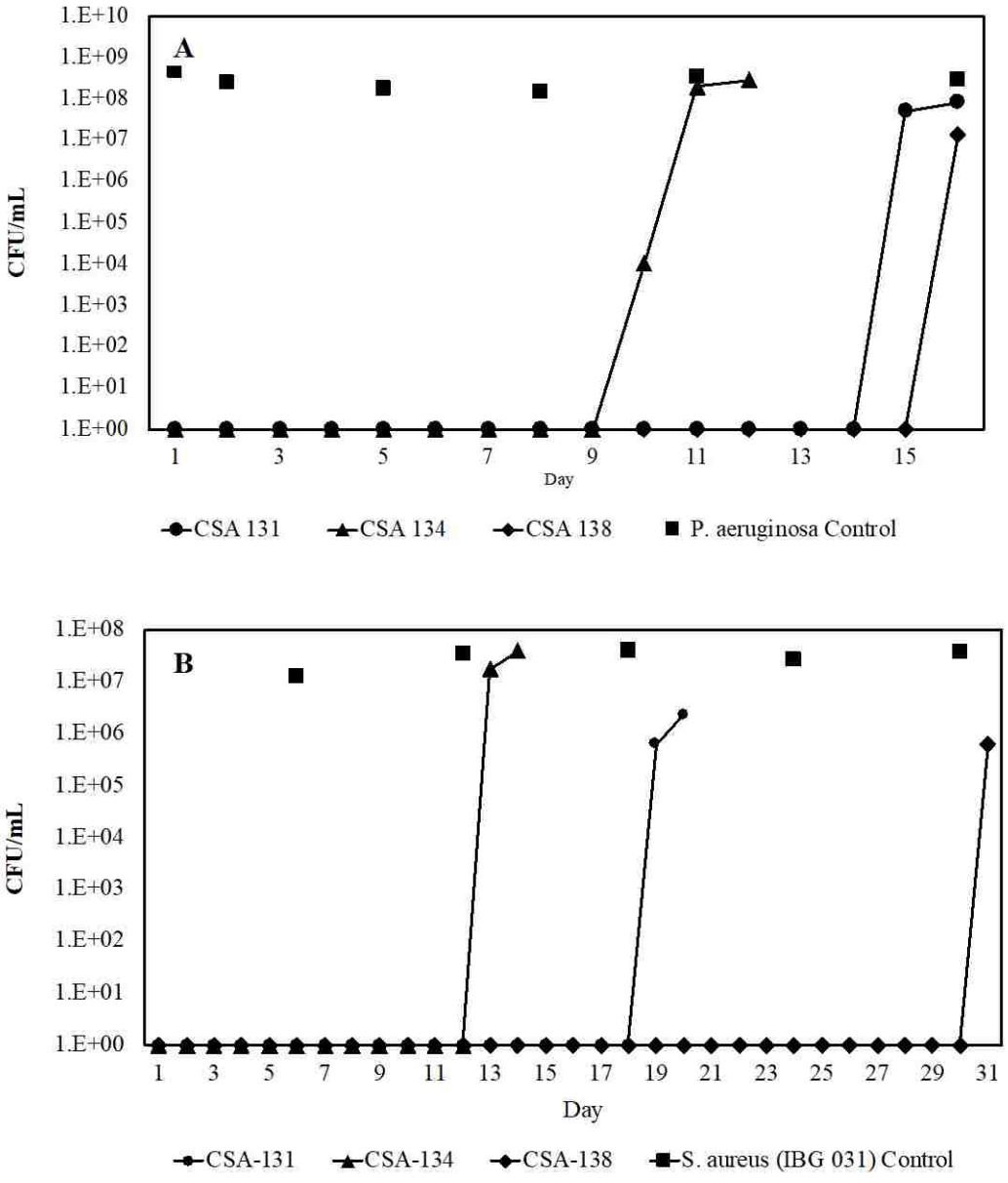

Figure 2-3: Bacterial population in nutrient media after 24 h incubation. Inoculated with *P. aeruginosa* ATCC 27853 (A), inoculated with *S. aureus* IBG 031 (B). Control lenses do not include any ceragenins. Lenses contained 1 % of selected ceragenins, relative to the dry weight of the lens. Every 24 h lenses were placed in fresh media and reinoculated.

2.10.2 Implanted medical device coatings

Implant-related infections affect thousands of patients each year [115], and active-release antimicrobial coatings have been designed in order to combat this issue. These coatings release antimicrobial agents into the surrounding tissue and fluids with the intent of preventing biofilm formation on the device and infection at the implant site [116,117]. However, due to the presence of sessile organisms, if a biofilm forms on a device or the device is implanted in the presence of an established biofilm, most conventional antibiotics cannot fully protect implanted devices. An active-release coating containing ceragenins is an attractive option because ceragenins exhibit antibacterial activity against established biofilms, they do not lose effect in the presence of proteases and other enzymes, and they are easily incorporated into stable polymer coatings.

An active-release coating containing CSA-13 was first developed and described by Williams *et al.* [118] on fracture fixation plates. Investigation of the polymerization of a silicone coating showed that the incorporation of CSA-13 in particulate form (18 % w/w) had no impact on the physical properties of the coating and SEM observation revealed that the CSA-13 was distributed evenly throughout the coating. Of critical importance, when placed in aqueous solution, CSA-13 eluted from the coating over a span of 30 days. Furthermore, thermal stability testing of the coating demonstrated that coated fixation plates retained stability at elevated temperatures, providing further evidence that the CSA-13-silicone combination would be a viable option for the coating of implanted devices [116,119]. In order to evaluate this coating *in vivo,* biofilms of methicillin-resistant *S. aureus* (MRSA) were grown on a polymer mesh. After being allowed to reach population densities of over 10^9 CFU cm^{-2}, the mesh was implanted on the tibia of sheep and then immediately covered with a fracture fixation plate that was coated with CSA-13-silicone. Following inoculation, each sheep in the control group developed infection, while those that received fixation plates

coated with CSA-13 were fully protected from developing infection over the course of the 12-week study. Investigation of the surrounding tissue showed that the coating was well tolerated, with no evidence of cytotoxicity or inhibition of wound healing. Remarkably, it was noted that there was an increase in bone healing in the presence of ceragenin.

The ability of this coating to prevent infection caused by planktonic bacteria was also evaluated *in vitro* and *in vivo* [120]. The coating was applied to porous titanium plug implants and placed in mouse models infected with MRSA. While control mice had to be euthanized per protocol shortly after the start of the experiment due to effects of infection, mice with CSA-13 coated implants were protected from infection for the duration of the 12-week study. Furthermore, CSA-13 released from implants did not damage skeletal attachment sites of the titanium plug implant compared to controls. Taken together, these *in vivo* studies provide evidence that ceragenin-containing coatings can provide an effective antimicrobial function to implanted devices, allowing for the eradication of both planktonic and biofilm-associated bacteria.

2.10.3 Bone fractures

Aside from their antimicrobial properties, AMPs have been shown to influence bone healing [121]. Considering this observation, the abilities of ceragenins to impact bone growth were determined. Selected ceragenins were tested in a rat femur-based model of bone regrowth to determine whether they would accelerate bone regrowth when used alone or in combination with bone morphogenic protein-2 (BMP-2), which is used clinically to accelerate bone regrowth. Of the ceragenins that were tested, CSA-90 displayed the most potent activity [122]. To determine if CSA-90 could positively impact bone regrowth while providing antibacterial protection of bone injury, a model of bone regrowth, complicated with infection, was used in a similar rat femur-based study.

As anticipated, CSA-90 functioned to both prevent infection and potentiate the activity of BMP-2 in repairing and regrowing bone. In contrast, untreated rats had to be sacrificed per protocol within two weeks of fracture due to declining health. Because open fractures are very often complicated by infection, most often due to pathogens that dwell on the skin including *S. aureus*, the ability of ceragenins to both aid in bone regrowth while also serving to prevent infection at the fracture site could provide profound benefit to patients.

2.10.4 Imaging infections

AMPs and ceragenins display affinity toward bacterial membranes, and efforts have been made to leverage this property into selective association of AMPs or ceragenins, labeled with imaging agents, for use in imaging bacterial infections [123,124]. As further evidence of the affinity of ceragenins for bacterial membranes, CSA-124 was covalently attached to nanoparticles consisting of a silver shell with a maghemite core [109]. Imaging of the nanoparticles confirmed selective association with intact bacteria, with particular affinity for *S. aureus. In vitro* MRI studies further verified that these nanoparticles were able to adhere to *S. aureus*, indicating their potential to be used as contrast agents for use in imaging deep tissue infections [125].

Technicium (99mTc)-labeling of CSA-13 was also investigated as a means of imaging infections in mice. CSA-13 was chosen specifically because its multiple amine groups allow it to form stable complexes with the metal ion. Following direct infection of the thigh muscle in mice with *S. aureus*, the CSA-13-99mTc complex was administered. Imaging showed that the complex accumulated at the infection site and also in the kidneys [126]. Further efforts were made to alter the binding between the ceragenin and the technicium in order to allow the amine groups to remain

free and available to form ionic interactions with bacterial membranes [127]. This modified complex has been shown to associate with *S. aureus* in *in vitro* studies.

2.10.5 Gastrointestinal diseases

Helicobacter pylori is carried by about half of the world's adult population. While carriers are often asymptomatic, infection can lead to severe ulceration and gastritis, and is associated with gastric adenocarcinoma. The emerging threat of antibiotic-resistant strains led Leszczynska *et al.* [128] to test whether ceragenins could be used as a viable treatment option. They found that CSA-13 displayed significantly lower minimum bactericidal concentrations (MBC) against a variety of *H. pylori* clinical isolates as compared to LL-37. Furthermore, under simulated gastric conditions in the presence of low pH and pepsin, CSA-13 retained its bactericidal activity while the activity of LL-37 was lost. Interestingly, *H. pylori*, with its unique defense mechanisms of incorporating host cholesterol into it membrane and activity through its HefC efflux pump, showed some resistance to ceragenins, which was based on the presence of cholesterol in the bacterial membrane [129].

The impact of CSA-13 in gastrointestinal infections caused by *Clostridium difficile* has been studied in a mouse model [130]. Oral administration of an active formulation of CSA-13 containing Eudragit and methylcellulose resulted in CSA-13 release in the terminal ileum and colon where the environmental pH is alkaline. The inhibition of *C. difficile* spore germination and cell viability by CSA-13 was measured at 4 μg mL^{-1}. Both subcutaneous and oral administration of CSA-13 decreased the concentration of *C. difficile* in fecal samples of mice, however *Peptostreptococcaceae* bacteria abundance increased suggesting that CSA-13 suppresses *C. difficile via* modulation of intestinal microbiota. Therefore, other microbial species and the balance of the gut microbiota should be considered with regard to further therapeutic application of CSA-

13 in gastrointestinal diseases. According to the observations from this study, the protective action of CSA-13 could be generated through the direct suppression of *C. difficile*, by lowering the levels of pro-inflammatory metabolites (endocannabinoids), or by increasing the levels of protective metabolites (citrulline, 3 aminoisobutyric acid, retinol, and ursodeoxycholic acid) in the intestine [130].

2.11 Conclusions

The central and critical roles that AMPs play in innate immunity have been well documented and include broad-spectrum antimicrobial activities, the ability to sequester microbial endotoxins and thereby inhibit inflammatory processes and additional activities that accelerate wound healing. Recognition of these roles has led to intense research of AMPs; for example, thousands of papers have been published describing activities of the human cathelicidin LL-37. The potential for therapeutic use of AMPs has also been well recognized; however, issues related to clinical use have also emerged: "AMPs possess some limitations that hamper their clinical and commercial development such as high production costs, potential toxicity, susceptibility to proteases (also in the wound fluid), and unknown pharmacokinetics" [131]. By abandoning peptide structure, while retaining overall morphology, ceragenins provide a means of reproducing the beneficial properties of AMPs without incurring many of the issues hampering clinical use of AMPs.

Current studies with ceragenins have focused on applications in tissues that express relatively high amounts of AMPs, and ceragenins have proven to be well tolerated in these tissues. However, less work has been done with potential systemic exposure to ceragenins. Use of ceragenins in coatings of medical devices and at bone fractures could lead to wider exposure, but no adverse events have been observed. Intraperitoneal injection of CSA-13 into mice in an infection model

showed efficacy without measured toxicity [132]. The possibility of systemic use of ceragenins exists, but the membrane-targeting activity of ceragenins argues that their most attractive uses will be in localized applications. With successful demonstration of efficacy *in vitro* in multiple animal models, it is anticipated that ceragenins will continue development toward clinical use and eventual applications in replacing or augmenting the activities of endogenous AMPs.

Chapter 3 Susceptibility of colistin-resistant, Gram-negative bacteria to antimicrobial peptides and ceragenins

3.1 Introduction

The continuous emergence of drug-resistant bacteria has led to dire predictions about a possible "post-antibiotic" era in which common infections will not be treatable with our current arsenal of antibiotics [133,134]. Of particular concern are Gram-negative bacteria because these organisms are inherently resistant to many antibiotics due to the permeability barrier provided by their outer membranes and the efflux pumps located therein [17,60]. To treat infections from Gram-negative infections, clinicians are increasingly using colistin, a member of the polymyxin family of antibiotics [135]. Colistin is considered the antibiotic of "last resort" because, while it has side effects including nephrotoxicity and ototoxicity, it is broadly active against Gram-negative bacteria [136-138]. Isolation of colistin-resistant bacteria in many countries underscores the need for development of novel strategies for targeting Gram-negative bacteria, including drug-resistant strains [139].

A central impediment to the development of new antibiotics/antimicrobials is that by the time that a new therapeutic has passed through clinical trials, resistant bacteria have emerged putting at risk the investment necessary for the development. It is evident that investigation of novel antimicrobials must include consideration of the likelihood of resistance development. Evolutionary pressures lead to generation of drug resistance among bacteria; however, these pressures also provide direction for the development of antimicrobials that are unlikely to engender resistance [135,140].

The ubiquity of endogenous antimicrobial peptides (AMPs) and the diversity of their primary sequences argue that they have played an important role in innate immunity for eons, that they have evolved independently dozens of times and that their mechanisms of action allow them to remain efficacious as antimicrobial agents even with extended bacterial exposure [141]. Although there are multiple mechanisms by which AMPs exert their antibacterial activities, in general AMPs are cationic and facially amphiphilic (e.g., they display cationic groups on one face of the molecule with hydrophobic side chains on the opposing face), and they interact with bacterial membranes [142]. Due to the broad-spectrum bactericidal activity of many AMPs and the idea that bacteria will not readily become resistant, multiple AMPs have entered clinical trials for treatment of a number of disease states [128,143,144]. However, there are challenges in clinical use of peptide therapeutics including relatively high costs of large-scale production and susceptibility to degradation by proteases [114,145].

The structures of colistin, AMPs and ceragenins have common features: multiple cationic groups and substantial hydrophobic character. All three types of antimicrobials are known to interact with bacterial membranes. Consequently, the emergence of highly colistin-resistant bacteria leads to the questions: (1) Are colistin-resistant bacteria also resistant to AMPs and ceragenins? (2) Does generation of resistance to colistin occur at the same rate as potential generation of resistance to AMPs and ceragenins? (3) Since the primary mechanism for bacterial resistance to AMPs and ceragenins is through modification of the lipid A portion of lipopolysaccharide (LPS) [146,147], how important are these modifications in resistance of Gram-negative bacteria to colistin?

To address these questions, we have compared the susceptibility of colistin-resistant, clinical isolates of *Klebsiella pneumoniae* to colistin, representative AMPs (LL-37, cecropin A and

magainin 1) and representative ceragenins. Our initial focus on *K. pneumoniae* was due to its known pathogenicity and its ability to transfer resistance genes to other Gram-negative bacteria [148,149]. To determine the relative rates at which Gram-negative bacteria become resistant to these antimicrobials, we have serially exposed colistin-susceptible, reference strains of *K. pneumoniae*, *Pseudomonas aeruginosa* and *Acinetobacter baumannii* to colistin and ceragenin CSA-131 (a second generation ceragenin) and monitored susceptibility to these antimicrobials. After up to 30 periods (24 h) of exposure to the antimicrobials, susceptibilities of the strains were determined with colistin, CSA-131 and LL-37. Strains that showed increased MICs with colistin and CSA-131 were grown in large quantity, LPS from these strains was isolated, truncated to lipid A, and structural modifications of lipid A, relative to lipid A in the reference strains, were determined by mass spectrometry. The same methods were used to characterize lipid A from the clinical isolates of *K. pneumoniae*.

Through these studies we found that high levels of resistance to colistin (MICs of 16 to >100 *times* the MICs with reference strains) do not correlate with comparable resistance to AMPs and ceragenins. We also found that upon serial exposure of Gram-negative bacteria to colistin or CSA-131, these bacteria became highly resistant to colistin (MICs increasing from 1-2 μg/mL to over 300 μg/mL) in a relatively short time, while modest increases in MICs (e.g., from 1 to 4 μg/mL) with the same strains were observed with CSA-131 over 30 days of exposure. Characterization of lipid A from susceptible and resistant strains showed the expected modifications of the glycolipid in the resistant strains; namely, increased fatty acid content and formation of phosphate esters with 4-aminoarabinose or ethanolamine. These modifications were found in the lipid A from the clinical isolates of *K. pneumoniae* and from the Gram-negative bacterial serially exposed to colistin and CSA-131. Nevertheless, while these strains were highly resistant to colistin, they were either

marginally resistant or fully susceptible to ceragenins and AMPs. These results suggest that lipid A modifications (increased lipid content and phosphate ester formation with 4-aminoarabinose or ethanolamine) increase MICs with colistin, ceragenins and AMPs, but these modifications do not appear to be responsible for the very high levels of colistin resistance seen in clinical isolates and with the Gram-negative bacteria serially exposed to colistin. These results also indicate that there is little or no cross resistance between colistin and ceragenins.

3.2 Materials and methods

3.2.1 Materials

Six clinical isolates of *K. pneumoniae* were obtained from the Antibacterial Resistance Leadership Group (ARLG, Newark, NJ); colistin-susceptible, reference strains of *K. pneumonia* (ATCC 13883), *Acinetobacter baumannii* (ATCC 19606) and *Pseudomonas aeruginosa* (ATCC 27853) were obtained from American Type Culture Collection (ATCC, Manassas, VA). Ceragenins CSA-13, CSA-131, CSA-44, CSA-138, and CSA-142 (Fig 1) were synthesized from a cholic acid scaffolding as previously described [50]. LL-37 (LLGDFFRKSKEKIGKEFKRIVQRIKDFLRNLVPRTES), cecropin A (KWKLFKKIEKVGQNIRDGIIKAGPAVAVVGQATQIAK-NH2), and magainin 1 (GIGKFLHSAGKFGKAFVGEIMKS), all with > 95% purity, were purchased from Anaspec (Fremont, CA) and used without further purification. Colistin (polymyxin E), Mueller–Hinton broth (MH) and Mueller–Hinton agar (MHA) were purchased from Sigma–Aldrich (St Louis, MO, USA).

3.2.2 Susceptibility testing

Minimum inhibitory concentrations (MICs) were determined using a broth microdilution method in a 96-well microdilution plate according to the Clinical Laboratory Standards Institute protocol [150]. Briefly, two-fold dilutions of antibacterial agents (colistin, LL-37, cecropin A, magainin 1, and ceragenins) in MH were dispended in separate wells of a 96-well plate. Aliquots (100 μL) of a prepared inoculum were added, and plates were incubated at 37 °C for 18-20 h. Also, negative and positive controls were included for each set of MIC measurements. The lowest concentrations of antibacterial agents inhibiting the visible growth of bacteria were used as the MICs. Minimum bactericidal concentrations (MBCs) were determined by taking 10 μL from each well and plating on MHA. The MBC was defined as the lowest concentration of an antibacterial agent giving no visible colonies after 24 h incubation at 37 °C.

3.2.3 Serial passage of bacteria with colistin and CSA-131

Serial passaging of *K. pneumoniae* (ATCC 13883), *P. aeruginosa* (ATCC 27853) and *A. baumannii* (ATCC 19606) were performed according to the protocol described previously [151]. Briefly, MICs (24 h) for the strains were determined, and bacteria growing at the highest concentrations of the antimicrobials were used to inoculate fresh medium. This process was repeated every 18-24 h. MICs were recorded every 24 h, and concentrations of the antimicrobials were adjusted to allow determination of MICs.

3.2.4 Time–kill curve analysis

Aliquots (100 μL) of inoculated MH (1×10^6 CFU/mL) were added to separate wells on a 96-well plate. CSA-131 was added, at a concentration of the MIC, two times the MIC (2xMIC), four times the MIC (4xMIC), and eight times the MIC (8xMIC), to the wells, and resulting mixtures were incubated at 37 °C. Aliquots (10 μL) were removed at varied intervals (0, 1, 2, 4, 8, 12, and

24 h), serially diluted in PBS, plated on MHA and incubated. Bacterial counts were made after 24 h at 37 °C. A negative control, including only bacteria in MH without the ceragenin, was used for measurement of uninhibited growth. Time-kill curves were plotted by log10 CFU/mL mean colony counts versus time. Ceragenins were considered bactericidal at a three-log reduction (CFU/mL) or greater relative to the initial inoculum [152].

3.2.5 Scanning electron microscopy (SEM)

To observe the effect of ceragenins on cell membranes, *K. pneumoniae* ATCC 13883 was cultured to mid-log phase and washed three times with PBS. Bacteria were re-suspended in PBS (OD_{600} = 0.2). CSA-131 (25 or 50 μg/mL) was added and the mixtures were incubated at 37 °C for 1 h. A control was prepared by incubating the bacterial suspension without adding CSA-131. After collection via centrifugation, cells were washed with PBS three times. Gluteraldehyde (2.5% (w/v)) was added to fix the cells at 4 °C overnight. Resulting material was washed five times with PBS at 5000 rpm for 10 min using a microhematocrit centrifuge (Hettich Mikro 20, Hettich, Tuttlingen, Germany) to remove the glutaraldehyde. Osmium tetraoxide (0.5 mL) was used as a second fixative reagent, and samples were stored at 4 °C overnight. Cells were washed with PBS five times at 14000 g for 8 min. A graded ethanol series including 10%, 30%, 50%, 70%, 90% (1 time), 100% (3 times) and HMDS (2 times) for 15 min each was used to dehydrate the cells. Samples were collected by centrifuge each time and the supernatant was discarded after each centrifugation. Finally, samples were exposed to air in a desiccator at room temperature for 24 h. To minimize the effect of dehydration on the cell membranes, drying through a CO_2 critical point dryer (Tousimis 931.GL, Research Corp, Rockville, MD, USA) and lyophilizer were applied. Interestingly, no differences in the quality of images obtained by either air-drying or critical point dryer were observed. Dried bacterial specimens were sputter-coated with 5-10 nm of a Gold-

Palladium alloy and visualized under a scanning electron microscope (FEI Helios NanoLab 600 SEM/FIB, Hillsboro, Oregon, USA) [82].

3.2.6 Transmission electron microscopy (TEM)

Primary sample preparation of TEM was done according to the method described in the SEM preparation. Fixation with osmium tetraoxide was performed for 2 hours rather than overnight, the pellets were washed three times with PBS. Washed cells were embedded in agarose low melt temperature and after being solidified, they were cut into small cubes of around 1 mm^3 and placed in a vial containing distilled water. Dehydration through the same graded ethanol series used in SEM was done followed by acetone (3 times). The samples were then immersed in 2:1 and 1:2 mixture of acetone: epoxy resin respectively and rotated for 1h for infiltration. The mixture was then replaced by 100% epoxy resin and incubated at 60°C overnight. Afterwards, samples were sectioned using an ultra microtome (MT-X; RMC, Tucson, AZ, USA), stained with uranyl acetate and lead citrate solutions, and observed with a STEM (FEI Helios NanoLab 600 STEM/FIB, Hillsboro, Oregon, USA).

3.2.7 Isolation and analysis of lipid A

Lipid A samples were isolated using the TRI Reagent method [153] and analyzed via mass spectrometry (ESI, negative ion mode, Agilent 6230 Series TOF Spectrometer). Using this method, we found the isolated lipid A showed loss of one phosphate group; consequently, a minor modification was applied to the published isolation method: heating time of extracted lipopolysaccharide was changed from 1 h to 30 min at 100 °C in order to obtain the diphosphate form of lipid A. With this modification to the published procedure, the mass spectral analyses gave results for lipid A comparable with other published studies [154-156].

3.3 Results

3.3.1 MICs and MBCs of colistin, AMPs and ceragenins

In an initial set of experiments, the MICs of colistin, LL-37, cecropin A, magainin 1, and ceragenins (CSA-13, CSA-131, CSA-44, CSA-138, and CSA-142) against colistin-resistant, clinical isolates of *K. pneumoniae* were determined and compared to those with a reference, colistin-susceptible strain of *K. pneumoniae* (ATCC 13883) (Table 3-1). The clinical isolates gave MICs of 16 to 200 µg/mL with colistin, and MICs with LL-37 and magainin 1 were relatively high against the reference strain as well as the clinical isolates. MICs were lower and less varied with cecropin A and the ceragenins, and only small changes in MIC were observed with cecropin A and CSAs -13, -44, and -131 with the various strains.

Table 3-1: MICs of colistin, AMPs and CSAs against a standard strain of *K. pneumoniae* (ATCC 13883) and colistin-resistant, clinical isolates.

	MIC (µg/mL)								
Strain	**Col**	**LL-37**	**Cec A**	**Mag 1**	**CSA-13**	**CSA-44**	**CSA-131**	**CSA-138**	**CSA-142**
K. pneumoniae (ATCC 13883)	2.0	32	2.0	64	2.0	1.0	1.0	3.0	3.0
K. pneumoniae (ARLG-1127)	32	64	2.0	64	2.0	1.0	1.0	2.0	2.0
K. pneumoniae (ARLG-1340)	100	100	nm	nm	2.0	1.0	1.0	3.0	4.0
K. pneumoniae (ARLG-1349)	16	64	4.0	64	2.0	1.0	3.0	3.0	8.0
K. pneumoniae (ARLG-1360)	64	100	4.0	150	2.0	1.0	2.0	6.0	6.0
K. pneumoniae (ARLG-1389)	200	100	4.0	200	6.0	2.0	3.0	8.0	8.0
K. pneumoniae (ARLG-1406)	64	64	4.0	100	3.0	1.0	3.0	6.0	16

nm = not measured
Col: Colistin, Cec A: cecropin A, Meg 1: Megainin 1

To verify that the activity of the ceragenins is bactericidal, MBCs of two lead ceragenins, CSA-44 and CSA-131, were determined with the colistin-resistant isolates. These results are

shown in Figure 3-1. These results show that both ceragenins are bactericidal at relatively low concentrations, with CSA-44 demonstrating bactericidal activity at concentrations only slightly above those of the corresponding MICs.

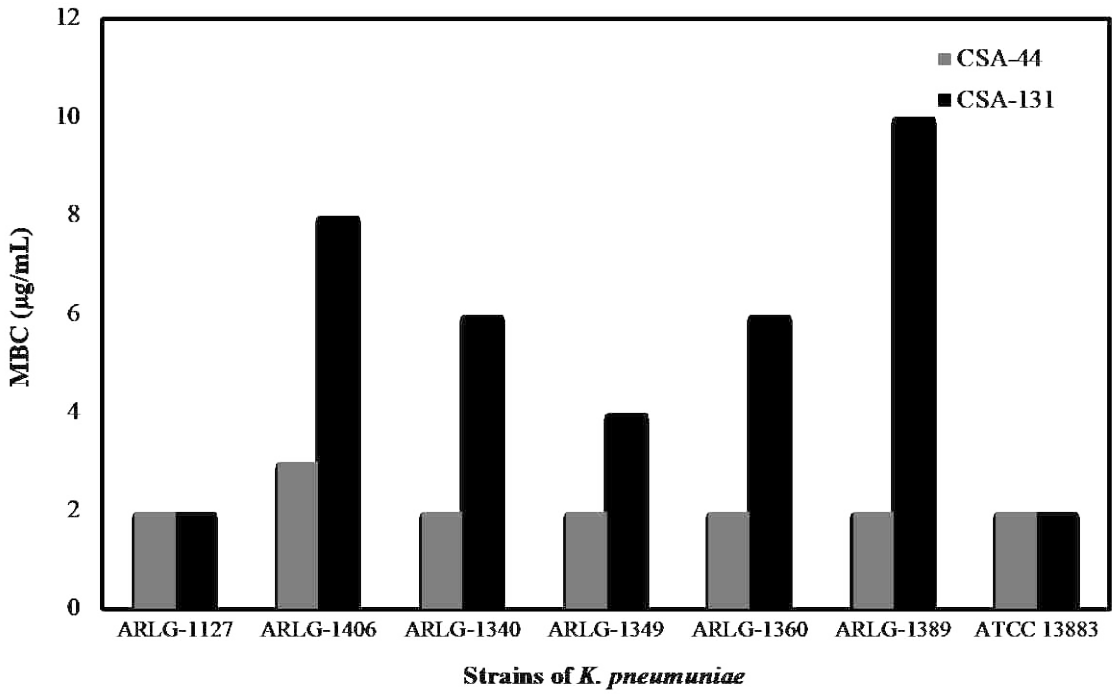

Figure 3-1: Ceragenins are bactericidal against colistin-resistant *K. pneumoniae*. MBCs of CSA-44 and CSA-131 against six clinical isolates of colistin-resistant *K. pneumoniae* and a reference strain (ATCC 13883).

3.3.2 Time-kill assays

Time-kill assays were performed to further differentiate between bactericidal and bacteriostatic activities using ceragenins CSA-44 and CSA-131. The rates of antimicrobial activity of these ceragenins against selected colistin-resistant strains ARLG-1127 and ARLG-1389 were compared to those with the reference strain (ATCC 13883) (Figure 2-1). Only minor differences were seen in the kinetics of bactericidal activity among the colistin-resistant and colistin-susceptible strains, again suggesting that colistin resistance does not significantly influence susceptibility to ceragenins. At two times the MICs for both ceragenins, the inoculum was decreased by at least three logs within one to two hours. At four times the MICs, the inoculum was

decreased to the detection limit (two logs) within the same time frame. At eight times the MICs (data not shown), results were comparable to those at four times the MICs.

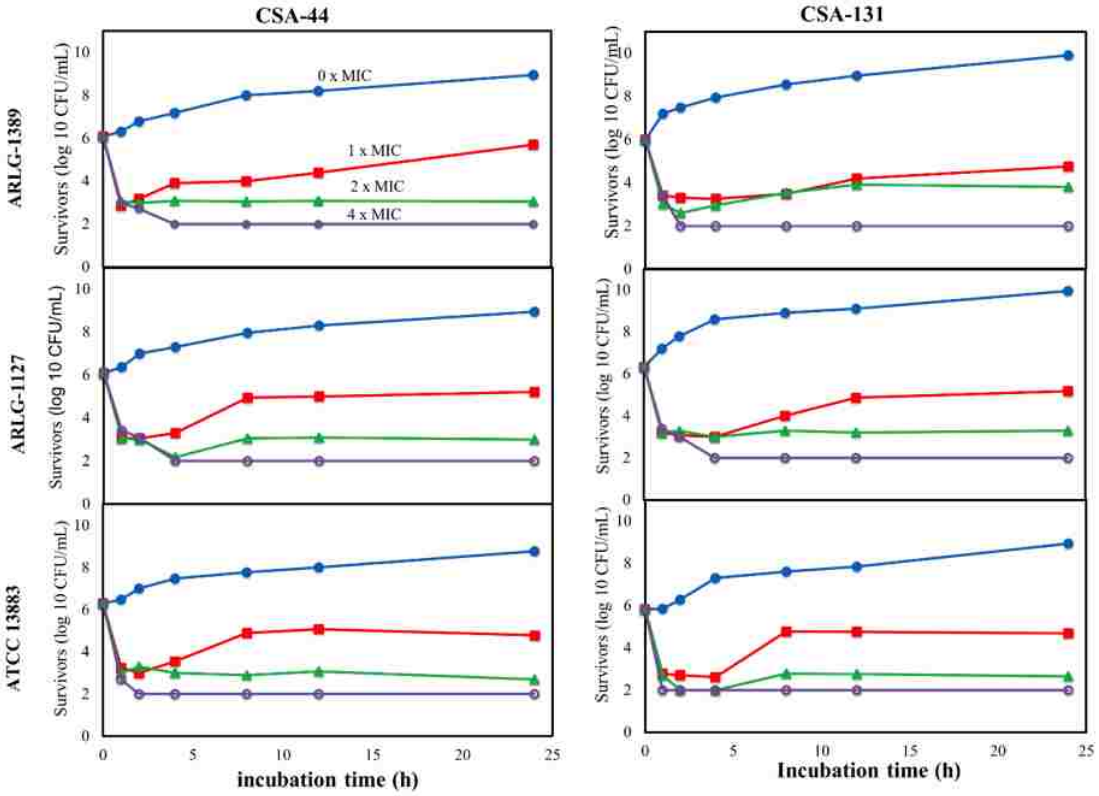

Figure 3-2: Rates of bactericidal activity of ceragenins are similar among colistin-resistant and colistin-susceptible strains. Time-kill curves with CSA-44 and CSA-131 against colistin-resistant K. pneumoniae strains (ARLG-1127 and ARLG-1389) and colistin-susceptible strain ATCC 3883. Detection limit is 2 logs (CFU/ml).

3.3.3 SEM

Ceragenins selectively target bacterial membranes [35], and to visualize the impact of a lead ceragenin, CSA-131, on membrane morphology, bacteria treated with the ceragenin were subjected to scanning electron microscopy (SEM) (Figure 3-3). In the control without ceragenin treatment, cells displayed the expected rod shape, although some surface roughness was observed as a result of the dehydration process (Figure 3-3 A). Nevertheless, there were substantial changes in the morphology of cells treated with CSA-131 (Fig Figure 3-3 B and Figure 3-3 C). Disruptions

in the cell membrane are evident along with increased roughness on the cell surface. These changes in morphology are dependent on the ceragenin concentration. Additionally, ceragenin-treated cells are shortened relative to untreated cells suggesting that ceragenin treatment prevented *K. pneumoniae* from reaching a regular length [33].

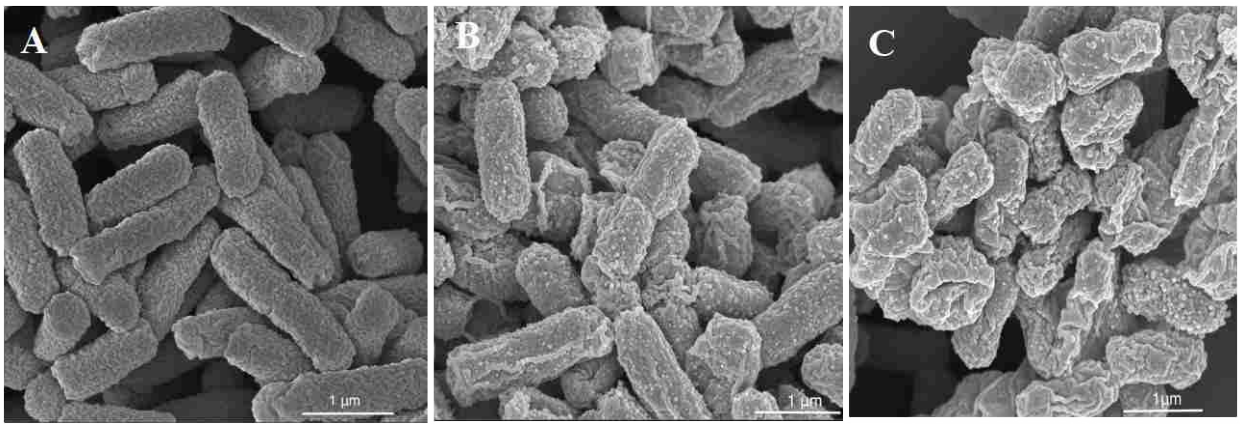

Figure 3-3: SEM images of *K. pneumoniae* (ATCC13883).(A)Control .(B)Treated with 25µg/ml CSA-131. (C) Treated with 50 µg/ml CSA-131 (magnification 50,000).

3.3.4 TEM

Membrane disintegration of *K.pneumoniae* ATCC 13883 treated with CSA-131 was observed via TEM (Figure 3-4). In the control sample, the typical round to ellipse shapes (depending on the sectioning direction) of *K.pneumoniae* with an evenly distributed cytoplasmic content was shown (Figure 3-4 A). However, exposure of the bacteria to the ceragenin evidently caused the disintegration of the membrane cells with significant blebbing and forming vesicles (Figure 3-4 B & C). Furthermore, ceragenin induced an obvious collapse in the plasma membrane, consequently creating denser intracellular components (Figure 3-4 B). Interestingly, treatment with higher concentrations of ceragenin formed substantial morphological alterations, including breaking the cell and releasing cytoplasmic components, making the cells seem empty inside (Figure 3-4 C) [35,54].

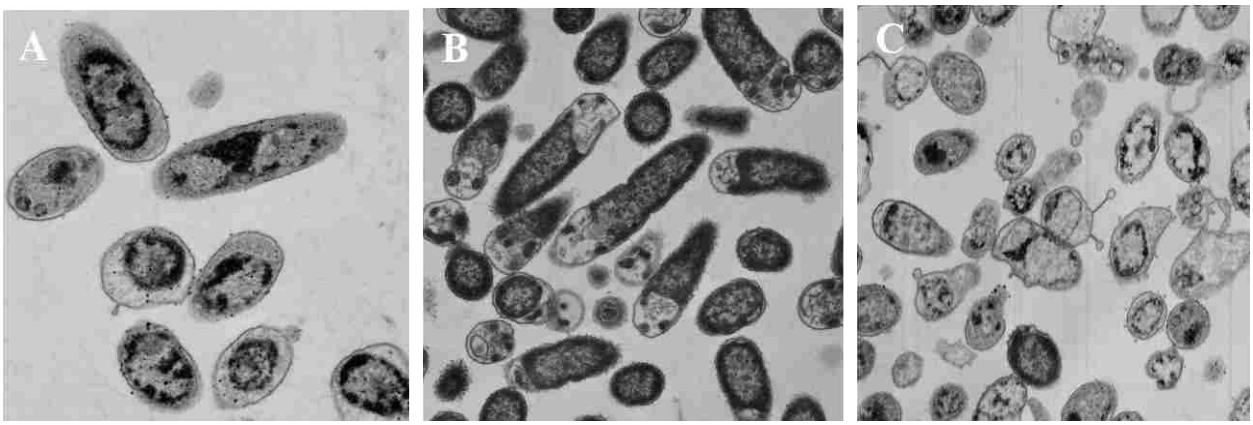

Figure 3-4: TEM images of *K. pneumoniae* (ATCC13883).(A)Control .(B)Treated with 25µg/ml CSA-131. (C) Treated with 50 µg/ml CSA-131 (magnification 35000).

3.3.5 Serial exposure of Gram-negative bacteria to colistin and CSA-131

To compare the rates at which *K. pneumoniae* and two other Gram-negative pathogens (*A. baumannii* and *P. aeruginosa*) acquire resistance to colistin and a lead ceragenin (CSA-131), these strains were serially exposed to both antimicrobials. Initially, all three strains were fully susceptible to colistin and the ceragenin (MICs of 1.0 or 2.0 µg/mL). At each 24 h time point, MICs were determined, and bacteria surviving at the highest concentration of antimicrobial were used for the subsequent MIC measurement. By 10 days (24 h time periods), the MICs of colistin against all three genera of bacteria rose to 350 µg/mL or higher Figure 3-5. Relatively small changes in MIC were observed with CSA-131 over the course of 30 days of exposure. Beginning and ending MICs are shown in Table 3-2.

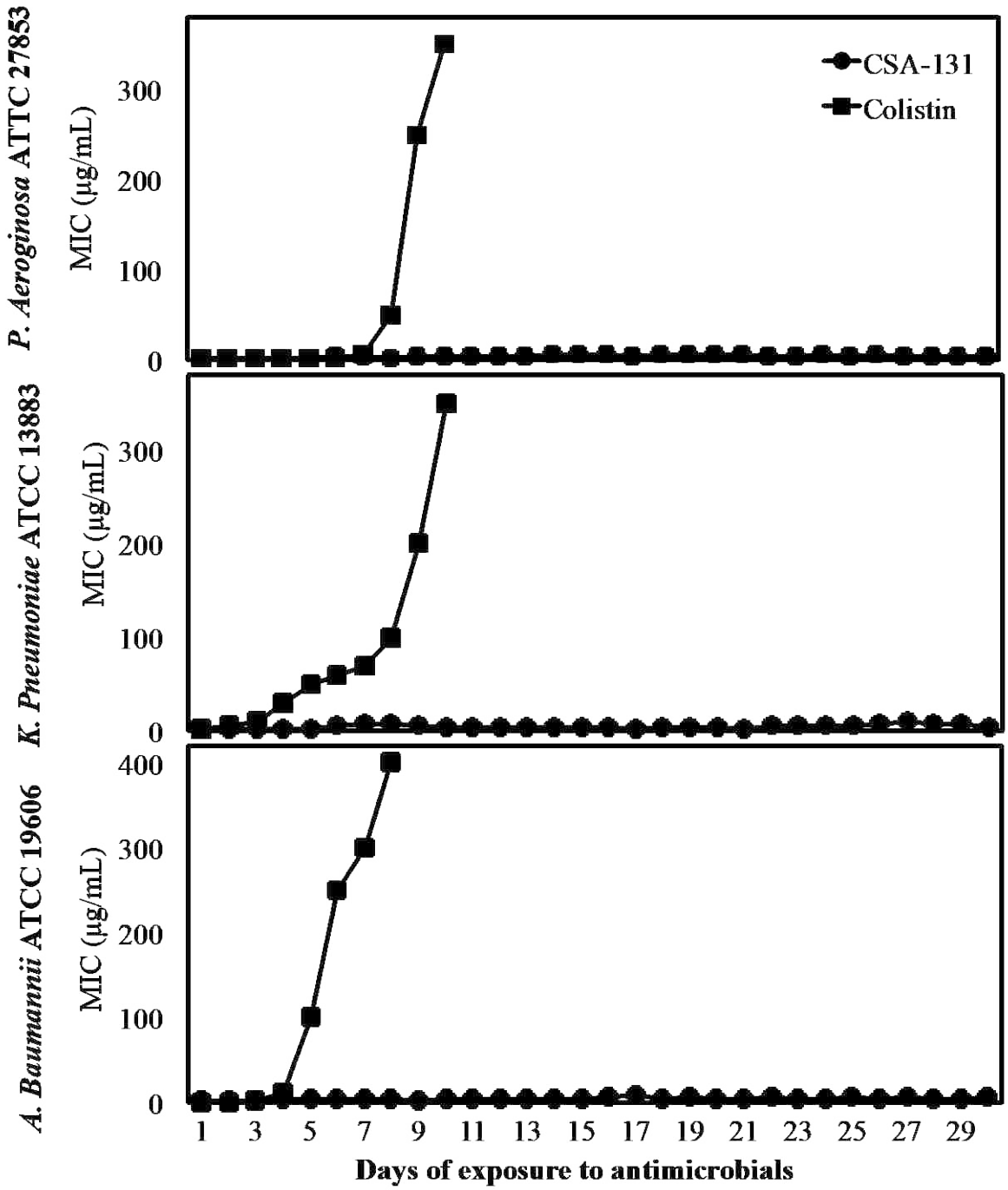

Figure 3-5: MICs of colistin and CSA-131 against *K. pneumoniae, A. baumannii* and *P. aeruginosa* after the number of days (24 h periods) of exposure.

At the end of the serial passaging experiments (10 days for colistin and 30 days for CSA-131), the MICs of the resulting organisms were determined with colistin, CSA-131 and AMPs LL-37,

magainin 1 and cecropin A. These results are shown in Table 3-2. Notably, CSA-131 retained activity against the highly colistin resistant strains. In contrast, relatively modest resistance to CSA-131 (1 to 8 times the MIC with the parent strain) translated into increased MICs for colistin (16 to 32 times the MIC with the parent strain). Resistance to colistin also increased MICs with AMPs (1.3 to 4 times the MIC with the parent strain). Finally, resistance to CSA-131 translated into comparable resistance to AMPs (2.3 to 8 times the MIC with the parent strain). These results suggest that colistin resistance includes mechanisms that do not strongly impact susceptibility to CSA-131 or the AMPs tested.

Table 3-2: MICs of colistin, CSA-131, LL-37, magainin 1, and cecropin A with susceptible standard strains of *K. pneumoniae*, A. *baumannii*, and *P. aeruginosa* and with strains serially exposed to colistin or CSA-131.

	MIC (∝g/ml)				
Strain	**Colistin**	**CSA-131**	**LL-37**	**Magainin1**	**Cecropin A**
K. pneumoniae ATCC 13883	2.0	1.0	32	64	2.0
Serially exposed to colistin*	350	1.5	64	82	16
Serially exposed to CSA-131**	32	8.0	100	150	24
A. Baumannii ATCC 19606	1.0	2.0	16	32	4.0
Serially exposed to colistin*	400	2.0	64	100	16
Serially exposed to CSA-131**	32	2.0	128	150	32
P. Aeruginosa ATCC 27853	1.0	2.0	32	64	4.0
Serially exposed to colistin*	350	2.0	64	100	8.0
Serially exposed to CSA-131**	32	4.0	100	150	16

* 10 days of exposure
** 30 days of exposure

3.3.6 Characterization of lipid A modifications in clinical isolates of *K. pneumoniae* and bacteria serially exposed to colistin and CSA-131

The lipid A portion of LPS is a primary target of colistin [157], ceragenins [54] and AMPs [158], and lipid A modifications have been observed as a mechanism for resistance generation to these antimicrobials [138,151,156,159,160]. Lipid A modifications include phosphate ester formation with 4-aminoarabinose and/or ethanolamine, which decrease the net negative charge of lipid A. To determine how modification of lipid A from *K. pneumoniae* correlated with resistance to colistin and CSA-131, LPS was isolated from three of the clinical isolates and bacteria serially exposed to colistin and CSA-131. The LPS was truncated to yield lipid A, and modifications to lipid A were observed via mass spectrometry. Observed masses are shown in Table 3-3 (mass spectra are shown in Supplementary Materials). Comparable masses have been observed for parent and modified lipid A [154-156].

Table 3-3: Masses of isolated lipid A from colistin-susceptible (ATCC 13883) and colistinresistant strains of *K. pneumoniae* and bacteria serially exposed to colistin and CSA-131

***K. pneumoniae* strain**	**Observed lipid A Mass (*m/z*)**	**Mass of parent lipid A structures (*m/z*)**	**Adaptations to parent lipid A structures**
ATCC 13883*	1795 1840 1853 1910		
ARLG 1389	2023 2209	1840 1840	Lauric acid Aminoarabinose and palmitic acid
ARLG 1349	2021 2209	1840 1840	Lauric acid Aminoarabinose and palmitic acid
ARLG 1360	2034	1910	Ethanolamine
ATCC 13883 serially exposed to colistin**	1795 1987	1795 1840	 Aminoarabinose and hydroxyl group
Serially exposed to CSA-131***	1840 2021 2152	1840 1840 1840	 Lauric acid Aminoarabinose and lauric acid

* ATCC 13883 is fully susceptible strain, so no modifications to lipid A are identified (this is the source of the parent lipid A structures.
**10 days of exposure
***30 days of exposure

3.4 Discussion

A central concern in the development of novel antimicrobial agents is the rapidity with which bacteria generate resistance, and this concern contributes to the paucity of development of new antibiotics. Since higher organisms have co-evolved with bacteria, the mechanisms by which high organisms control bacterial growth may provide guidance for development of antimicrobial agents to which bacteria do no readily generate resistance. AMPs represent one of the key means by which higher organisms control bacterial growth. As mimics of AMPs, ceragenins share structural features with these peptides; specifically, multiple cationic (positive) charges juxtaposed with hydrophobic structure. Notably, colistin shares these structural features. However, while AMPs and ceragenins are active against Gram-positive bacteria, colistin and the polymyxins in general are only weakly active against these organisms. This observation argues that, at least for Gram-positive bacteria, colistin has a different mechanism of action than AMPs and ceragenins. Nevertheless, all three classes of antimicrobials are active against Gram-negative bacteria, which leads to the concern that colistin resistance translates to resistance to AMPs and ceragenins. The studies presented herein lay this concern to rest; highly colistin-resistant bacteria largely remain susceptible to AMPs and ceragenins.

The ceragenins tested in these studies and cecropin A gave MICs in the single μg/mL range, and MICs remained in this range with colistin-resistant clinical isolates (Table 3-1). The clinical isolates were up to hundreds of times more resistant to colistin than the reference strain, while the MICs with LL-37 and magainin 1 increased by factors of ca. 2-3. Thus, some cross resistance is evident, but not to the magnitude observed with colistin.

Further characterization of the most active ceragenins, CSA-131 and CSA-44, demonstrated the potent bactericidal activity of these compounds (Figure 3-1and Figure 3-2) SEM and TEM

(Figure 3-4) confirmed earlier studies demonstrating that ceragenins interact with bacterial membranes. Morphological changes to Gram-negative bacterial membranes are a hallmark of the activity of many AMPs, and we have shown, via TEM, that similar changes occur in bacterial membranes upon treatment with a ceragenin [35]. The SEM images (Figure 3-3) provide a three-dimensional representation of these changes.

Serial exposure of Gram-negative pathogens to colistin demonstrates the rapidity with which these organisms generate resistance (Figure 3-5). MICs rose to 350 μg/mL within 10 days of serial passaging. In contrast, only small changes in MIC with CSA-131 were observed (Table 3-2). CSA-131 retained activity against the highly colistin-resistant bacteria, while the MICs with AMPs increased by factors of two to eight. Bacteria that were serially exposed to CSA-131 displayed resistance to colistin (increases by factors of 16 to 32), but their MICs with colistin were much lower (32 μg/mL) than those serially exposed to colistin. Together, these data suggest that there may be some common resistance mechanisms among colistin, AMPs and ceragenins, but that the mechanism(s) that bacteria employ to become highly resistant to colistin is very different from mechanism(s) used to increase MICs with AMPs and ceragenins.

Two-component systems (e.g., PhoP/PhoQ and PmrA/PmrB) are known to instill resistance to AMPs [161], and this resistance is mediated by changes to the structure of lipid A resulting in incorporation of aminoarabinose and/or ethanolamine [154,158]. For example, in *Salmonella typhimurium* this modification is caused by two-component signal transduction systems including PhoP-PhoQ and PmrA-PmrB [161]. The presence of positive charges on AMPs activates PhoQ, which is a membrane-associated protein kinase, and activated PhoQ phosphorylates PhoP, which leads to upregulation of a host of proteins including PagP leading to the addition of palmitate to membrane-associated lipid A. This change increases the hydrophobic character of lipid A and

membrane stiffness. The same signal transduction system also leads to further modification of lipid A through formation of phosphate esters with ethanolamine and L-4-amino arabinose [156,163,164]. These changes decrease the net negative charge of the membrane and further decreases the affinity of AMPs to the bacterial membrane. These defenses, however, are metabolically costly to bacteria, and absent AMPs or other threats, bacteria shut down these systems and exist in AMP-susceptible forms. It is also interesting to note that although resistance to AMPs has been observed *in vitro*, no evidence of resistance *in vivo* has been observed to this point [41].

The action of MCR-1, characterized as a cause of colistin resistance, has also been proposed to cause addition of ethanolamine to the parent structure [138], although in a recent study of colistin-resistant, clinical isolates of *K. pneumoniae*, plasmid-associated genes *mcr-1* and *mcr-2* were not detected [133]. These changes to lipid A lead to a decrease in the overall negative charge on the surface of the bacteria and a subsequent a loss of affinity for positively charged antimicrobials. In a previous study, we observed that serial exposure of Gram-negative bacteria to CSA-13, a first generation ceragenin, led to modifications of lipid A with aminoarabinose and increases in MIC [151]. Characterization of lipid A from three colistin-resistant, clinical isolates of *K. pneumoniae* showed aminoarabinose or ethanolamine modification to lipid A (Table 3-3). Similar modifications were observed with *K. pneumoniae* serially exposed to colistin and CSA-131. These modifications appear common to bacteria resistant to colistin or serially exposed to CSA-131. However, these changes do not correlate with the high levels of resistance to colistin, suggesting that another mechanism renders these bacteria highly colistin resistance.

The highest increase in MIC observed after serial exposure (30 days) to CSA-131 came with *K. pneumoniae* (an increase from 1.0 to 8.0 μg/mL); changes with *A. baumannii* and *P. aeruginosa* were smaller (Table 3-2). Serial exposure of Gram-negative bacteria to CSA-13 led to much larger

increases in MIC (MICs > 20 μg/mL). As noted, this resistance was correlated with aminoarabinose modifications to lipid A [151]. CSA-131 has a longer lipid chain than CSA-13, and we hypothesize that this longer lipid chain allows CSA-131 to interact more strongly with membranes containing modified lipid A than CSA-13. Ultimately, this stronger interaction with CSA-131 would allow more effective traversal of the outer membrane and subsequent targeting of the cytoplasmic membrane.

3.5 Conclusions

While specific mechanisms for resistance of Gram-negative bacteria to polymyxins, including colistin, have been identified, multiple mechanisms likely influence resistance [162]. At least one of these mechanisms causes very high resistance to colistin but does not appear to impact susceptibility to AMPs and ceragenins. Lipid A modifications may impact the antimicrobial activity of colistin, AMP and ceragenins modestly, but they do not account for the very high MICs for colistin with clinical isolates of *K. pneumoniae* and Gram-negative bacterial strains serially exposed to colistin. The fact that lead ceragenins (CSA-44 and CSA-131) retain bactericidal activity against highly colistin-resistant bacteria provides further support for development of these compounds as broad-spectrum antibacterial agents in multiple potential clinical applications.

3.6 Appendix A

Supporting information for susceptibility of colistin-resistant, Gram-negative bacteria to antimicrobial peptides and ceragenins.

Mass spectra (ESI, negative ion mode, Agilent 6230 Series TOF Spectrometer) of lipid A isolated from the indicated strains of *K. pneumoniae*. Col-R strain is *K. pneumoniae* (ATCC 13883)

serially exposed to colistin for 10 days. CSA-R is *K. pneumoniae* (ATCC 13883) serially exposed to CSA-131 for 30 days.

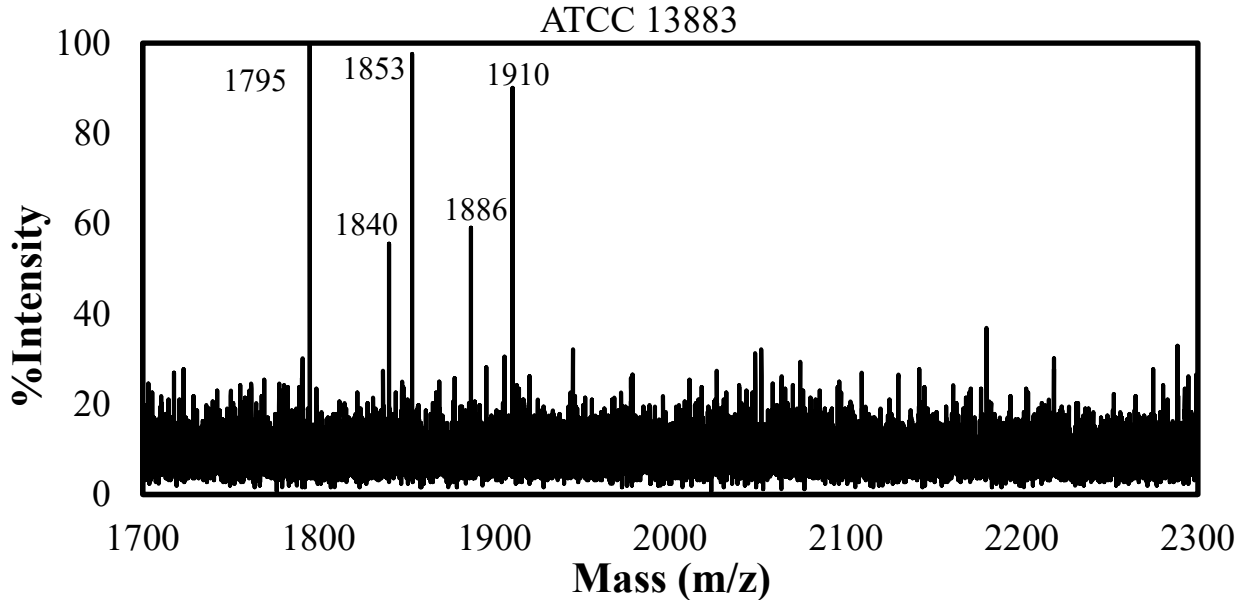

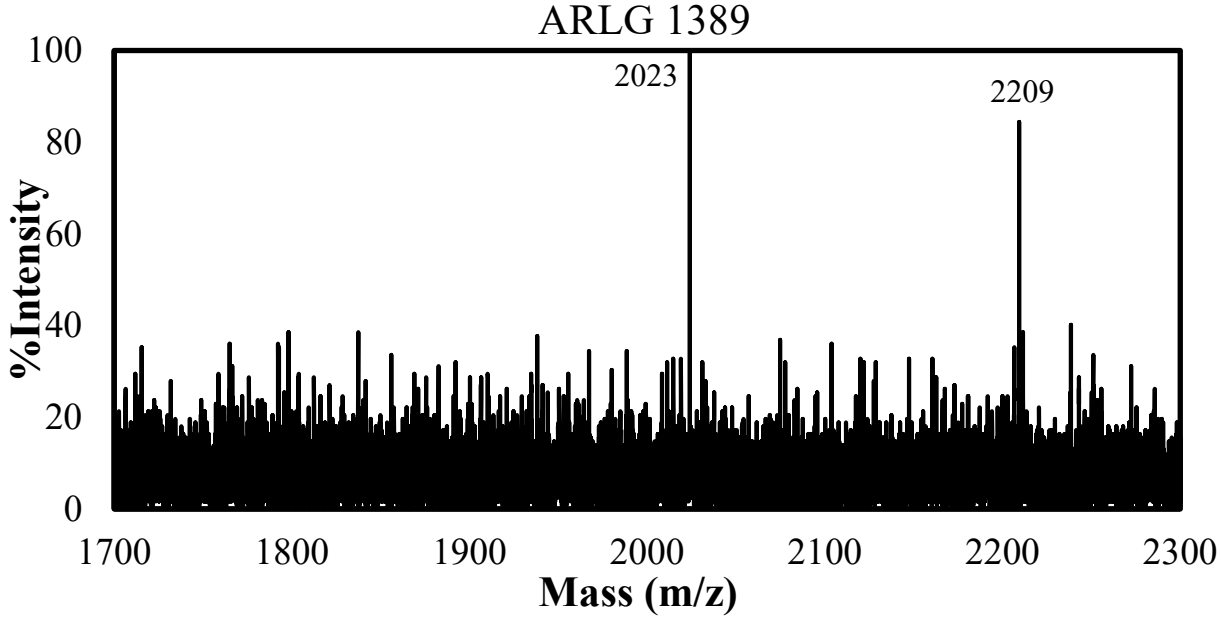

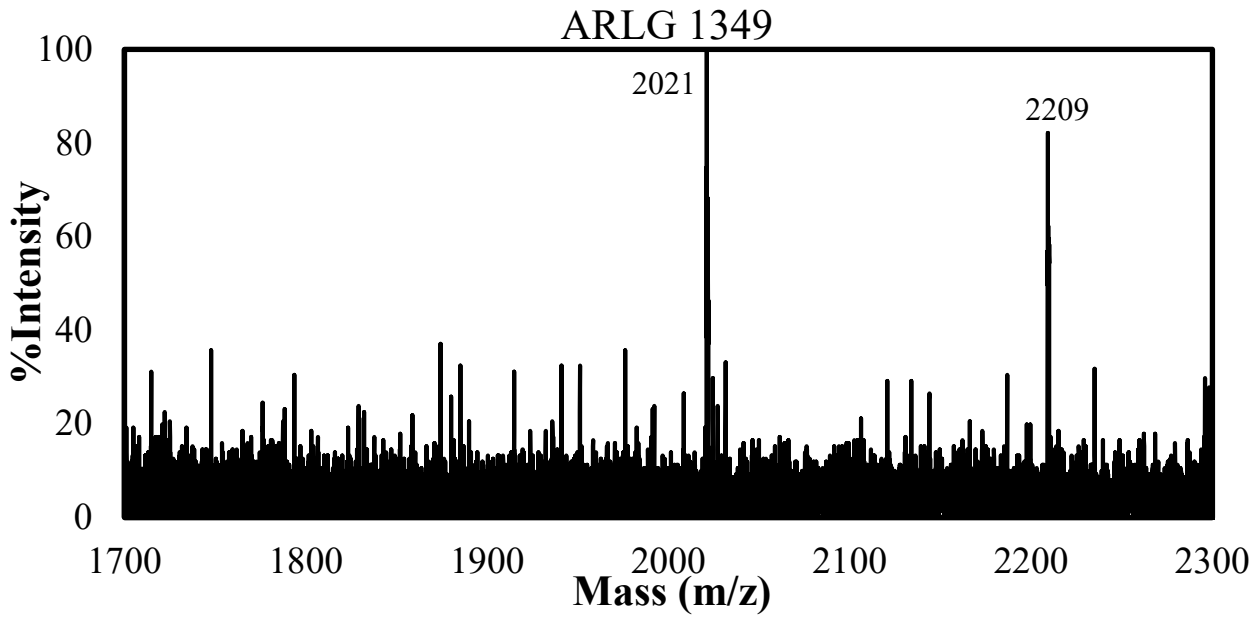
ARLG 1349
2021
2209
%Intensity
Mass (m/z)
100
80
60
40
20
0
1700
1800
1900
2000
2100
2200
2300

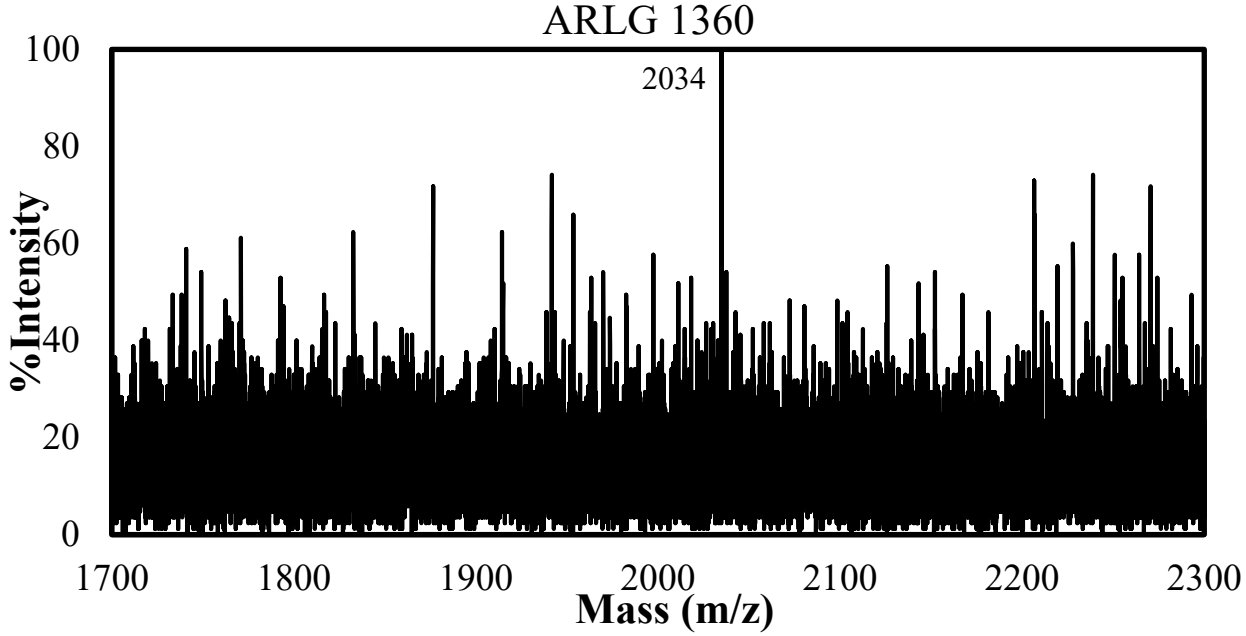
ARLG 1360
2034
%Intensity
Mass (m/z)
100
80
60
40
20
0
1700
1800
1900
2000
2100
2200
2300

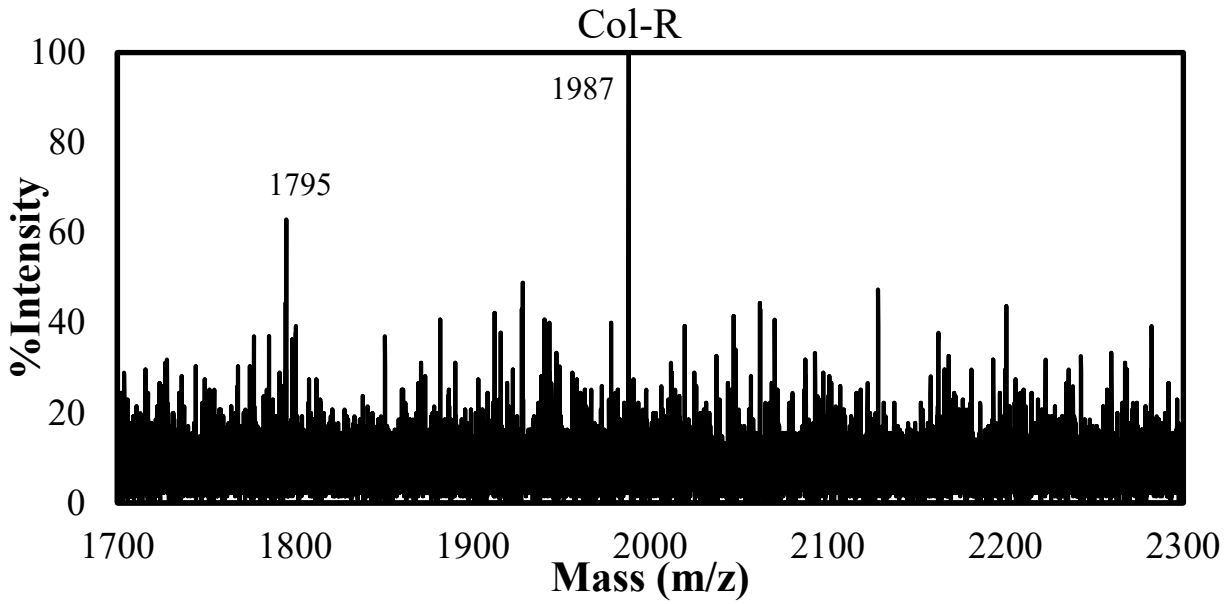
Col-R
100
80
60
40
20
0
%Intensity
1987
1795
1700
1800
1900
2000
2100
2200
2300
Mass (m/z)

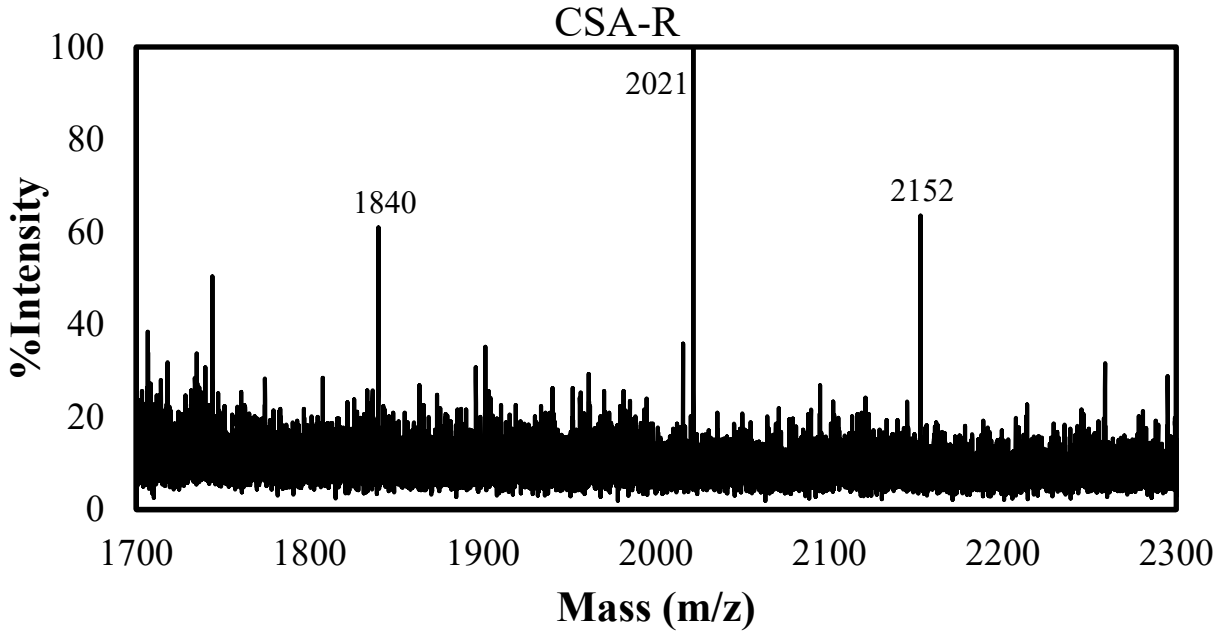
CSA-R
100
80
60
40
20
0
%Intensity
2021
1840
2152
1700
1800
1900
2000
2100
2200
2300
Mass (m/z)

3.7 Appendix B

Proposed structures for lipid A isolated from the indicated strains that match the mass spectral data. Changes from the parent structures are in red. Locaton of acylation (addition of a fatty acid) and phosphate ester formation may not reflect exact structure (i.r., mass spectral data do not provide positional information for modifications).

ATCC 13883

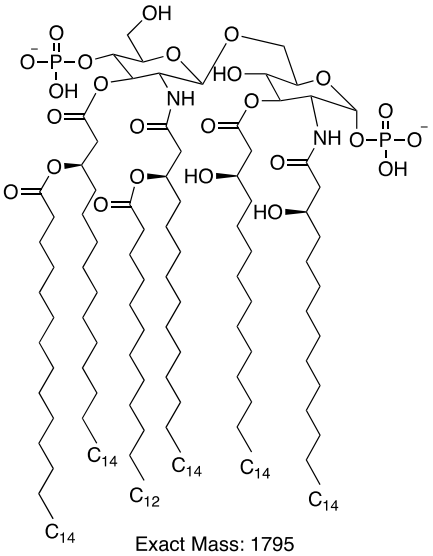

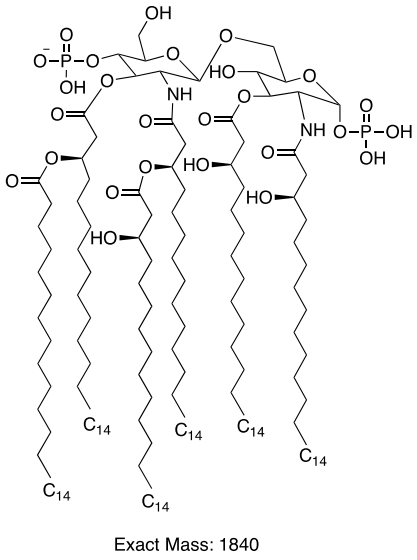

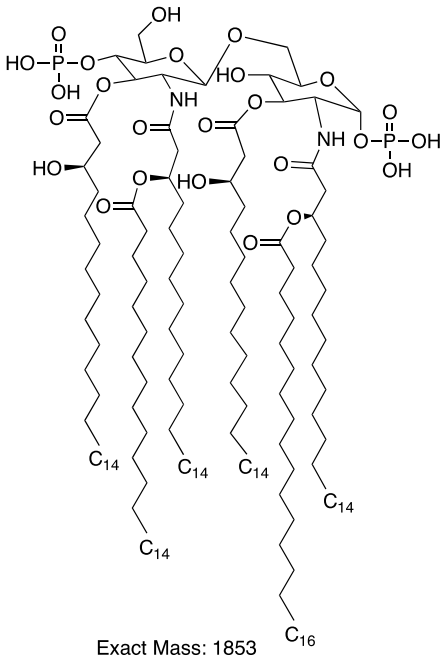

Exact Mass: 1853

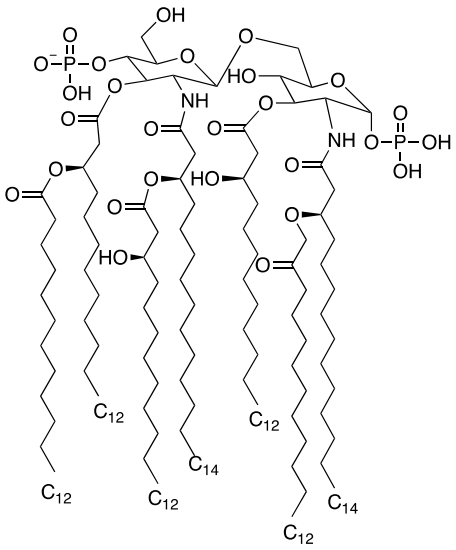

Exact Mass: 1910

ARLG 1389, ARLG 1349

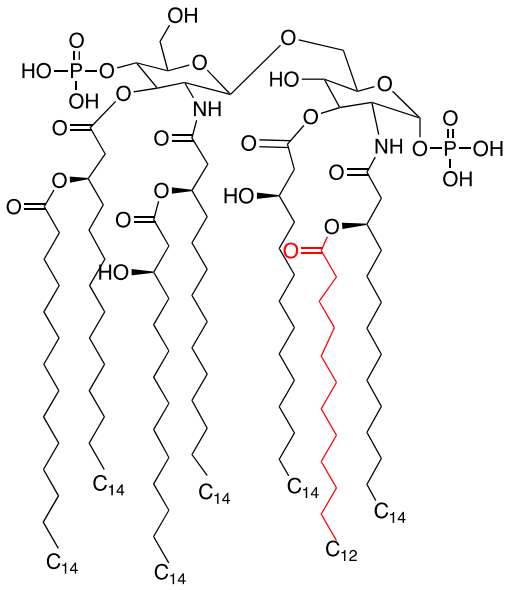

Exact Mass: 2023

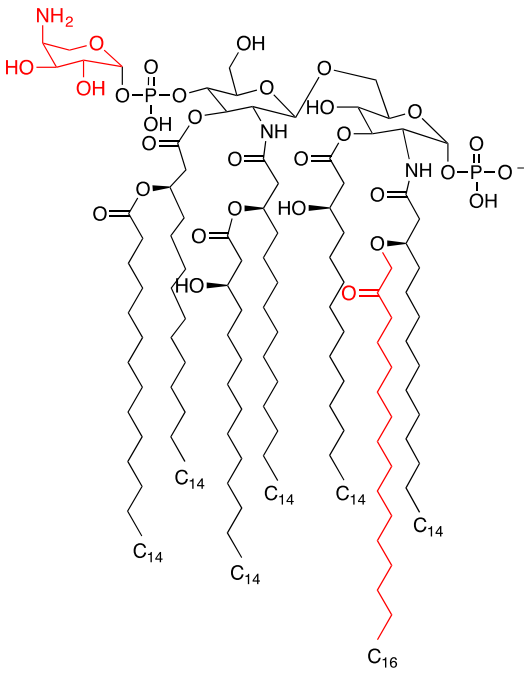

Exact Mass: 2209

ARLG 1360

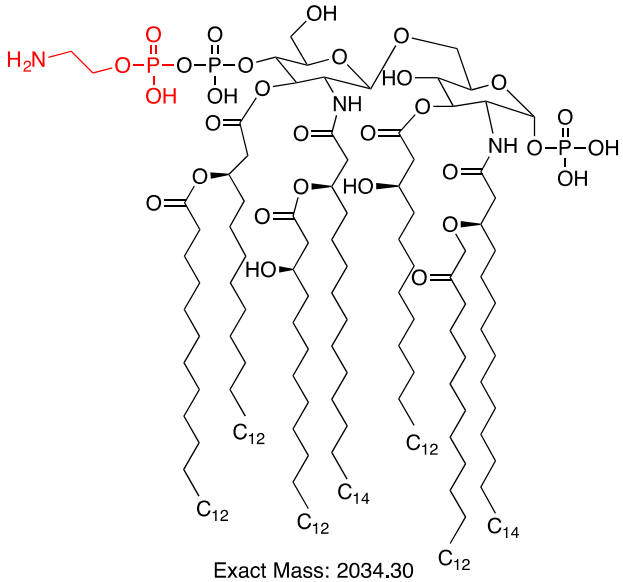

Exact Mass: 2034.30

Col-R (Colistin Resistant made by serial passaging)

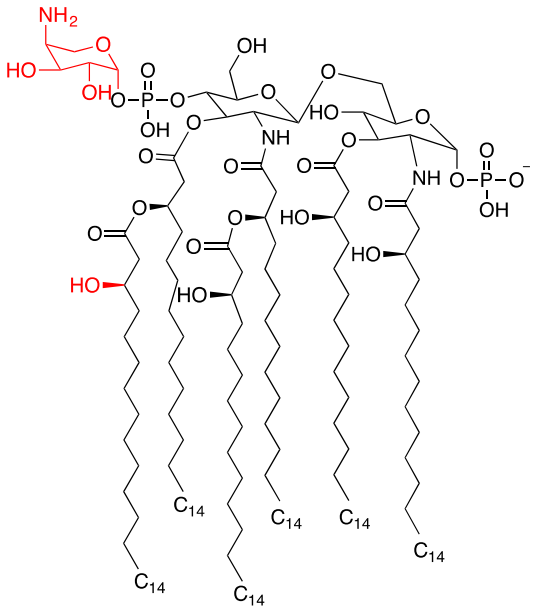

Exact Mass: 1987

CSA-R (CSA resistant made by serial passaging)

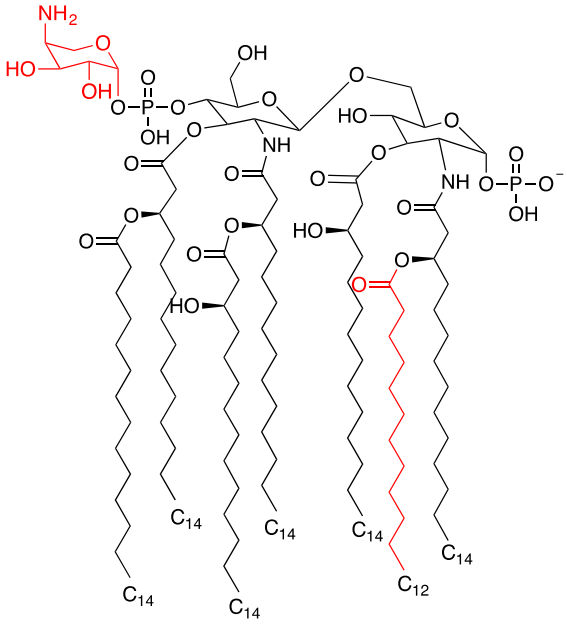

Exact Mass: 2153

Chapter 4 Proteomic analysis of resistance of Gram-negative bacteria to chlorhexidine and impacts on susceptibility to colistin, antimicrobial peptides and ceragenins

4.1 Introduction

Chlorhexidine (Figure 4-1) is a potent antiseptic agent that has been in use since the 1950s [165]. It is used extensively in healthcare settings in hand washing, patient bathing, treatment of gingivitis, skin antisepsis, and other antimicrobial applications [166]. Chlorhexidine is sparingly soluble in water, and thereby normally formulated with either acetate or gluconate to form water-soluble salts. Chlorhexidine has been found to have antibacterial, antifungal, and even some anti-viral activities [167]. Although chlorhexidine has proven to be an effective antimicrobial agent in hospital settings, it has limitations. While data show that chlorhexidine is active against planktonic bacterial cells, it is less effective against biofilms. After treatment of methicillin resistant *S. aureus* (MRSA) and multi-drug resistant (MDR) *Pseudomonas aeruginosa* biofilms grown on hospital grade-surfaces, these pathogens were shown to maintain up to 11% and 80% of their cell viability respectively [168]. Additionally, recent studies found that various clinical isolates of *Klebsiella pneumoniae*, from before and after the widespread use of chlorhexidine, show a significant difference in susceptibility to the antimicrobial [169,170]. Notably, it has been shown that development of resistance is stable; bacteria do not revert to susceptible forms after being grown for an extended time in antimicrobial-free medium, suggesting that resistance is mutational rather than adaptational [169].

Due to the prevalent use of chlorhexidine, especially in clinical settings, there has been increasing concern about whether repeated exposures of bacteria to sub-lethal doses of chlorhexidine is a factor in the emergence of multi-drug resistant bacteria [171]. For example, Bhardwaj *et al*, found that serial exposure of vancomycin-resistant *Enterococcus faecium* to

chlorhexidine resulted in reduced susceptibility to other membrane-targeting antimicrobials such as daptomycin [172]. Of particular concern is the role of exposure to chlorhexidine in generation of colistin resistance. The prevalence of Gram-negative, drug-resistant bacteria has resulted in increased use of colistin (Figure 4-1), which is considered an antibiotic of "last resort." However, colistin resistant organisms have been increasingly isolated from clinical settings [173,174]. Wand *et al.* [170] recently reported cross-resistance between chlorhexidine and colistin. They found that in chlorhexidine-adapted strains of *K. pneumoniae*, the minimum inhibitory concentrations (MIC) for colistin increased by a factor between 16 and 32 with five of the six strains tested. However, when colistin-resistant *K. pneumoniae* were tested for chlorhexidine susceptibility, Wand *et al.* found that MICs of chlorhexidine were the same with colistin-susceptible and colistin-resistant strains. On the other hand, Curiao *et al.* [175] reported that at least in *Salmonella*, there are multiple mutations leading to chlorhexidine resistance that are not necessarily associated with colistin resistance.

Cross resistance of bacteria to chlorhexidine and colistin may be due to common features of these antimicrobials. For example, both are cationic (positively charged) with hydrophobic functionality. Notably, most endogenous antimicrobial peptides (AMPs, representative sequences are shown in Figure 4-1) also display these features: cationic groups juxtaposed with hydrophobic side chains [14,176]. We recently reported [177] that highly colistin-resistant bacteria are susceptible to both AMPs and non-peptide mimics of AMPs, termed ceragenins. This finding led to the question of whether generation of chlorhexidine resistance results in cross resistance to ceragenins and AMPs. Reported herein are investigations of the means by which Gram-negative bacteria become resistant to chlorhexidine and how this resistance influences susceptibility to colistin, AMPs and ceragenins. Rather than focus on mutations, changes to the proteome were investigated to obtain

an understanding of multiple possible alterations in gene expression that lead to resistance. We found that, as expected, induction of resistance in Gram-negative bacteria to chlorhexidine resulted in decreased susceptibility to colistin; nevertheless, organisms remained susceptible to ceragenins. Changes to the proteome of chlorhexidine-resistant organisms, relative to a parent strain, were in the outer membrane proteins as well as proteins associated with chaperones, efflux pumps, flagella and cell metabolism.

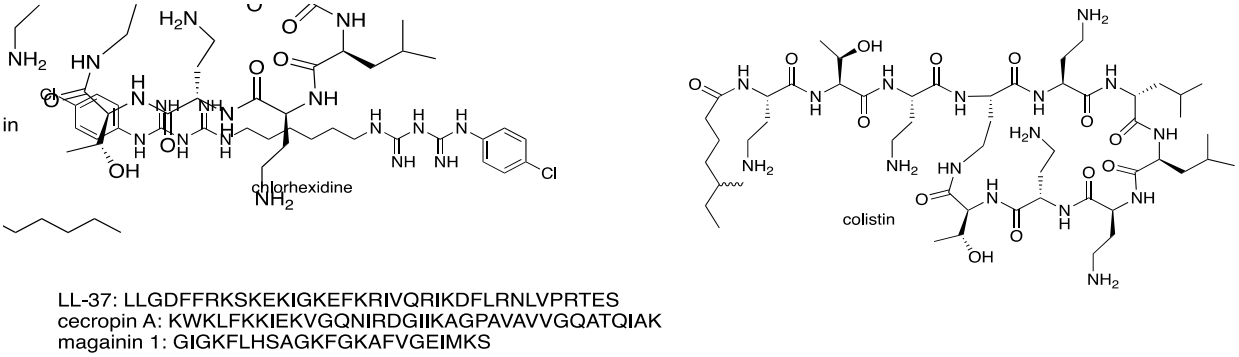

Figure 4-1: Structures of chlorhexidine, colistin and sequences of LL-37, cecropin A and magainin 1.

4.2 Material and methods

4.2.1 Materials

K. pneumoniae (ATCC 13883), *Acinetobacter baumannii* (ATCC 19606) and *P. aeruginosa* (ATCC 27853) were obtained from the American Type Culture Collection (ATCC, Manassas, VA). Chlorhexidine, colistin (polymyxin E), congo red and coomassie brilliant blue dyes were purchased from Sigma–Aldrich (St Louis, MO, USA).

4.2.2 Susceptibility testing

MICs were determined using a broth microdilution method in a 96-well plate according to the Clinical Laboratory Standards Institute protocol (2006) as described in detail in section 3.2.2

4.2.3 Serial passage of bacteria with chlorhexidine

Serial passaging of bacteria was performed according to a protocol described in section 3.2.3.

4.2.4 Colony morphology assay

MHA plates were made in 60 x 15mm petri dishes with the addition of Congo red (40 mg/L) and Coomassie brilliant blue (20 mg/L) dyes. Bacterial cultures were grown overnight in MH broth at 37 °C. An aliquot of bacterial culture (1 µL) was then spotted onto the MHA dyed plates and incubated at 37 °C for 24 h [178]. Images were acquired using a stereo microscope (Stemi 2000, Zeiss).

4.2.5 Proteomic sample preparation

Three independent studies were performed for the proteomics analyses and one single colony was used for each independent study. Both wild-type (ATCC 27583) and drug-resistant *P. aeruginosa* were cultured in TSB (25 mL) to an OD600 nm of 0.5. Cells were pelleted at 3750 x g for 10 min at room temperature followed by three washes with ice-cold PBS. Cell pellets were lysed in 1% sodium dodecyl sulfate (1 mL) in Tris buffer (50 m*M*, pH 8). Cells were briefly sonicated to further lyse the cells. Protein concentration was determined by bicinchoninic acid (BCA) protein assay (Thermo Fisher Scientific, Waltham, MA, USA). Protein digestion was carried out using filter-assisted digestion. Aliquots of 50 µg of protein were transferred to centrifugal filters (30 kD molecular weight cutoff), denatured with guanidine (100 µL, 6 *M*

guanidinium hydrochloride, 100 m*M* Tris, pH 8.5), and centrifuged for 15 min at 14000 x g. This step was repeated three times to remove SDS entirely. Cell lysate was reduced by DTT (20 m*M* in 6 *M* guanidinium hydrochloride) at 65 °C for 5 min. After cooling for 5 min, alkylation was performed with iodoacetamide (50 m*M*, 1 h incubation at room temperature in the dark). The mixture was then washed two times with ammonium bicarbonate buffer (25 m*M*, pH 8.5). The washed, alkylated protein sample was re-suspended in ammonium bicarbonate (ABC, 100 µL) followed by overnight digestion at 37 °C with trypsin (1 µg, Sigma-Aldrich Proteomics Grade). After trypsin digestion, peptides were isolated by spinning down the mixture (14,000 x g, 30 min.) with one rinse of the filter using ABC (100 µL, centrifugation 14,000 x g for 30 min.). The combined filtrate was vacuum dried using a speedvac (Sorval). The dried sample was immediately re-dissolved in 50 µL of buffer (0.1% formic acid in Optima-grade water) for mass spectrometry analysis [179].

4.2.6 Mass spectrometry data acquisition

Mass spectrometry data were collected using an Orbitrap Fusion Lumos mass spectrometer (Thermo Fisher Scientific, Waltham, MA, USA) coupled to an EASY-nLC 1200 liquid chromatography (LC) pump (Thermo Fisher Scientific, Waltham, MA, USA). A capillary RSLC column (EASY-spray column pepMap ® RSLC, C18, 2 µm, 100 Å, 75 µm × 25 cm) was used for separation of peptides. The mobile phase was comprised of buffer A (0.1% formic acid in Optima water) and buffer B (Optima water and 0.1% formic acid in 80% acetonitrile).

Elution of peptides was performed at 300 nL/min with the following gradients over 2 h: 3–25% B for 80 min; 25–35% B for 20 min; 35–45% B for 8 min; 45–85% B for 2 min and 85% for 8 min. Data were acquired using the method described by Peng *et al* [180]. Briefly, using the top

speed method (3 s cycle) and a resolution of 120,000 at 200 m/z, a full scan MS was obtained in the orbitrap with a target value of 3e5 and a maximum injection time of 60 ms. Detection of fragment ions in the linear ion trap was performed with a target AGC value of 1e4 and a maximum injection time of 250ms.

Label-free quantification (LFQ) values were obtained using PEAKS (version 8.5) and the Swiss-Prot validated *P. aeruginosa* proteome (5638 sequences May 2018) with a reverse sequence decoy database concatenated and included during the search. After the removal of contaminants, low scoring peptides and reverse matches, the LFQ values for the top 3 peptides were summed and transformed by a logarithm of 2. The proteins were then separated into wild type and mutant groups, and only those with at least three correct LFQ values were used for quantification. Accordingly, two-tailed heteroscedastic t-tests were conducted to compare wild type versus mutant groups. The acquisition of gene ontology terms and functional clusters, as well as the identification of molecular functions and biological process, was conducted using the Database for Annotation, Visualization and Integrated Discovery (DAVID) and Uniprot. Information about protein-protein interaction networks was retrieved from STRING (v10).

4.3 Results and Discussion

4.3.1 Susceptibility of tested Gram-negative bacteria to antimicrobials

Our results in Chapter 3 has shown that Gram-negative bacteria become resistant to colistin following exposure to a sublethal concentration of colistin; however, colistin resistance does not correlate with higher MIC levels for AMPs or ceragenins. To determine whether resistance to chlorhexidine also leads to cross-resistance against other antimicrobials, Gram-negative strains

were serially exposed to chlorhexidine for 10 days with MIC determination every 24 h. Serial exposure of Gram-negative bacteria to chlorhexidine resulted in a rapid four- to eight-fold increase in MICs of chlorhexidine within 10 days (Figure 4-2).

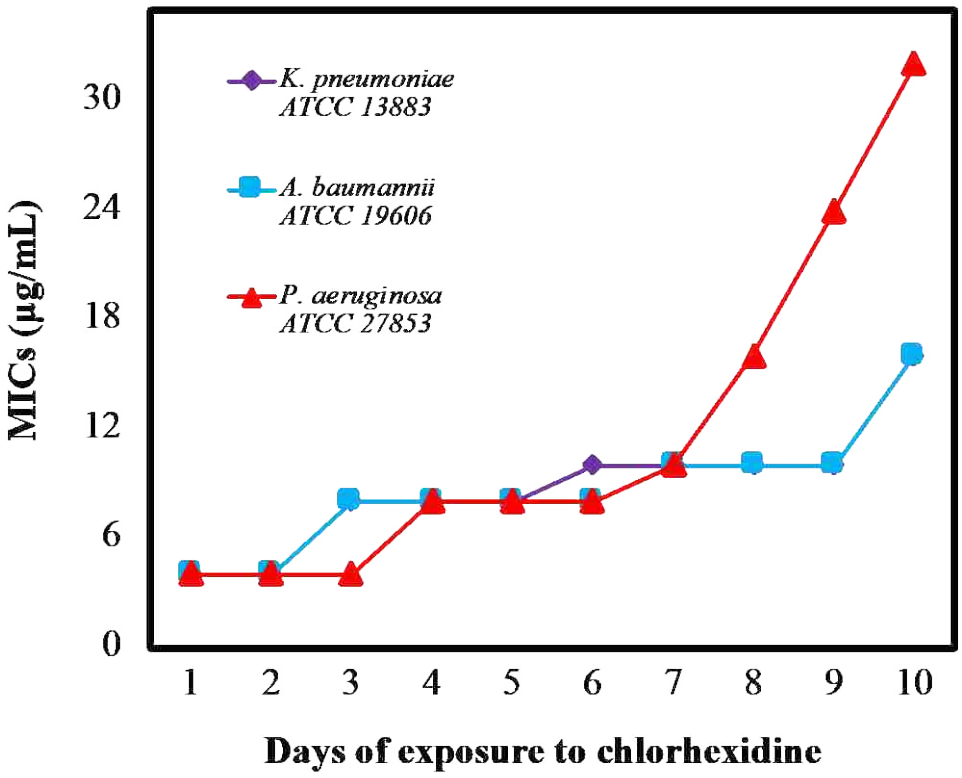

Figure 4-2: MICs of chlorhexidine against *A. baumannii*, *P. aeruginosa* and *K. pneumoniae* after the number of days exposure to chlorhexidine.

MICs of AMPs (LL-37, cecropin A, magainin 1), lead ceragenins (CSA-44 and CSA-131) and colistin were measured with the chlorhexidine resistant strains (Table 4-1). Notably, the chlorhexidine-resistant organisms showed decreased susceptibility to colistin (8- to 32-fold increases in MICs) in spite of not having been exposed to colistin. In contrast, MICs of representative AMPs were the same with the original strains and the chlorhexidine-resistant organisms. Similarly, the MICs of lead ceragenins (CSA-44 and CSA-131) were unchanged with the original and chlorhexidine resistant bacteria. Although chlorhexidine-resistant Gram-negative

bacteria showed decreased susceptibility to colistin, as earlier reported by Wand *et al*. [170] and seen in our studies, colistin-resistant Gram-negative bacteria did not show an increased MIC with chlorhexidine (data not shown). Overall, these results support the idea that exposure of Gram-negative bacteria to chlorhexidine can lead to cross-resistance to colistin, while susceptibilities to AMPs and ceragenins remain unchanged.

Table 4-1: MICs of chlorhexidine, colistin, CSA-131, CSA-44, LL-37, magainin 1, and cecropin A with susceptible standard strains of K. pneumoniae, A. baumannii, and P. aeruginosa and with strains serially exposed to chlorhexidine and colistin.

Strain	CHX	Col	CSA-131	CSA-44	LL-37	Magainin 1	Cecrop
K. pneumoniae ATCC 13883	4	2	1	1	32	64	2
Serially exposed to CHX	16	16	1	1	32	64	nm
A. baumannii ATCC 19606	4	1	2	2	16	32	4
Serially exposed to CHX	16	16	2	2	16	32	nm
P. aeruginosa ATCC 27853	4	1	2	2	32	64	4
Serially exposed to CHX	32	32	2	2	32	64	nm

CHX: chlorhexidine, Col: colistin. All tested bacteria are serially exposure to chlorhexidine for ten passages. All the MICs are results of three independent experiments. nm: not measured.

4.3.2 Colony morphology

Control strains of each type of Gram-negative bacteria produced colonies of circular and smooth morphology (Figure 4-3 A-C). The serially passaged strains of *A. baumannii* and *K. pneumoniae*, however, formed colonies of irregular shape and had rough surfaces (Figure 4-3 D-F). Although *P. aeruginosa* serially exposed to chlorhexidine produced colonies which were circular, they also had slightly rough surfaces and formed undulating margins. All three serially

passaged strains grew larger colonies that covered more surface area than their respective controls. These changes in morphology may be a response to LPS modifications. For example, in *Pseudomonas stutzeri*, it has been shown that chlorhexidine resistance accompanies a loss of low-mass LPS species in SDS-PAGE gels. Because these strains showed cross-resistance, the shift to higher-mass LPS suggests that multidrug resistance is accompanied by LPS production which favors larger polysaccharide components [181]. And, as demonstrated in Gram-negative *Vibrio cholerae*, colony morphology can shift from smooth to rough in response to extracellular polysaccharide changes [182]. The connection between extracellular polysaccharides and colony morphology is further supported by *Salmonella enterica,* which shifts from rough to smooth morphology when short O-antigen chain LPS production is up-regulated [183]. Because capsular polysaccharides have been shown to shield *K. pneumoniae* from polymixins, including colistin [184], the increased mass of the polysaccharides contained within LPS may be the bridge between resistance to the two classes of antimicrobials, either by introducing additional mass or by changing the organization of the capsule. Generally, proposed mechanisms of colistin resistance in Gram-negative bacteria involve LPS modifications [185,186]. Thus, chlorhexidine resistance potentially brings about colistin resistance through one or more modifications to LPS.

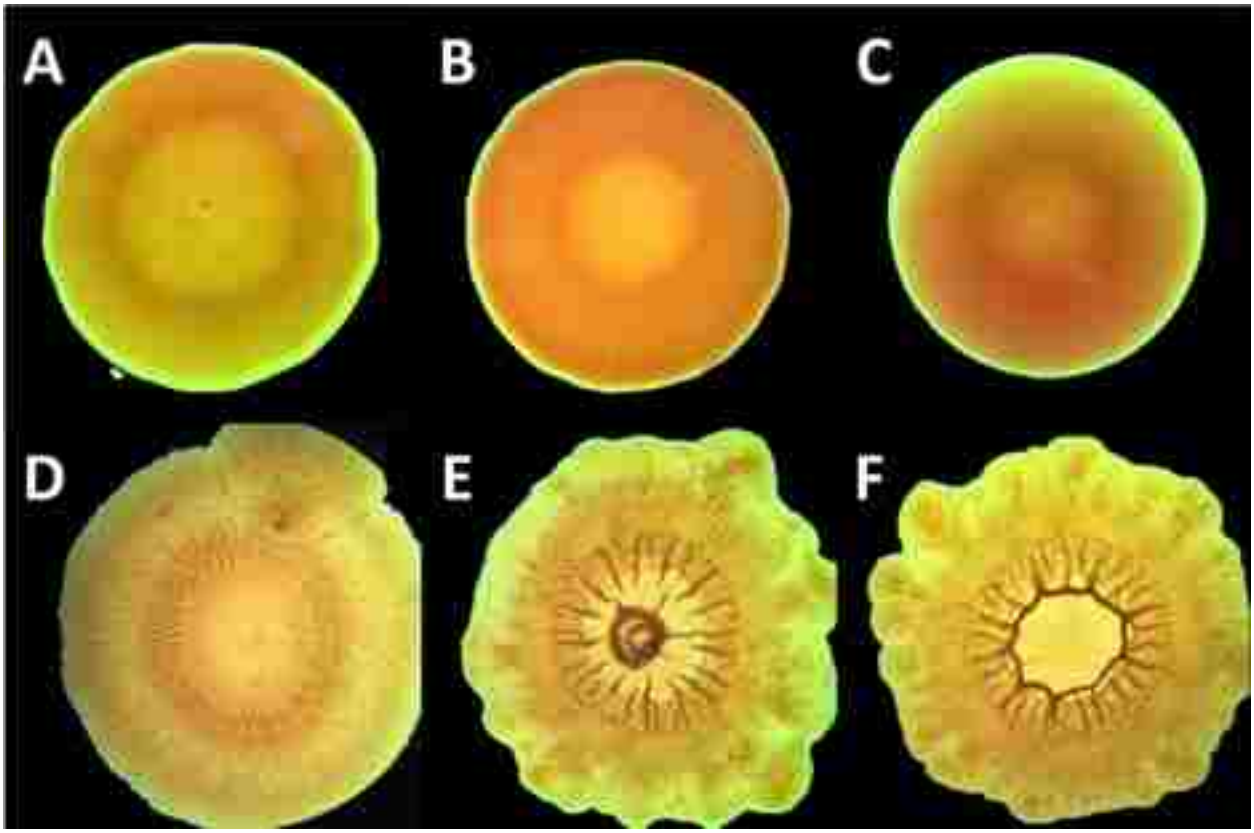

Figure 4-3: Colony morphology of *A. baumannii* and, *P. aeruginosa* and *K. pneumoniae* upon exposure to chlorhexidine. Bacterial strains *P. aeruginosa* (A, D), *A. baumannii* (B, E), and *K. pneumoniae* (C, F) were serially passaged with chlorhexidine (D-F) and the resulting colony morphology was compared with untreated colonies (A-C).

4.3.3 Proteomics

Proteomics has been established as an effective method of analyzing biological processes and is particularly valuable for examining resistance to antibiotics [187,188]. For *P. aeruginosa*, a recent study has unveiled several differences in protein expression associated with low and high levels of ciprofloxacin resistance [189]. On the whole, though, proteomic data on chlorhexidine-resistant *P. aeruginosa* remain scarce, in particular regarding cross-resistance with colistin, for which, to the best of our knowledge, no data on differential expression inherent to resistance are yet available. We have evaluated cross-resistance between colistin, chlorhexidine, AMPs and their mimic, ceragenins, and we further analyzed the proteome of chlorhexidine-resistant *P. aeruginosa* using

reference strain ATCC 27853 for comparison.

We used label-free quantitation to compare the relative concentrations of proteins within the proteome of wild-type and chlorhexidine-resistant *P. aeruginosa*. We observed substantial alterations of the proteome of the resistant strain relative to the wild-type strain, with several highly abundant proteins reduced in relative concentration and increased in a collection of proteins with distinct connections to antibiotic resistance as outlined below. A total of 330 proteins (out of 528 proteins) were differentially expressed at a significant level (2-fold-change, $p < 0.05$), following exposure to chlorhexidine. Identification, function and biological functions of some proteins differentially expressed between the chlorhexidine-resistant and wild-type *P. aeruginosa* are listed in Table 4-2 in the same order that they are mentioned in the text. Large changes in protein expression indicate that the general protein concentration can vary dramatically in response to treatment [183,188].

We searched for relationships among the most upregulated (12.5% of the total differentially expressed) and the most downregulated (12.5% of the total differentially expressed) proteins and assigned them to functional clusters. The numbers of differentially expressed proteins for each cluster are shown in Figure 4-4. Functional clusters containing the largest number of upregulated proteins are involved in microbial metabolism in diverse environments, carbon metabolism, ATP binding, nucleotide binding and translation of proteins. Conversely, functional clusters containing the largest number of downregulated proteins include nucleotide-binding, ATP-binding, cytoplasm and nucleotide phosphate-binding proteins.

A

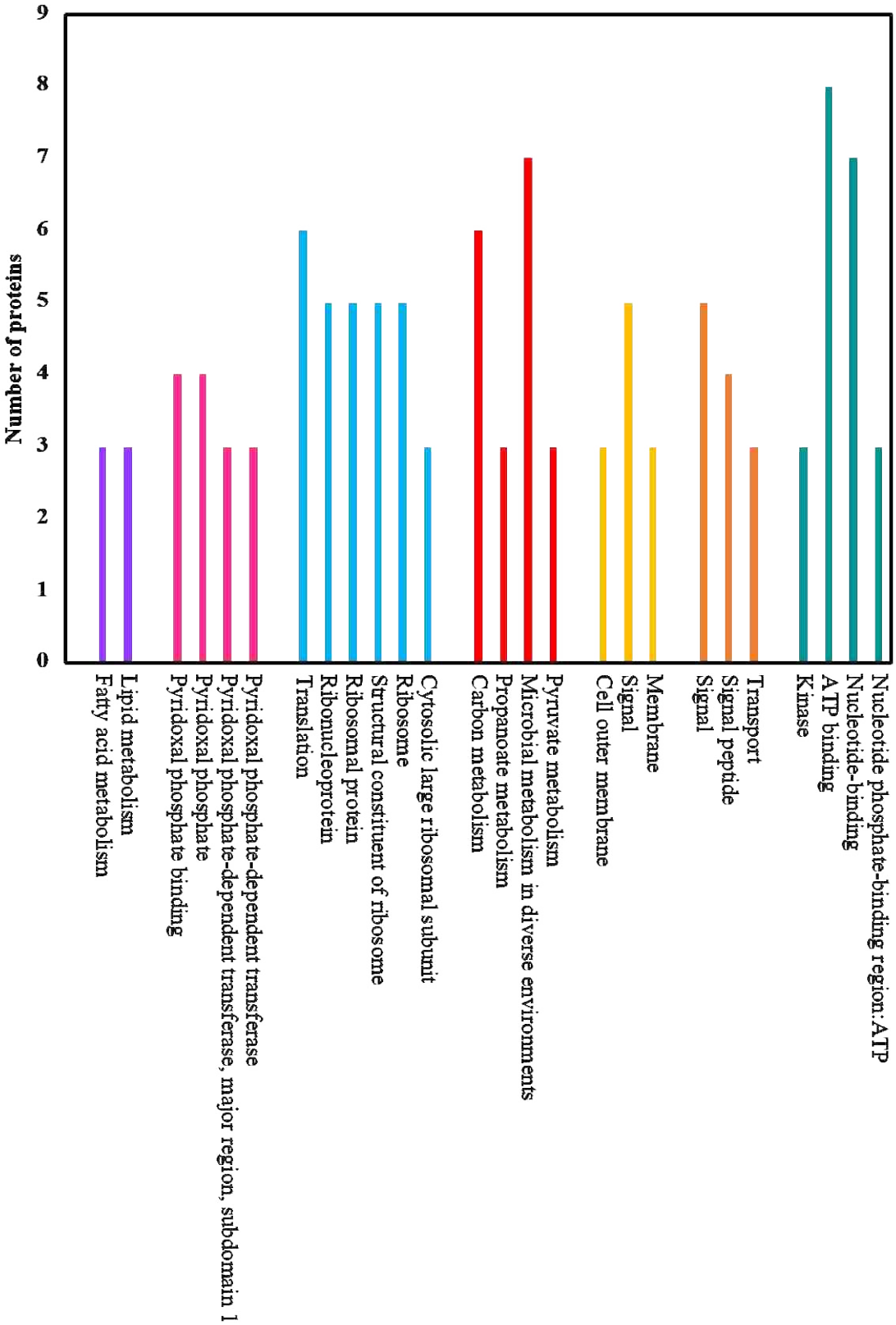
Number of proteins
0
1
2
3
4
5
6
7
8
9
Nucleotide phosphate-binding region:ATP
Nucleotide-binding
ATP binding
Kinase
Transport
Signal peptide
Signal
Membrane
Signal
Cell outer membrane
Pyruvate metabolism
Microbial metabolism in diverse environments
Propanoate metabolism
Carbon metabolism
Cytosolic large ribosomal subunit
Ribosome
Structural constituent of ribosome
Ribosomal protein
Ribonucleoprotein
Translation
Pyridoxal phosphate-dependent transferase
Pyridoxal phosphate-dependent transferase, major region, subdomain 1
Pyridoxal phosphate
Pyridoxal phosphate binding
Lipid metabolism
Fatty acid metabolism

B

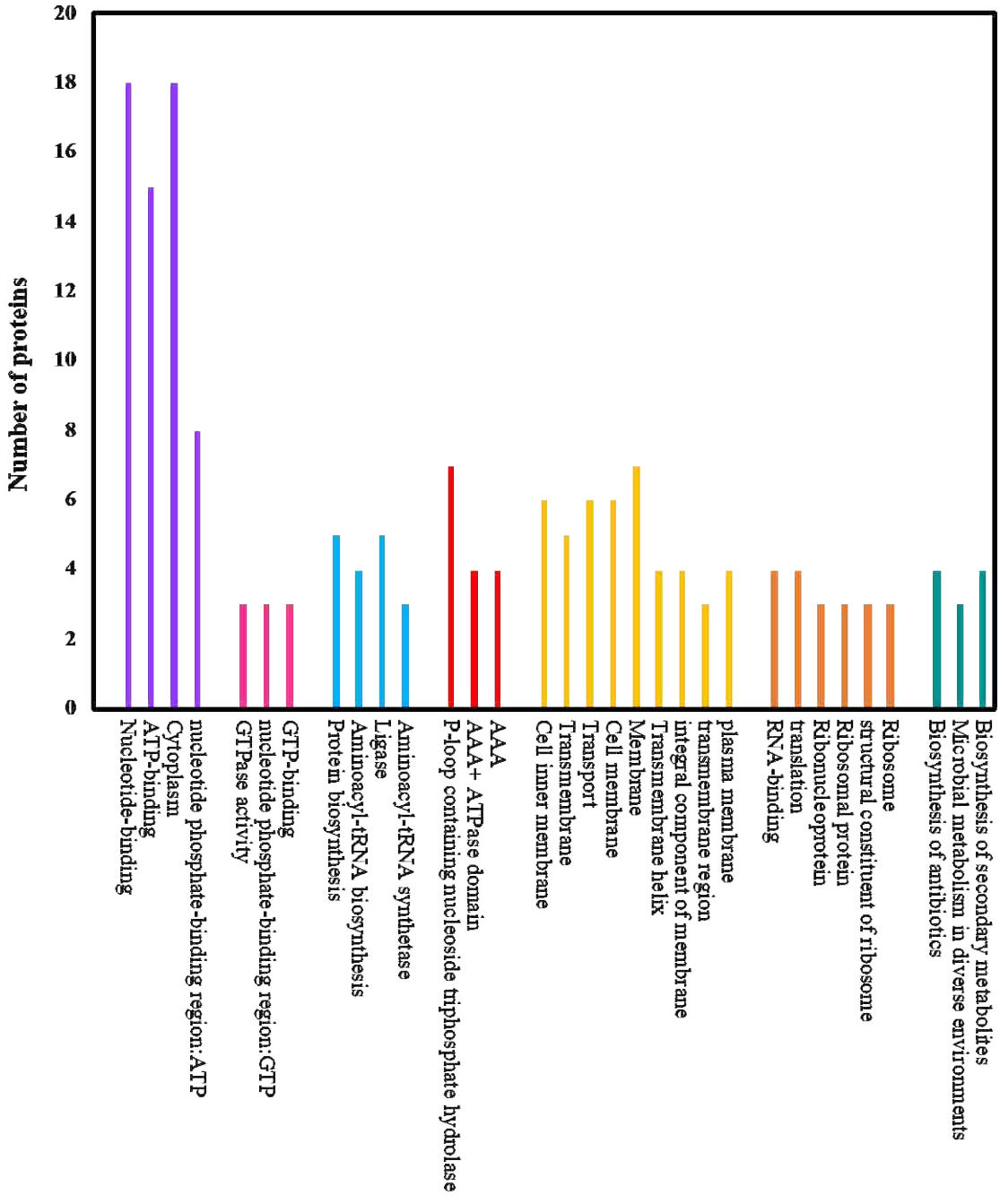

Figure 4-4: Functionally similar proteins (colored groups) among the most significantly (≥2 fold changes, $p < 0.05$) upregulated (A) and downregulated (B) proteins of chlorhexidine-resistant *P. aeruginosa* against wild type. Each bar within the colored group represents a different functional connection between proteins within that group.

4.3.3.1 Modifications in membrane proteins following exposure to chlorhexidine

Due to the positive charge on chlorhexidine, its initial interactions with Gram-negative bacteria are thought to occur at negatively-charged regions of LPS. Further, reduced susceptibility to chlorhexidine has been previously reported in association with modifications in the cell membrane, including modifications to LPS [181,190]. LPS modifications that have been associated with decreased bacterial susceptibility to cationic agents, such as chlorhexidine, include charge-reducing modifications in LPS and size reduction of the O-antigen polymer [190].

In this study, several changes in the expression of proteins associated with the cell membrane were noted following chlorhexidine exposure. As shown in Table 2, OprF was one of the most highly upregulated proteins in our study. OprF is a multifunctional protein that helps maintain cell shape, interacts with peptidoglycan layers, and is associated with forming non-specific channels for passive diffusion of ions, small polar nutrients and antibiotics [191,192]. It has been shown that inactivated OprF decreases virulence and increases outer membrane vesicle formation in *P. aeruginosa* [193]. Additional work has been done on the role of OprF in modifying quorum sensing and promoting virulence factor production in *P. aeruginosa*. Loss of functioning OprF was accompanied by loss of quorum sensing network activity and virulence factor production [194].

Protein network analysis (Figure 4-5) showed that the relative increase in OprF is accompanied by an increase in LptD concentration, a protein involved in the assembly of LPS for OM biogenesis. Mutant, non-functional LptD in *P. aeruginosa* increases the permeability of the outer membrane and results in compromised barrier function [195]. Therefore, upregulation of LptD in our data suggests that exposure to chlorhexidine decreases the permeability of the OM in *P. aeruginosa.*

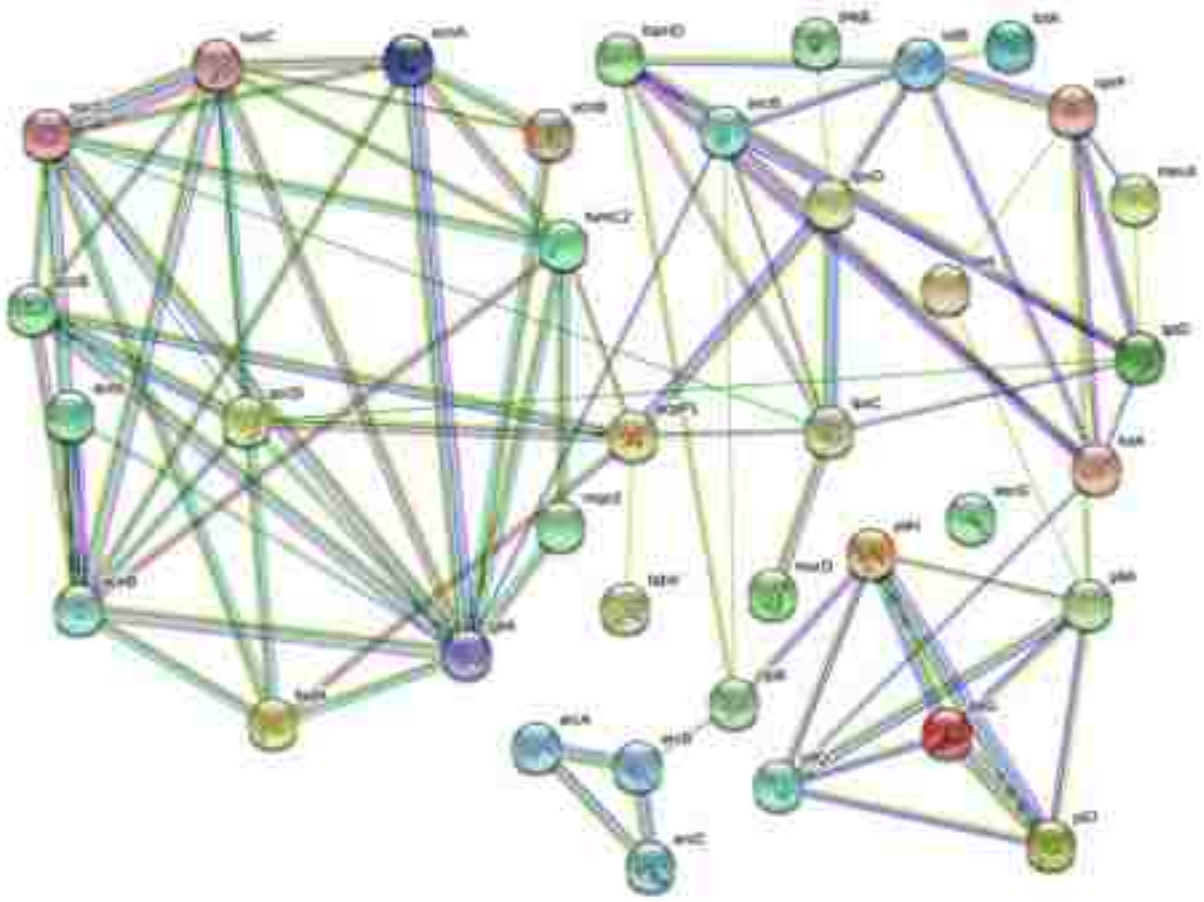

Figure 4-5: The most significantly upregulated proteins in chlorhexidine-resistant *P. aeruginosa* are highly interconnected. The connections between OprF to LptD, TolB, OprI, and LolA suggests that LPS production may be significantly changed (relevant proteins are in the top right corner.)

OprF also is connected to TolB (Figure 4-5), part of the Tol-Pal system, which contributes to the biogenesis of the OM and plays a key role in maintaining OM integrity. A significant upregulation of TolA, another part of Tol-Pal system, was also observed upon exposure of the cells to chlorhexidine in our proteomics data. Biochemical studies have identified interactions between TolA and OM porins [196], which are consistent with our results where both TolA and OM porin F, OprF, are upregulated.

Studies have shown that mutant *tol* genes in *E. coli* increased susceptibility to antibiotics [197]. The absence of TolA in *E. coli* K-12 has been shown to cause a substantial reduction in the surface expression of O antigen (O7-specific) LPS and less lipid A-core oligosaccharide. Its absence is also correlated with attenuated growth rate and dramatic morphological changes [198]. In *tol* mutants of *Vibrio cholera*, filamentation has also been reported [199]. This observation is consistent with our morphological study in which treatment with chlorhexidine caused dramatic morphological changes and altered flagella protein regulation in the Gram-negative bacteria.

An increase in the expression of a ligase enzyme associated with peptidoglycan biosynthesis (MurD*)* was also observed. Upregulation of MurD may result in a protective modification by increasing the thickness or cross-linking the peptidoglycan layer, which subsequently reduces the efficacy of chlorhexidine by affecting its transportation. Mur enzymes have been an attractive target for the development of antibacterial inhibitors owing to the fact that these enzymes are highly conserved molecules specific to bacteria with a known structure and function. However, no Mur inhibitors are clinically used as antimicrobials [200].

Of note, a protein which increased with chlorhexidine resistance was PagL, a deacetylase which removes the R-3-hydroxymyristate at position 3 of lipid A. PagL is activated by the *phoP/phoQ* two-component system, a regulatory system controlling genes for virulence within *Salmonella* [201,202]. Though usually inhibited by 4-amino-4-deoxy-L-arabinose and phosphoethanolamine modifications of lipid A, PagL deacetylation of lipid A has been tied to increased polymyxin resistance in *Salmonella* strains lacking these modifications. In a later study, overexpression of a *pagL*-specific sRNA, Sr006, was shown to increase *pagL* mRNA, lipid A deacetylation, and polymyxin B resistance in *P. aeruginosa.* The same study also demonstrated that a *pagL* knockout resulted in decreased polymyxin B resistance [203]. Therefore, upregulation of

PagL in chlorhexidine-resistant *P. aeruginosa* indicates that the mechanism of action for resistance to chlorhexidine could be partly in common with that of polymyxins.

Interestingly, protein network analysis (Figure 4-5) suggested that PagL is connected to LpxD, a significantly upregulated protein which is involved in lipid A biosynthesis along with LpxC, another upregulated protein. Previous MALDI-TOF analysis of the lipid A extracted from RamA-overexpressing strains of *K. pneumoniae* revealed that RamA increases colistin/polymyxin resistance levels [204]. This increase was accomplished through RamA directly binding to lipid A biosynthesis genes such as *lpxC* causing lipid A structural modifications. However, no RamA overexpression was observed in our study. We also found several outer membrane lipoproteins including LolA, BamD and OprI upregulated following chlorhexidine exposure. These results suggest that the increased lipoprotein synthesis of BamD and OprI might be required for appropriate sorting of lipoproteins by carrier proteins, like LolA, to the outer membrane under certain stress conditions such as antibiotic exposure [205].

4.3.3.2 Altered chaperone protein regulation following exposure to chlorhexidine

The Clp chaperones and proteases are highly conserved proteins found across the prokaryotes, in the mitochondria of eukaryotes and the chloroplasts of plants. Previous studies showed that ClpB is a chaperone associated with resistance to high temperature in *E. coli*. Furthermore, inactivation of the *clpB* gene of *Leptospira interrogans* resulted in reduced virulence and attenuated the *in vitro* growth of the cells under stress conditions, suggesting that ClpB plays a major role in bacterial survival under stress conditions [206]. Upregulation of ClpB upon exposure to chlorhexidine was also observed in our study, confirming that ClpB is essential for stress tolerance against inducing factors like antimicrobial agents where proteins tend to unfold and aggregate. Clp

protease, a periplasmic chaperone protein, was also reported to be upregulated in biofilm upon chlorhexidine treatment [207].

One of the protein translocation systems through the inner membrane involves Sec proteins in a chaperone-based pathway where immature proteins are targeted to a Sec translocase such as SecG, SecE, and SecY using the chaperone SecB for transport across the inner membrane. Our data showed upregulation of SecG and SecB while SecA was downregulated. Previous reports showed that loss of function of SecG leads to a significant increase in membrane depolarization, hydroxyl radical formation and cell death in aminoglycoside-treated cells. The redox-responsive two-component system (Arc) was also shown to have an associated role [208]. Interestingly, our proteomics profile revealed the upregulation of ArcA, ArcB and ArcC that encode arginine deiminase, ornithine carbamyltransferase and carbamate kinase, respectively. The Arc two-component system contains ArcB, a quinone-sensitive sensor kinase that controls the redox state of the cellular quinone pool via modulating the phosphorylation state of the transcription factor ArcA [208,209].

4.3.3.3 Efflux pump activity following exposure to chlorhexidine

A previous proteomics study correlated an increase in the expression of MexCD-OprJ efflux systems with a reduction in susceptibility to ciprofloxacin in *P. aeruginosa* [189]. Additionally, the transcriptome of *P. aeruginosa* revealed that MexCD-OprJ efflux pump was significantly upregulated after treatment with chlorhexidine [210]. Another study showed that increased expression of SmvA, an efflux pump of the major facilitator superfamily (MFS), is associated with increased resistance to chlorhexidine in *K. pneumoniae* [211]. However, in our study, exposure to chlorhexidine did not increase the relative expression of SmvA or Mexcd-Oprj efflux systems.

Although we did not find upregulation of SmvA or Mexcd-Opri, we found that multidrug resistance protein MexA was significantly upregulated. MexA functions as the periplasmic linker component of the MexAB-OprM efflux system that confers multidrug resistance, possibly indicating that this system plays a role in chlorhexidine response. Conversely, other research has shown that the overexpression of efflux pumps does not impact the antimicrobial efficacy of chlorhexidine, and it has been proposed that this is largely due to the limited solubility of chlorhexidine in the bacterial membrane core [212].

4.3.3.4 General cell metabolism following exposure to chlorhexidine

Proteomic platform analysis showed that many proteins associated with energy metabolism and many enzymes associated with glycolysis, fatty acid biosynthesis, and the TCA cycle were upregulated in the resistant strain. For example, upregulation of AceE and AceF, two enzymes involved in the conversion of pyruvate to acetyl-CoA and CO_2, was observed. In addition, proteins associated with acetyl-CoA carboxylase such as AccD and AccB were also upregulated. These proteins are involved in the first step of the subpathway that synthesizes malonyl-CoA from acetyl-CoA. Furthermore, significant upregulation was observed in proteins FadA, FabV and AcpP1, which are all involved in lipid metabolism. FadA catalyzes the final step of fatty acid oxidation, in which acetyl-CoA is released. FabV catalyzes the reduction of a carbon-carbon double bond in an enoyl moiety that is covalently linked to Acp as an acyl carrier protein of the growing fatty acid chain. Consistent with our results, increased expression of several proteins associated with fatty acid synthesis, such as Acp, was also observed in biofilm of *Delftia acidovorans* following chlorhexidine exposure [208]. Finally, a substantial number of proteins associated with the TCA cycle were upregulated. Succinate-CoA ligase enzymes (SucC and SucD), fumarate hydratase (FumC1), malate:quinone oxidoreductase 2 (MqO2) and citrate synthase (GltA) were the upregulated

proteins related to the first step of the cycle. Aconitate hydratase enzymes (AcnA and AcnB) were the upregulated proteins involved in isocitrate synthesis.

The acquisition of antimicrobial resistance may be energetically costly for bacteria, and in a normal environment, high-energy expenditure lowers the general fitness of bacteria. Therefore, bacteria will usually only take on metabolic costs if environmental pressures, such as antibiotics, dictate its necessity [213]. The upregulation of metabolic proteins by *P. aeruginosa* shown in this study could be a result of the intrinsic linkage between bacterial metabolism and antibiotic resistance.

4.3.3.5 Altered flagella protein regulation in chlorhexidine resistant strain

Of interest in our proteomics data is the upregulation of Pil proteins (PilA, PilG, PilH, PilJ, PilQ) involved in fimbriae formation and motility. Formation of pili, or fimbriae, has been correlated with virulence in pathogens such as *P. aeruginosa*, *E. coli*, *A. baummanii*, *V. cholerae* and *Streptococcus* spp. Presence of pili enables bacteria to bind to a surface or tissue, which initiates interaction with the host and increases biofilm formation [213-215]. It has been previously reported that overexpression of flagellar genes is associated with increased tolerance to antimicrobial agents, including chlorhexidine, in *Salmonella*, which may now be extended to chlorhexidine tolerance in *Pseudomonas* [190,216,217]. Twitching motility is a bacterial movement on a solid surface that occurs in a wide variety of pathogens including *P. aeruginosa*. Twitching motility is mediated by a complex chemosensory pathway including PilG, PilH, PilI, PilJ and PilK and is also involved in biofilm formation [218,219]. The upregulated proteins identified in our study, including PilG, PilH and PilJ, suggest that exposure to chlorhexidine increased the twitching

motility which contributes to virulence and biofilm formation. It is known that type IV pili in *P. aeruginosa* are assembled from PilA, a single protein subunit, which is transferred out of the cell via outer membrane secretin PilQ to form fimbrial strands. The upregulation of PilA and PilQ suggests that the biosynthesis of pili, which is associated with adhesion and accumulation of *P. aeruginosa* on surfaces, increased in chlorhexidine-exposed bacteria [220]. Overall, the observed alterations in Pil proteins in our comparison of the proteomes of chlorhexidine-susceptible and resistant bacteria are associated with biofilm formation and virulence, suggesting that further investigation of biofilm formation in chlorhexidine-resistant bacteria would be a meaningful line of research.

Table 4-2: Identification, function and biological process of proteins differentially expressed between chlorhexidine-resistant and wild type *P. aeruginosa*.

	Accession No.	Protein	Function	Biological Process	Fold Change
1	P13794	Outer membrane porin F (OprF)	Porin activity, structural role in determining cell shape and growth in low osmolarity medium.	Adhesion of symbiont to host, ion transport, regulation of cell shapes.	62.38
2	Q9I5U2	LPS-assembly protein LptD (LptD)	Assemply of lipopolysaccharide at the surface of the outer membrane.	Gram-negative-bacterium-type cell outer membrane assembly, lipopolysaccharide export, response to organic substance.	7.83
3	P50601	Tol-Pal system protein TolB (TolB)	Maintains outer membrane integrity during outer membrane invagination of cell division.	Cell cycle, cell division, protein import.	15.36
4	P50600	Tol-Pal system protein TolA (TolA)	Role in outer membrane invagination during cell division, maintains outer	Bacteriocin transport, cell cycle, cell division.	285.55

			membrane integrity.		
5	Q9HVZ9	UDP-N-acetylmuramoyl alanine—D-glutamate ligase (MurD)	Cell wall formation, catalyzes addition of glutamate to UDP-N-acetylmuramoyl-L-alanine (UMA).	Cell cycle, cell division, cell wall organization, peptidoglycan biosynthetic process, regulation of cell shape.	3.63
6	Q9HVD1	Lipid A deacylase PagL (PagL)	Has 3-O-deacylase activity, hydrolyzes ester bond at the 3 position of lipid A.	Lipid A metabolic process, lipopolysaccharide metabolic process.	Large Positive
7	Q9HXY6	UDP-3-O-acylglucosamine N-acyltransferase (LpxD)	Catalyzes N-acylation of UDP-3-O-acylglucosamine with 3-hydroxyacyl-ACP as the acyl donor.	Lipid A biosynthetic process.	Large Positive
8	P47205	UDP-3-O-acyl-N-acetylglucosamine deacetylase (LpxC)	Catalyzes hydrolysis of UDP-3-O-myristoyl-N-acetylglucosamine	Lipid A biosynthetic process.	108.97

			to UDP-3-O-myristoylglucosamine and acetate.		
9	Q9I0M4	Outer-membrane lipoprotein carrier protein (LolA)	Transports lipoproteins from inner membrane to outer membrane.	Chaperone-mediated protein transport across periplasmic space, lipoprotein localization to outer membrane.	Large Positive
10	P33641	Outer membrane protein assembly factor BamD (BamD)	Assembly and insertion of beta-barrel proteins to the outer membrane.	Cell envelope organization, protein insertion into membrane.	58.42
11	P11221	Major outer membrane lipoprotein (OprI)	***	***	973.45
12	Q9HVN5	Chaperone protein ClpB (ClpB)	Stress-induced multi-chaperone system involved in recovery from heat induced damage.	Protein metabolic process, protein refolding, response to heat.	152.40
13	Q9HV52	Protein-export membrane protein SecG (SecG)	Participates in protein export by sequence similarity.	Intracellular protein transmembrane transport, protein secretion, protein transport by the Sec complex.	Large Positive

14	Q9HU56	Protein-export protein SecB (SecB)	Molecular chaperone that binds precursor proteins and maintains them in a translocation-competent state. Binds receptor SecA.	Protein tetramerization, protein transport.	Large Positive
15	Q9LCT3	Protein translocase subunit SecA (SecA)	Sec protein translocase complex, couples hydrolysis of ATP to protein transfer, SecB receptor.	Protein import, protein targeting, protein transport by the Sec complex.	0.84
16	P13981	Arginine deiminase (ArcA)	Conversion of L-arginine to L-citrulline.	Arginine catabolic process to ornithine, arginine deiminase pathway.	70.59
17	P08308	Ornithine carbamoyltransferase, catabolic (ArcB)	Catalyzes phosphorolysis of citrulline in catabolism of arginine.	Arginine biosynthetic process via ornithine, arginine catabolic process to ornithine, arginine deiminase pathway, urea cycle.	650.66
18	P13982	Carbamate kinase (ArcC)	Synthesizes CO_2 and NH_3 from	Arginine deiminase pathway, carbamoyl	290.09

			carbamoyl phosphate.	phosphate catabolic process.	
19	P52477	Multidrug resistance protein MexA (MexA)	Periplasmic linker of MexAV-OprM efflux system, efflux pump for n-hexane and p-xylene efflux.	Protein homooligomerization, response to antibiotic.	35.89
20	Q59637	Pyruvate dehydrogenase E1 component (AceE)	Catalyzes conversion of pyruvate to acetyl-CoA and CO_2.	Glycolytic process.	3014.55
21	Q59638	Dihydrolipoyllysine-residue acetyltransferase component of pyruvate dehydrogenase complex (AceF)	Catalyzes acetyl-CoA and enzyme N_6-(dihydrolipoyl)lysine to CoA and enzyme N_6-(S-acetyldihydrolipoyl)lysine.	Glycolytic process.	40.67
22	Q9HZA7	Acetyl-coenzyme A carboxylase carboxyl transferase subunit beta (AccD)	Synthesizes malonyl-Coa from acetyl-CoA.	Fatty acid biosynthetic process, malonyl-CoA biosynthetic process.	129.73

23	P37799	Biotin carboxyl carrier protein of acetyl-CoA carboxylase (AccB)	Facilitates transfer of the carboxyl group to form malonyl-CoA in fatty acid biosynthesis.	Fatty acid biosynthetic process.	180.37
24	Q9HZJ3	3-ketoacyl-CoA thiolase (FadA)	Catalyzes the final step of fatty acid oxidation (in which acetyl-CoA is released).	Fatty acid beta-oxidation.	Large Positive
25	Q9HZP8	Enoyl-[acyl-carrier-protein] reductase [NADH] (FabV)	Catalyzes the reduction of a carbon-carbon double bond in the final reduction of the elongation cycle of fatty acid synthesis (FAS II).	Fatty acid biosynthetic process.	87.20
26	O54439	Acyl carrier protein 1 (AcpP1)	Fatty acid chain carrier.	Lipid A biosynthetic process.	46.21
27	P53593	Succinate—CoA ligase [ADP-forming] subunit beta (sucC)	Provides succinate binding specificity in the coupling of hydrolysis of	Nucleoside triphosphate biosynthetic process, protein autophosphorylation, tricarboxylic acid cycle.	1522.01

			succinyl-CoA with synthesis of ATP or GTP in TCA cycle.		
28	Q51567	Succinate—CoA ligase [ADP-forming] subunit alpha (SucD)	Provides coenzyme A and phosphate binding specificity in the coupling of hydrolysis of succinyl-CoA with synthesis of ATP or GTP in TCA cycle.	Nucleoside triphosphate biosynthetic process, tricarboxylic acid cycle.	44.3522
29	Q9I587	Fumarate hydratase class II 1 (FumC1)	Catalyzes the stereospecific interconversion of fumarate to L-malate.	Fumarate metabolic process, malate metabolic process, tricarboxylic acid cycle.	68.94
30	Q9HVF1	Probable malate:quinone oxidoreductase 2 (Mqo2)	Catalyzes the redox reaction between (S)-malate and a quinone to form oxaloacetate and a reduced quinone.	Ethanol oxidation, tricarboxylic acid cycle.	923.77

31	P14165	Citrate Synthase (GltA)	Catalyzes the formation of citrate (and CoA) from oxaloacetate and acetyl-CoA.	Tricarboxylic acid cycle.	316.01
32	Q9I3F5	Aconitate hydratase A (AcnA)	Catabolism of short chain fatty acids via TCA cycle, 2-methylcitrate cycle I, catalyzes isomerization of citrate to isocitrate.	Anaerobic respiration, propionate metabolic process (methylcitrate cycle), response to oxidative stress, tricarboxylic acid cycle.	40.00
33	Q9I2V5	Aconitate hydratase B (AcnB)	Catabolism of SCFAs via TCA cycle, 2-methylcitrate cycle I, isomerization of citrate to isocitrate, hydration of 2-methyl-cis-aconitate to (2R,3S)-2-methylisocitrate.	Propionate catabolic process (2-methylcitrate cycle), tricarboxylic acid cycle.	1161.97

34	P04739	Fimbrial protein (PilA)	Assembles type IV pili.	Cell adhesion involved in single-species biofilm formation, pathogenesis, regulation of calcium-mediated signaling, single-species biofilm formation on inanimate substrate, type IV pilus-dependent motility.	105.67
35	P46384	Protein PilG (PilG)	Pilus biosynthesis and twitching motility, receives environmental signals and transduces them to pilus assembly machinery.	Phosphorelay signal transduction system.	46.57
36	P43501	Protein PilH (PilH)	Member of the signal transduction system that regulates twitch motility and pilus function.	Phosphorelay signal transduction system.	81.69
37	P42257	Protein PilJ (PilJ)	Member of the signal transduction system that	Chemotaxis.	182.73

			regulates twitch motility and pilus function.		
38	P34750	Fimbrial assembly protein PilQ (PilQ)	Biogenesis and secretion of type IV fimbiae, essential for formation of pili.	Protein secretion, type IV pilus biogenesis.	Large Positive

4.4 Conclusion

We have demonstrated that prolonged exposure of Gram-negative bacteria to chlorhexidine results in significantly reduced susceptibility to colistin but not to AMPs and ceragenins. This suggests that there may be a specific mechanism for resistance of Gram-negative bacteria to chlorhexidine that causes even higher resistance to colistin but does not affect susceptibility to AMPs and ceragenins. These observations are consistent with the reported decrease in susceptibility of chlorhexidine-resistant *K. pneumoniae* to colistin [211]. The fact that lead ceragenins (CSA-44 and CSA-131) retain bactericidal activity against highly colistin and chlorhexidine resistant bacteria is further support for the development of these compounds as broad-spectrum antibacterial agents to potentially be used in multiple clinical applications.

To understand the changes to Gram-negative bacteria that lead to chlorhexidine and colistin resistance but do not impact AMPs and ceragenins, an in-depth quantitative proteomic study was performed with a parent strain of *P. aeruginosa* and its chlorhexidine-resistant progeny. It is likely that proteins involved in resistance to chlorhexidine function similarly in other Gram-negative bacteria. Our study suggests that increased expression of membrane proteins such as OprF, LptD,

and the Tol-Pal system is responsible for chlorhexidine resistance, but this is not the only pathway contributing to resistance. For example, chlorhexidine resistance is also associated with upregulation of PagL, which is affected by the two-component regulatory system *phoP/phoQ*. Additionally, upregulation of flagella proteins, chaperones and proteins associated with energy metabolism were also observed in the chlorhexidine-resistance pathway. Upregulation of some of these proteins also correlates with colistin resistance. Co-resistance with colistin suggests that LPS modification along with changes in expression of associated membrane proteins could be involved in the primary mechanism of chlorhexidine resistance. The fact that exposure of Gram-negative bacteria to chlorhexidine may lead to colistin resistance and possible drug resistance among Gram-positive organisms suggests that wide-spread use of chlorhexidine should be reconsidered. In order to decrease the speculated effect of chlorhexidine on the development of colistin-resistant strains, application of other antimicrobials such as ceragenins could be a safe choice considering its lower risk of cross-resistance.

Chapter 5 Ceragenins are active against drug-resistant *Candida auris* clinical isolates in planktonic and biofilm forms

5.1 Introduction

Candida auris has emerged as a global threat; from the initial report from in Japan in 2009, it has spread and been isolated on five continents [221-223]. *C. auris* can be a substantial cause of nosocomial infections in some settings and associated with high levels of mortality [224,225]. Of particular concern is the drug resistance found among many isolates. Resistance to azole antifungal agents with clinical isolates is common, and resistance of some strains of *C. auris* to all three classes of commonly used antifungals (azoles, polyenes and echinocandins) has been observed [226,227]. The emergence of this pathogen has led to efforts to better track and characterize infections [228], and it provides a strong impetus for the development of novel antifungal agents active against drug-resistant organisms [229].

Higher organisms have faced threats from fungal pathogens for hundreds of millions of years, and evolutionary pressures have yielded antifungal innate-immune functions effective against organisms in both planktonic and biofilm forms. Antimicrobial peptides (AMPs) constitute a key component of these innate-immune defenses, and AMPs from a variety of sources have shown potent antifungal activities [230,231]. The prevalence of AMPs, in organisms ranging from mammals to amphibians to insects to plants, suggests that AMPs retain antimicrobial activities over extended periods without generation of widespread resistance. Recognizing the antifungal activities of AMPs and their anticipated retention of potency with extensive use, substantial efforts have been made to develop antifungal AMPs for clinical use [231]. Impediments to clinical use include the

relative high cost of large-scale preparation of peptide therapeutics as compared to small molecules and the instability of linear peptides in the presence of ubiquitous proteases.

Recently, antifungal activities of selected ceragenins were reported [82], with MICs of ceragenins comparable to or below those measured with amphotericin B, fluconazole and AMPs omiganan and LL-37 with multiple strains of *Candida albicans*. Fungi in the genera of *Paecilomyces*, *Cryptococcus*, *Aspergillus*, *Scedosporium*, *Rhizopus*, *Blastomyces* and *Apophysomyces* also proved susceptible to the ceragenins tested. Atomic force microscopy images of *C. albicans* untreated and treated with ceragenin CSA-13 showed changes in surface morphology of cells treated with the ceragenin, which were interpreted as showing membrane activity. Studies of mechanisms of antifungal activities of AMPs have concluded that membrane perturbation plays a key role [83,232], while increases in damage by reactive oxygen species (ROS) and attenuation of mitochondrial functions, leading to apoptosis, have been observed [84,86,233]. In a recent study, magnetic nanoparticles adorned with either the AMP LL-37 or CSA-13 resulted in generation of ROS in *Candida* spp [87].

Considering the need for novel antifungal agents in the face of the growing threat of *C. auris* infection, our objectives in the studies described herein were to determine the antifungal activity of selected ceragenins against isolates of *C. auris* collected by CDC and to compare these activities with those of representatives of the three major classes of antifungal agents. Activities measured included both MICs and minimum fungicidal concentrations (MFCs) on planktonic organisms. Because fungi may grow in sessile form in biofilms, we also measured the activities of selected ceragenins against established biofilm forms of *C. auris*. To better understand the antifungal activities of ceragenins, SEM images of *C. auris*, with and without ceragenin treatment, were acquired. Although ceragenins are well tolerated in a variety of routes of administration

[119,120,122,132], topical application to skin or mucosal tissues to treat fungal infections represents an attractive use of the antimicrobials. To determine the potential for use in this venue, different formulations of ceragenins CSA-44 and CSA-131 were evaluated in an *ex vivo* vaginal porcine mucosal tissue model infected with *C. albicans* or *C. auris* and compared to nystatin or a commercial cream containing miconazole.

5.2 Materials and methods

5.2.1 Materials and fungal strains

CDC (Atlanta, GA) has catalogued over 100 clinical isolates of *C. auris* for use in determining susceptibility patterns, and these were used in initial studies with ceragenin CSA-131. These isolates represent all four of the known clades of *C. auris* and originated from various countries. These isolates were characterized as susceptible or resistant to fluconazole and echinocandins based on the MICs published by CDC (https://www.cdc.gov/fungal/diseases/candidiasis/recommendations.html), although *C. auris*-specific breakpoints have not yet been established. Ten additional isolates of *C. auris* and one strain of *C. albicans* (ATCC 90028, Manassas, VA) were used to further characterize susceptibility to other ceragenins. Three antifungal drugs belonging to the three main classes of commonly used antifungal compounds including amphotericin B (Fisher Scientific, Pittsburgh, PA), fluconazole and caspofungin (Sigma-Aldrich, St. Louis, MO, USA) were used in comparison. The culture media used included Sabouraud dextrose broth (SDB) or agar (SDA) and 1640-RPMI (Sigma-Aldrich, St. Louis, MO, USA) buffered at pH 7.0 with 165 m*M* of MOPS (Sigma-Aldrich, St. Louis, MO, USA). Published protocols for growth of *Candida* spp. have used either SDB or RPMI [234-236], and to observe any medium-dependent changes in susceptibility, MICs and MFCs were measured in both media.

5.2.2 Determination of susceptibility profiles of planktonic fungi

MICs of the *C. auris* strains were measured according to the broth microdilution protocol from the Clinical and Laboratory Standards Institute M27-A3 document [237]. With the entire CDC collection, RMPI medium was used in the measurement; inocula of 0.5 to 2.5 x 10^3 CFU/mL were prepared and used to seed pre-prepared drug plates containing CSA-131. These plates were incubated at 35 °C and read after 24 hours. With the smaller collection (10 isolates), two different media, SDB and RPMI, were used to evaluate the antifungal activity of all four classes of antifungal compounds used in this study. MFCs were determined by plating 10 µL from each well of the MIC plate (after 24 h incubation) on SDA plates and measuring the lowest concentration of the antibiotic which eliminated 99.9% (three-log reduction) of the colonies formed on the plates after 48 h of incubation at 35 °C [238].

5.2.3 Determination of susceptibility profiles of fungal biofilms

To quantify the biofilm formed by clinical isolates of *C. auris* and determine the sessile susceptibility profile of ceragenins, metabolic activity within biofilms was imaged using 2,3-bis-(2-methoxy-4-nitro-5-sulfophenyl)-2H-tetrazolium-5-carboxanilide (XTT) as described by Moss *et al* [236]. In this assay, metabolic activity of cells in the biofilm is measured based on their reduction of XTT. Initially, biofilms were formed in a sterilized polystyrene flat-bottomed 96-well microtiter plates (Sarstedt, USA) incubated at 35 °C for 48 h and washed three times with PBS to remove planktonic cells. Ceragenins were then added to the wells in a concentration range of 1-128 µg/mL and incubated for 24 h. A 10 m*M* menadione (Sigma-Aldrich, St. Louis, MO, USA) solution was prepared in 100% acetone and added to an XTT solution (0.5 mg/mL) to achieve a final concentration of 1 µM menadione. Aliquots of the XTT/menadione solution (100 µL) were added to each well containing biofilm and negative control wells. Plates were wrapped

in aluminum foil and incubated at 37 °C for 2 h. Aliquots of the supernatant (70 µL) were removed from each well and the optical density was measured at 490 nm using a microtiter plate reader. Corresponding optical density values for each strain were subtracted from the negative control values to calculate sessile minimum inhibitory concentrations (SMICs). The $SMIC_{50}$ and $SMIC_{80}$ represent the concentration of the drug where the absorbance of the biofilm decreased by 50% or by 80%, respectively, compared to the biofilm formed by the same strain in the absence of the drug. Results are from three independent experiments.

5.2.4 Scanning electron microscopy of C. auris

To observe the effect of ceragenins on cell membranes, *C. auris* CDC 390 was cultured to mid-log phase and washed three times with PBS. Fungi were re-suspended in PBS (OD_{600}=0.2). CSA-131 (25 or 50 µg/mL) was added and the mixtures were incubated at 37 °C for 1 h. A control was prepared by incubating the fungal suspension without adding CSA-131. SEM sample preparation was performed as described in detail in section 3.2.5.

5.2.5 Confocal laser scanning microscopy

To observe the effects of treatment of fungal biofilms with CSA-131, aliquots (300 µL) of *C. albicans* and *C. auris* CDC383 (10^6 CFU/mL) were placed into separate single wells in a Lab-Tek® Chamber Slide™ (Nunc, Inc., Naperville, IL, USA) and incubated for 48 h. The biofilms were treated with CSA-131 (50 µL of a 50 µg/mL solution) and incubated for 24 h at 35 °C. After incubation, the solution was carefully removed, and the wells were washed three times with PBS. Biofilms were stained with BacLight Live/Dead Viability Kit (L13152, Molecular Probes, Inc) according to the manufacturer's instructions, and observed at 60x magnification using a confocal laser scanning microscope (Olympus FluoView FV1000).

5.2.6 Assays in *ex vivo* tissue

Ex vivo experiments were performed using porcine vaginal mucosal explants as previously described [235]. Normal healthy porcine vaginal tissue was excised from animals at slaughter (Theurer's Quality Meats, Lewiston, UT) and transported to the laboratory on ice. Tissue was trimmed and collected in RPMI 1640 media supplemented with penicillin (50 IU/mL, MP Biomedicals, Solon, OH) and streptomycin (50IU/mL, MP Biomedicals, Solon, OH). Antibiotics were included to decolonize normal flora, which may interfere with biofilm formation. Explants of uniform size were obtained using a 5 mm biopsy punch. Excess muscle was trimmed away with a scalpel. After antibiotic washout (3 changes of RPMI 1640 media followed by 30 min incubation at 37 °C), explants were transferred mucosal side up onto a PET 0.4 μm cell culture insert (BD Falcon, Franklin Lakes, New Jersey) and inoculated with 2 μL (10^5 CFU/explant) of *C. auris* (CDC 390) or *C. albicans* (ATCC 90028) prepared from overnight cultures in Todd Hewitt Broth. Following 2 h and 24 h incubation at 37 °C, explants (n=3) were treated with CSA-44L or CSA-131L (100 μL, 0.5% active) or CSA-44H and CSA-131H (2% active) in a HEC gel formulation and subsequently incubated for 24 h at 37 °C. For studies of cream formulations, aliquots of the test articles (100 μL) were spread evenly over explants. Tissues were suspended in a neutralizing broth (250 μL, Dey/Engley (HiMedia Laboratories, West Chester, Pennsylvania)), vortex mixed (highest setting for 4 m), and then serially diluted in PBS (Sigma, St. Louis, MO) and plated or plated neat. Samples were spread on Tryptic Soy Agar containing 5% sheep blood (BD Falcon, Franklin Lakes, New Jersey) using a spiral plater (Microbiology International, Frederick, MD) then incubated for 24 h at 37°C.

5.2.7 Statistical analysis

Analysis of variance (ANOVA) were performed by Dunnett's multiple comparison posttest using the GraphPad PRISM software (GraphPad Software, Inc., La Jolla, CA).

5.3 Results and discussion

5.3.1 Susceptibility of planktonic fungi to ceragenins

The susceptibilities of 100 clinical isolates to a lead ceragenin, CSA-131, were determined, and the distribution of CSA-131 MIC values ranged from 0.5-1 μg/mL (Table 5-1). The overall mode was 1 μg/mL and both the MIC_{50} and the MIC_{90} were 1 μg/mL. CSA-131 showed activity against all four clades of *C. auris* with no variation in activity between the clades. There was no loss in activity for those isolates which were previously determined to be resistant to fluconazole and/or an echinocandin.

Table 5-1: MICs of CSA-131 with fluconazole-resistant, fluconazole-susceptible and echinocandin-resistant *C. auris* isolates

C. auris Isolate	No. Isolates	Range	Mode	MIC_{50} (μg/mL)	MIC_{90} (μg/mL)
fluconazole-susceptible	30	0.5 - 1.0	N/A	0.5	1.0
fluconazole-resistant	70	0.5 - 1.0	1.0	1.0	1.0
echinocandin-resistant	7	0.5 - 1.0	1.0	1.0	1.0

To verify that other lead ceragenins also demonstrated activity against *C. auris*, studies were performed with a smaller collection of isolates and activities were compared to those with a strain of *C. albicans*. Both MICs and MFCs were measured in SDB or RMPI with CSA-44, CSA-131, CSA-142, CSA-144 and representatives of the three major classes of antifungal agents. As

observed with the larger collection of *C. auris* isolates, MICs of CSA-131 were either 0.5 or 1.0 μg/mL, and they were similar with CSA-44 and CSA-144 (Table 5-2). MICs were relatively higher with CSA-142. The strains tested gave relatively high MICs with fluconazole, and one of the strains (CDC383) showed resistance to caspofungin. As compared to caspofungin, amphotericin B and fluconazole, the ceragenins gave lower MFCs, suggesting greater fungicidal activity as compared to these other antifungal agents. Among the representative antifungal agents, caspofungin is the most closely related to ceragenins; it is a cationic molecule appended with a lipid chain. Similarly, ceragenins are cationic, and a lipid chain is required for activity. Nevertheless, caspofungin-resistant *C. auris* strains (e.g., CDC383) were fully susceptible to ceragenins. In general, the medium in which MICs and MFCs were determined did not play a substantial role; with many antifungal agents and organisms, MICs were identical in both media, as were MFCs.

Table 5-2: Comparison of the susceptibility (µg/mL) of clinical isolates of *C. auris* to selected ceragenins and three major classes of antifungal agents in SDB and RPMI.

Strains	CSA-44 SDB (RPMI)	CSA-131 SDB (RPMI)	CSA-142 SDB (RPMI)	CSA-144 SDB (RPMI)	CPF SDB (RPMI)	AMB SDB (RPMI)	FLZ SDB (RPMI)
***C. auris* CDC381**	0.5 [2.0]*	0.5 [8.0]*	4.0 [32]*	0.5 [2.0] (1.0 [8.0])	2.0 [64]*	1.0 [48] (1.0 [64])	16 [>100] (32 [>100])
***C. auris* CDC382**	0.5 [4.0]*	0.5 [8.0]*	4.0 [24]*	1.0 [8.0]*	nm	nm	nm
***C. auris* CDC 383**	0.5 [8.0] (0.5 [16])	1.0 [10] (0.5 [8.0])	2.0 [64]*	1.0 [8]*	32.0 [64] (16 [48])	1.0 [32] (1.0 [64])	64[>100] (>100 [>100])
***C. auris* CDC384**	0.5 [4.0]*	0.5 [4.0]*	4.0 [24]*	1.0 [8.0]*	nm	nm	nm
***C. auris* CDC385**	0.5 [16]*	0.5 [4.0]*	8.0 [32]*	1.0 [8.0]*	nm	nm	nm
***C. auris* CDC386**	0.5 [8.0]*	1.0 [8.0] (0.5 [8.0])	4.0 [32]*	0.5 [8.0] (1.0 [16])	2.0 [64]*	2.0 [48] (1.0 [64])	64[>100] (>100[>100])
***C. auris* CDC387**	0.5 [8.0]*	0.5 [8.0]*	4.0 [32]*	0.5 [8]*	nm	nm	nm
***C. auris* CDC388**	1.0 [8.0]*	0.5 [4.0]*	4.0 [24]*	2.0 [8.0]*	nm	nm	nm
***C. auris* CDC389**	0.5 [8.0]*	0.5 [8.0]*	4.0 [24]*	1.0 [8.0]*	nm	nm	nm
***C. auris* CDC390**	0.5 [8.0] (1.0 [32])	0.5 [4.0] (0.5 [8.0])	4.0 [16]*	1.0 [8.0]*	2.0 [100]*	4.0[64]*	64 [>100] (>100 [>100])
***C. albicans* ATCC 90028**	0.5 [8.0] (0.5 [16])	0.5 [4.0] (0.5 [8.0])	2.0 [8.0]*	2.0 [8.0]*	2.0 [32] (1.0 [8.0])	2.0 [100] (2.0 [64])	24 [>100] (32 [>100])

CPF: caspofungin, AMB: amphotericin B, FLZ: fluconazole
nm: not measured
*Same result in both media.

5.3.2 SEM of ceragenin-treated fungi

As described above, membrane disruption has been identified as a major mechanism of antifungal activity of AMPs [232,239], among other possible mechanisms. Changes in cell morphology upon treatment with AMPs have been attributed to membrane interactions, these include loss of smooth cell surfaces with marked invagination at high AMP concentrations. Similar

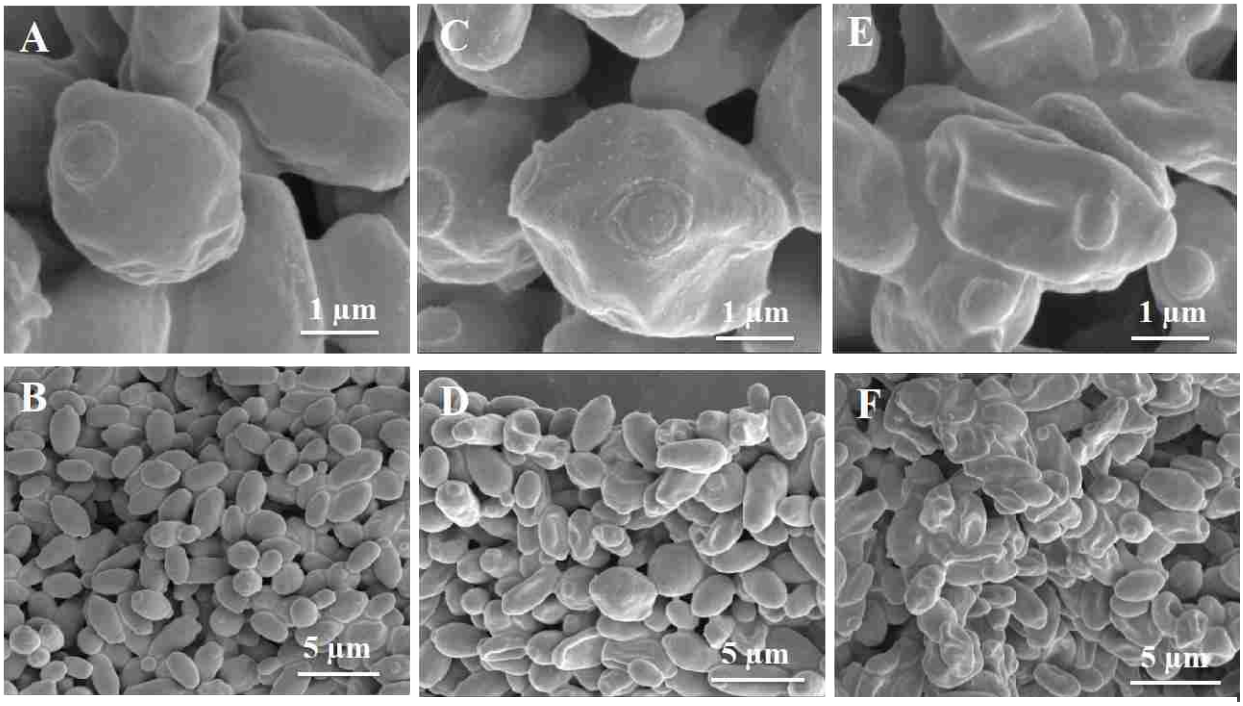

Figure 5-1: Scanning electron photomicrograph of untreated *C. auris* CDC390 (A and B) and treated with CSA-131 25 µg/mL (C and D) and 50 µg/mL (E and F).

morphological changes in *C. albicans* were observed with the human AMP LL-37 and the ceragenin CSA-13 [82]. The impacts of CSA-131 on the morphology of *C. auris* are shown in Figure 5-1. As with *C. albicans* treated with LL-37 or CSA-13, CSA-131 alters cell shape; at 50 µg/mL CSA-131 causes cells to buckle in upon themselves and some cells appear to have merged. These changes in cell morphology were observed at concentrations well above MFCs, and antifungal activity may be due to more subtle changes in cell permeability at lower concentrations of the ceragenin. At MFCs, little or no morphological changes in fungal cells are apparent.

5.3.3 Susceptibility of fungal biofilms to ceragenins

The abilities of bacteria and fungi to form biofilms, in which sessile organisms reside, contribute to drug resistance and protection of persister organisms that provide sources for chronic infections. The abilities of *C. albicans* to form biofilm are well established [240-243]; however, differing results for biofilm-forming propensities of *C. auris* have been reported [244,245]. Using a

measure of metabolic activity, we compared biofilm forming properties of a *C. albicans* reference strain to those of four isolates of *C. auris* (CDC 381, CDC-383, CDC 386 and CDC 390). Biofilms were grown under identical conditions, and as reported [246], *C. auris* strains were less efficient than the *C. albicans* strain at biofilm formation. Using the XTT-based assay, metabolic activity of the *C. auris* biofilms was measured as approximately 50% of that of *C. albicans* (Figure 5-2).

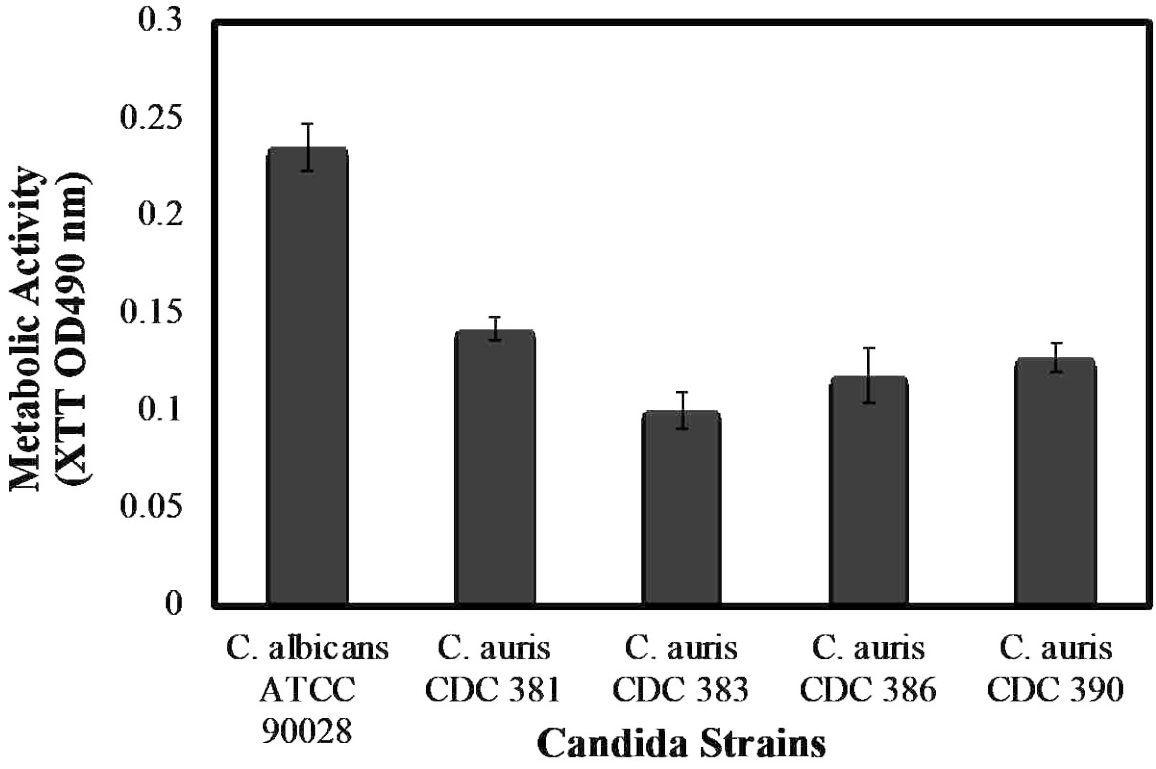

Figure 5-2: Biofilm formation by four selected strains of *C. auris* compared to *C. albicans* (ATCC 90028) at 48 h.

Having established the biofilm-forming characteristics of *C. auris* isolates, we used metabolic activity of biofilms to determine the activities of representative ceragenins and antifungals against sessile organisms making up these biofilms. Concentrations necessary to reduce biofilms by 50 and 80% are shown in Table 5-3. The ceragenins, amphotericin B and caspofungin demonstrated strong activity against the biofilms, while fluconazole was much less active. Because fluconazole

was weakly active against these organism in planktonic form, it is not surprising that biofilms were less susceptible to this antifungal as compared to others included in the study. Observing SMIC(80%) results, it is apparent that the sessile form of *C. auris* CDC390 becomes particularly resistant to all of the antifungals.

Table 5-3: Susceptibility profiles of sessile fungi (biofilm) to CSA-44, CSA-131 and three antifungal compounds.

	SMIC 50% [SMIC 80%] (μg/mL)				
Antimicrobial	*C.albicans* ATCC 90028	*C.auris* CDC 381	*C.auris* CDC 383	*C.auris* CDC 386	*C.auris* CDC 390
CSA-44	2.0 [8.0]	4.0 [16]	2.0 [8.0]	2.0 [4.0]	4.0 [64]
CSA-131	2.0 [4.0]	2.0 [32]	2.0 [4.0]	2.0 [4.0]	4.0 [64]
AMB	2.0 [8.0]	4.0 [16]	2.0 [4.0]	<1.0 [1.0]	8.0 [>64]
CPF	2.0 [8.0]	4.0 [32]	8.0 [32]	8.0 [64]	8.0 [100]
FLZ	64 [200]	64 [>200]	64 [>200]	32 [200]	100 [>200]

CPF: caspofungin, AMB: amphotericin B, FLZ: fluconazole

5.3.4 Confocal laser scanning microscopy of fungal biofilms

To observe the antibiofilm properties of a lead ceragenin, biofilms of *C. albicans* and *C. auris* were treated with CSA-131, stained and imaged via confocal microscopy (Figure 5-3. Untreated biofilms exhibited expected aggregates of live cells, while treated biofilms showed comparable aggregates of dead cells. As with Gram-negative bacteria [93], the ceragenin was able to penetrate the extracellular matrix and exert antifungal activity without significantly compromising the

biofilm morphology. The antibiofilm property of the ceragenins compliments their ability to inhibit biofilm formation as reported in a recent study in which CSA-131, incorporated into a hydrogel, prevents biofilm formation on a medical device for extended periods [247].

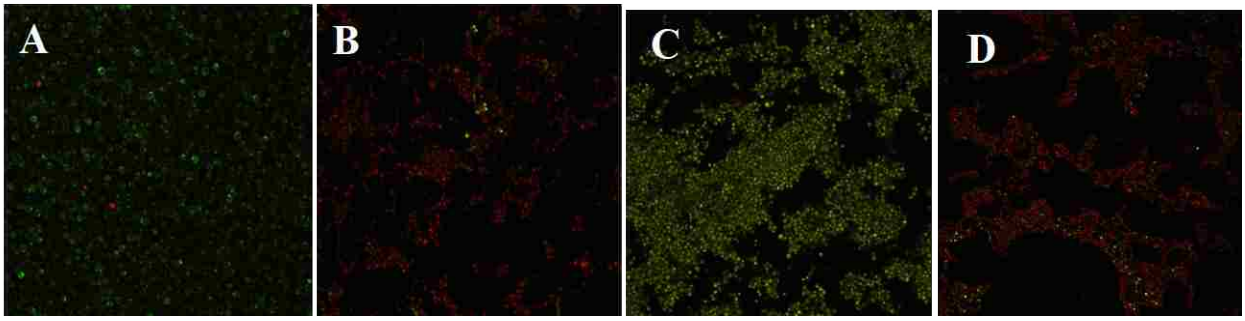

Figure 5-3: Confocal laser scanning micrographs (60 x magnification) of stained fungal biofilms. Green: live cells; red: dead cells. **A**: *C. albicans*, untreated. **B**: *C. albicans*, CSA-131 treated (50 µg/mL). **C.** *C. auris*, untreated. **D**: *C. auris*, CSA-131 treated (50 µg/mL).

5.3.5 Antifungal activity of formulated ceragenins in tissue explants

There are many potential applications of novel antifungal agents, and some of the most widely useful would involve topical application to skin or to mucosal tissues. For these types of applications, lead ceragenins would need to be formulated into gels or creams. Hydroxyethylcellulose (HEC, typically used at 2.7% in water) can be used to form a lubricating gel into which antimicrobial compounds can be formulated. Pluronic F127 is a non-ionic surfactant that has shown compatibility with ceragenins with concomitant decreases in cytotoxic properties [80,239]. Combining HEC, pluronic and either CSA-44 or CSA-131 at 0.5% (44L and 131L) or 2.0% (44H and 131H) gave stable, lubricious gels. These percentages of ceragenins are comparable to those of antifungals incorporated into commercially available antifungal products.

Porcine vaginal mucosal explants were used to determine the antifungal activities of these gels. Nystatin (a polyene antifungal related to amphotericin B) was used as a comparator and the

HEC-pluronic combination (vehicle) was used to observe effects of these compounds on the fungi. Fungal infection with either *C. albicans* or *C. auris* was established over 2 and 24 h of incubation, followed by treatment for 24 h with the test formulations. Over this time course, fungal populations grew to over 10^6 CFU per explant (Figure 5-4). In all experiments, the vehicle had no impact on fungal growth.

At two hours, nystatin decreased fungal counts with *C. auris* and *C. albicans* by ca. one log, but only with *C. albicans* was this reduction statistically significant. In contrast, both ceragenins, at both concentrations, significantly reduced fungal counts at two hours, with reductions as great as five logs (CSA-131 at 2%). At 24 h, nystatin-treated explants supported fungal counts comparable to controls with both species of fungi. At 24 h, the most potent activity of ceragenins was observed with *C. albicans*, with fungal counts significantly reduced relative to both control and nystatin-treated explants. With the highest concentrations of ceragenin (2%), fungal counts were reduced by more than four logs. Although the activity of the ceragenins, at 24 h, was not as dramatic with explants colonized with *C. auris*, significant reductions (ca. three logs) were observed with the highest concentration of the ceragenins. Significant reduction was also observed with the lower concentration (0.5%) of CSA-44.

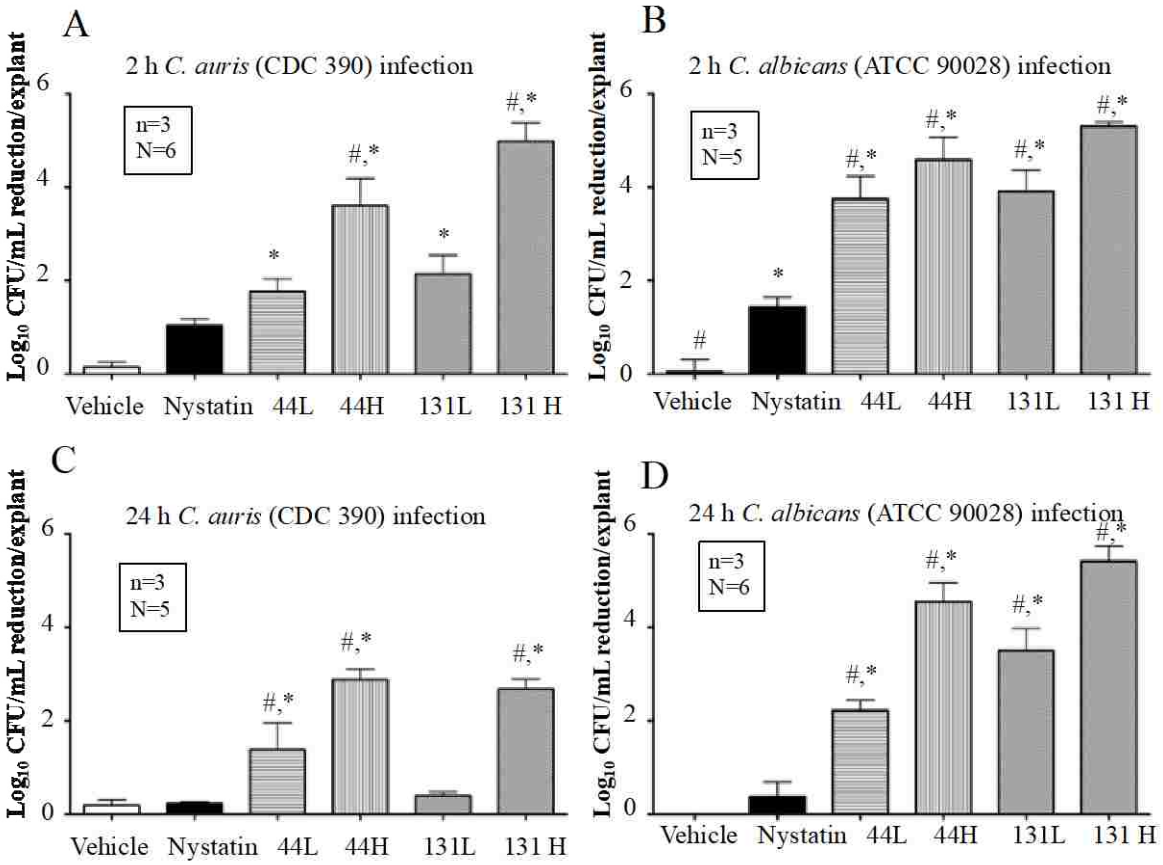

Figure 5-4: Antifungal activities of nystatin (100,000 USP nystatin units) compared to HEC/pluronic formulations of CSA-44 and CSA-131 in porcine vaginal mucosal tissue explants. Log_{10} CFU reduction from untreated growth control following 2 h (A and B) and 24 h (C and D) infections of *C. auris* or *C. albicans* on porcine vaginal mucosa (PVM). Data presented are means and standard errors of the means (SEMs). Analysis of variance (ANOVA) followed by Dunnett's multiple comparison posttest were performed using the GraphPad PRISM software (GraphPad Software, Inc., La Jolla, CA). *significantly different from growth control ($p<0.5$); #significantly different from nystatin ($p<0.5$). CSA-44L or CSA-131L: 0.5% active, CSA-44H or CSA-131H: 2% active in a HEC gel formulation.

CSA-44 was also formulated into a cream and compared to commercial Monistat 7 in the porcine vaginal mucosa infection model. Based on efficacy of the ceragenins in the gel formulation, a concentration of 1% CSA-44 in a cream was used and compared to Monistat 7 (2% miconazole in cream formulation). No other formulations were evaluated in this assay. With *C. albicans*, Monistat 7 reduced fungal counts by a statistically significant amount at two hours, as compared to the growth control, but this effect was negligible at 24 h. With this organism, the CSA-44 cream

formulation reduced counts by more than three logs at two hours and by ca. two logs at 24 h, both of which measurements were significantly different from both the vehicle and the Monostat 7-treated explants (Figure 5-5). Explants colonized with *C. auris* were not significantly affected by Monostat-7 treatment at 2 and 24 h. In contrast, the CSA-44-containing cream significantly reduced *C. auris* counts at both time points (> 2 log and >1 log reductions, respectively).

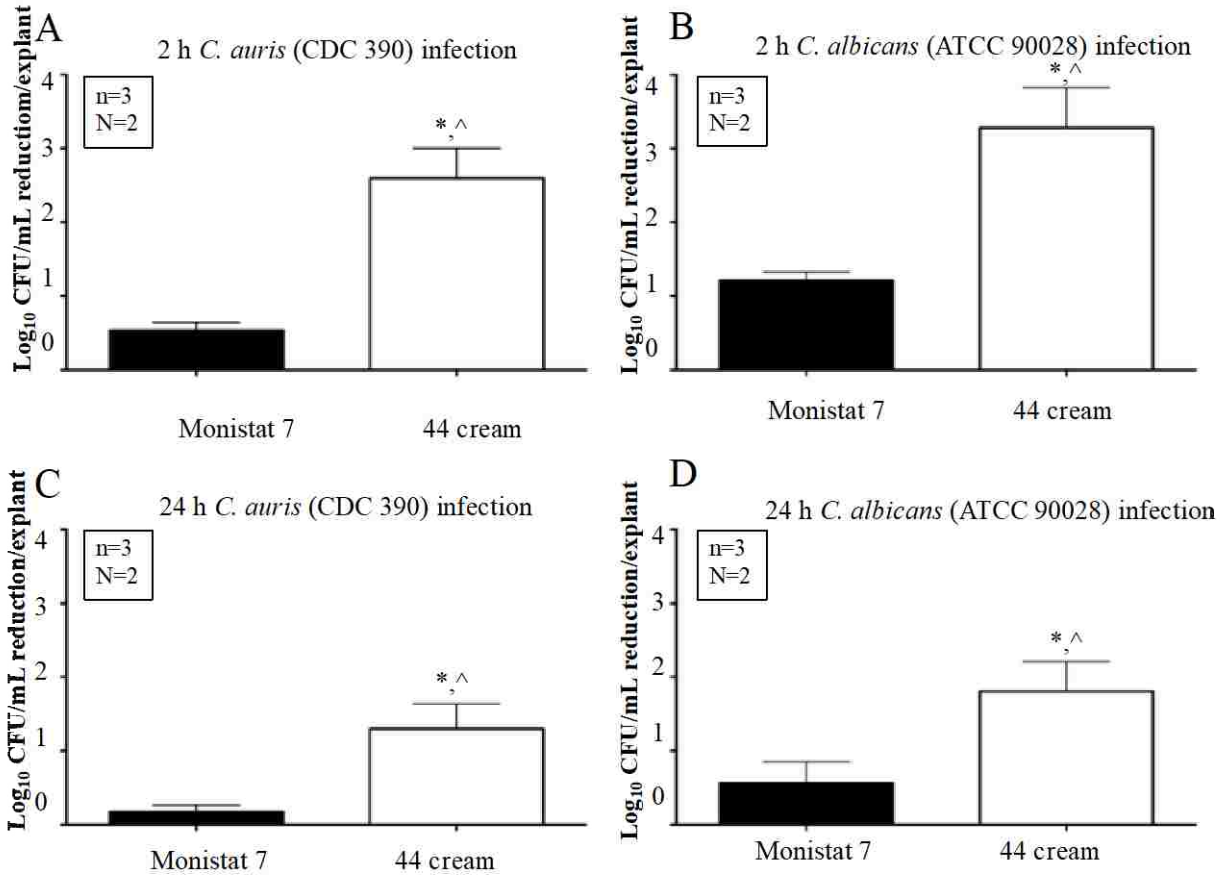

Figure 5-5: Antifungal activities of Monistat 7 (2% miconazole) compared to a cream formulation of CSA-44 (1%) in porcine vaginal mucosal tissue explants. Log_{10} CFU reduction from untreated growth control following 2 h (A and B) and 24 h (C and D) infections of *C. auris* or *C. albicans* on porcine vaginal mucosa (PVM). Data presented are means and standard errors of the means (SEMs). Analysis of variance (ANOVA) followed by Dunnett's multiple comparison posttest were performed using the GraphPad PRISM software (GraphPad Software, Inc., La Jolla, CA). *significantly different from growth control ($p<0.5$); ^significantly different from Monistat 7 ($p<0.5$).

5.4 Conclusions

The spread of *C. auris*, the high mortality rates in patients with infection and the high prevalence of drug resistance among clinical isolates underscore the need for the development of novel antifungal agents. The mechanisms common to endogenous AMPs provide direction for investigation of therapeutics that mimic antimicrobial activities that nature has honed over millions of years. Due to their simple structures, ceragenins are attractive candidates for development of novel antifungal agents; they can be prepared at a large scale and they are stable in the presence of ubiquitous proteases. The ceragenins display antifungal activities with *C. auris* comparable to the most active agents tested, and they do not show cross resistance with other antifungals. The ceragenins also retain activity against sessile organism in established biofilms. In formulated forms, ceragenins are active against high inocula of fungi in mucosal tissue. The substantial antifungal activities of these ceragenin formulations compared to nystatin and Monistat 7 highlight their potential for use as novel antifungals for topical or mucosal applications.

Chapter 6 Preclinical testing of a broad-spectrum antimicrobial endotracheal tube coated with an innate immune synthetic mimic

6.1 Introduction

Tissues in the airways provide innate immune defenses against microbial colonization, and a key component of these defenses is the production of antimicrobial peptides (AMPs) [248,249]. These defenses limit microbial transfer from the highly-colonized oropharynx to the nearly sterile lung tissues. Nearly 50 million patients worldwide are intubated annually with endotracheal tubes (ETTs) to assist breathing. The abiotic surfaces of ETTs provide a breeding ground on which microbes can readily form biofilms [250-252], because the surfaces do not provide an innate immune function comparable to surrounding tissues. Biofilms that form on these abiotic surfaces are a nidus for continual inoculation of surrounding tissues while providing an avenue for microbial transfer into the lungs leading to pneumonia. Ventilator-associated pneumonia remains a major healthcare burden [252,253], adding to lengths of intensive care, costs of hospitalization and increasing the use of antibiotics. Infections associated with mechanical ventilation lead to endotoxin-driven inflammation [254], which in turn can result in sepsis and remote organ damage (e.g., acute kidney injury), brain damage in neonates [255,256] and delirium in elderly patients [257,258]. Prevention of biofilm growth on ETTs may result in significant clinical improvements, reduced antibiotic usage, emergence of fewer multidrug resistant bacteria, reduction of endotoxin-driven adverse clinical outcomes and shorter duration of length of stay in the ICU.

It is increasingly recognized that microbial colonization of ETTs is polymicrobial [250,251,259]. The presence of different microbial pathogens in close proximity to each other in the biofilm matrix enables horizontal gene transfer of plasmids encoding for resistance to conventional

antibiotics and thereby facilitates the emergence of new drug-resistant strains [260,261]. Initial studies of ETT colonization focused on both Gram-positive and Gram-negative pathogens; however, fungi are now understood to contribute to ETT colonization [250,251,259]. Of particular concern are highly drug-resistant organisms. For example, while colistin is considered the antibiotic of "last resort" for Gram-negative bacteria, highly colistin-resistant bacteria have been isolated from a variety of tissues [262-264]. These bacteria are generally resistant to other antibiotics, with many characterized as extended-spectrum beta-lactamase producing organisms. Due to the relatively few antifungal agents available, recent identification of *Candida auris* as a drug-resistant fungal pathogen has led to fears of untreatable infections [265].m

Efforts to prevent ventilator-associated infections have included use of systemic antibiotics [266-268] as well as silver-releasing ETTs [269,270]. Recent studies by Stulik *et al.*[266] and Burnham *et al.* [267] have shown that systemic administration of antibiotics has little effect on airway colonization, and this ineffectiveness is likely due to the rapidity with which bacteria form biofilms and the insensitivity of these biofilms to most antibiotics. Silver-releasing ETTs showed promise in preventing bacterial colonization [269,270], with a concomitant reduction in risk of infection in patients ventilated for more than 24 h. However, silver-releasing ETTs have not gained widespread use in hospitals [270].

An attractive approach for prevention of microbial colonization of ETTs would be to provide an innate immune-like function on their abiotic surfaces. This function would necessarily mimic the activities of endogenous AMPs: broad-spectrum antibacterial activity, anti-fungal activity and the ability to sequester bacterial endotoxins to minimize inflammation. The use of AMPs to provide an innate immune-like function to ETTs has been proposed [271].

As mimics of AMPs, ceragenins also associate with endotoxins [63], inhibiting the processes that lead to release of inflammatory cytokines. As small molecules, ceragenins can be readily prepared at a large scale, and because they are not peptide based, they are not substrates for proteases.

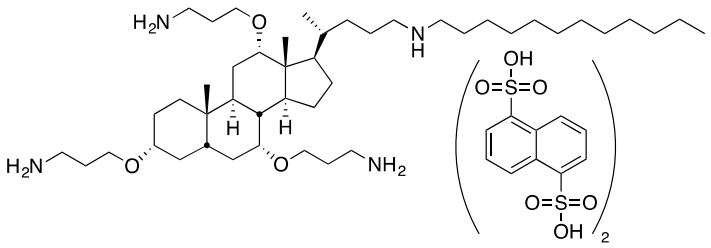

Figure 6-1: Structure of CSA-131(NDSA).

As functional mimics of AMPs, ceragenins are well suited for providing innate immune-like functions to the abiotic surfaces of medical devices. Herein we describe the incorporation of a lead ceragenin, CSA-131 (Figure 6-1), into a thin film, comprised of a lubricious hydrogel, on ETTs. The hydrogel film provides a reservoir of the ceragenin and facilitates controlled release of the ceragenin over extended periods. As the ceragenin is released, it prevents bacterial and fungal biofilm formation and sequesters endotoxins. In its optimized form, the coating is applied via dip coating with a mixture containing the ceragenin, followed by polymerization of the hydrogel. The resulting coating can be sterilized by ethylene oxide without adduct formation. *In vivo* experiments showed that the coated ETT is well tolerated, and no systemic exposure to ceragenin was observed. The Food and Drug Administration (US) has recognized the need for ETTs that prevent microbial colonization, and the coated ETT described herein was recently granted Expedited Access Pathway designation pursuant to the 21st Century Cures Act.

6.2 Materials and methods

6.2.1 Coating

CSA-131(NDSA) was jet milled (Fluid Energy, Telford, PA) to give particles of less than one micron in size. The resulting material was added to Hydromer Coating Solution 2018-20M (Hydromer, Branchburg, NJ) in quantities equal to 10 weight percent relative to the amount of non-volatile material in the coating solution and remained as a suspension of particles. To prepare ETT segments, tubes (7.5 mm id, Flexicare, Irvine, CA) were cut into 5 mm segments. For coating, intact tubes and tube segments were washed with isopropanol and hexanes and fully dried. Tubes and segments were dip coated, and the coating was then cured at 71.1 °C for 1 h. With tube segments, weight differences were determined and used to calculate average coating thickness. Coated tubes and tube segments were subjected to standard ethylene oxide (ETO) sterilization procedures (Steris, San Diego, CA), and ETO-treated segments were used to quantify ETO adduct formation with CSA-131 via mass spectrometry (Agilent 6230 TOF, Santa Clara, CA). To determine the total amount of CSA-131(NDSA) in the coatings, segments (5 mm) of coated ETTs were immersed (1 ^{mL}) in an acidic solution of isopropanol (90% isopropanol, 10% 1 *M* HCl in water) for three 4 h intervals. After each interval, the resulting solution was concentrated under vacuum, reconstituted in water and the CSA-131 concentration was determined via LC/MS (using an internal, mass-labeled standard) or HPLC-ELSD. To visualize the coating, coated and uncoated ETT segments (1 cm) were stained with crystal violet (2% w/v in ethanol) for 30 sec, then rinsed with distilled water five times. Segments were dried under vacuum for 1 h. Sections (ca. 1 mm) were cut and imaged with a light microscope (Axiovert 135, Zeiss, Germany) equipped with a digital camera.

6.2.2 CSA-131 elution studies

6.2.2.1 Elution from the inner lumen

Coated, intact ETTs (7.5 mm id, 28 cm length) were oriented in a drip flow reactor at a 30˚ angle. The proximal end of the ETT was connected to a peristaltic pump delivering 1 mL/min of sterile PBS. Aliquots of the aqueous solution were collected from the distal end of the ETT in separate vessels at time points of 30 and 60 min, 2, 4, 8, 24, 48, 72 and 96 h. The resulting solutions were lyophilized and reconstituted with minimal water prior to CSA-131 concentration determination via LC/MS (using an internal, mass-labeled standard) or HLPC-ELSD.

6.2.2.2 Elution from the outer lumen

The ends of intact ETTs (7.5 mm id, 28 cm length) were plugged with stoppers, and the tubes were placed in a PVC hose (2.5 cm id, 30 cm length) to approximate the size of an adult trachea. The hose was filled with PBS (120 mL), sealed at the ends with stoppers, and incubated at 37 °C. The resulting solution was collected and replenished with fresh PBS at 24, 48, 72 and 96 h. The resulting solutions were lyophilized and reconstituted with minimal water prior to CSA-131 concentration determination via LC/MS (using an internal, mass-labeled standard) or HLPC-ELSD.

6.2.3 Efficacy tests

6.2.3.1 Microbial cultures

Bacterial and fungal cultures were prepared from fresh colonies placed in media and incubated overnight at 37 °C. *Pseudomonas aeruginosa* (PA01, ATCC 47085), MRSA (BAA-41), and *Klebsiella pneumoniae* (ATCC 13883) were cultured in trypticase soy broth (TSB). *Candida albicans* (ATCC 90028) and *C. auris* (CDC 0383) were cultured in Sabouraud Dextrose Broth

(SDB). Bacterial and fungal cultures were pelleted and washed three times in PBS and the re-suspended in PBS. Optical density (OD) readings were performed at 600 nm. Aliquots of cultures were diluted in 10% TSB for bacteria or 10% SDB for fungi to a population of 10^6 CFU/mL and 10^3 CFU/mL, respectively.

6.2.3.2 Determination of antimicrobial properties of coated ETTs

To determine antimicrobial properties of CSA-131(NDSA) coatings, coated ETTs were cut to 5 mm segments and placed in sterile culture tubes. Inoculation solutions were prepared containing 10^6 CFU/mL (bacteria) or 10^3 CFU/mL (fungi), and these solutions (1 mL) were used to immerse ETT segments resulting in a surface area to volume ratio of 0.3 cm^2/mL. Tubes were capped and incubated at 37 °C for 24 h. Microbial growth was confirmed when the surrounding growth medium gave a turbidity greater than 0.5 McFarlands or when less than a three-log reduction was observed relative to controls with uncoated ETT segments. The latter measurement was made by removing aliquots (10 µL) from the growth media, serially diluting the aliquots, plating them on nutrient agar (TSA for bacteria and SDA for fungi), incubating for 24 h at 37 °C with bacteria and 48 h at 35 °C for fungi and counting resulting colonies. All ETT segments were tested in triplicate with uncoated ETT segments used as controls.

6.2.3.3 Quantification of biofilm growth

Coated ETT segments (5 mm) were treated as described above. For evaluation with mixed-species inocula, bacterial cultures (10^6 CFU/mL) were mixed (0.5 mL of each) before addition of ETT segments, or a fungal culture (10^3 CFU/mL, 0.5 mL) was mixed with a bacterial culture (10^6 CFU/mL, 0.5 mL) before addition of ETT segments. At 24 h intervals, ETT segments were removed (three at each time point), gently rinsed with PBS to remove planktonic organisms, immersed in neutralizing buffer (1 mL, Dey-Engley, Sigma Aldrich) and sonicated (bath sonicator)

for 15 min. The resulting solutions were serially diluted and plated on agar (TSA for bacteria and SDA for fungi), incubated for 24 or 48 h at 35 or 37 °C and colonies were counted.

6.2.4 SEM of microbial biofilms

ETT segments (1 cm) were incubated with bacterial and fungal cultures (1 mL) as described above for the indicated time periods. Controls were prepared by incubating uncoated ETT segments with the same cultures for the same time periods. After incubation, segments were gently washed with Sorensen buffer (0.1 *M*, pH 7.2) then fixed, dehydrated and sputter-coated as described in detail in section 3.2.5.

6.2.5 Measurement of endotoxin levels associated with coated and uncoated ETTs

Endotoxin levels were quantified using a *Limulus* amebocyte lysate (LAL) assay with a kinetic chromogenic readout (Charles River Laboratories, Charleston, SC). Assays were performed according to the manufacturer's instructions with an *Escherichia coli* endotoxin standard to establish a standard curve. Responses to the endotoxin standard were measured at varied concentrations of CSA-131, and no interference in endotoxin quantification was observed. Uncoated and coated ETT segments (5 mm) were inoculated with *P. aeruginosa* (PA01, 10^6 CFU) in TSB and incubated at 37 °C. Aliquots of the fluid were removed at specified times (0, 4 and 8 h) and assayed for endotoxin. At 24 h, tube segments were removed, gently washed with PBS, immersed in neutralizing broth and sonicated for 15 min. Aliquots of the resulting broth were assayed for endotoxin.

6.2.6 Intubation studies

Six pigs, weighing approximately 35-45 kg, were used in this safety evaluation study. On the day of the procedure, each animal was anesthetized and prepped acutely. Each animal was implanted with a coated or uncoated endotracheal tube and monitored under anesthesia for 24 h. Blood samples were collected at various time points during the study for pharmacokinetic and cytokine analysis. After the test period, the animals were euthanized and a limited necropsy performed. The trachea, oropharyngeal area, and collateral structures (lungs) were grossly examined for abnormalities that may be attributed to the test article.

6.3 Results and discussion

The hydrogel used in the coating is a polyurethane-based, medical-grade, lubricious material developed by Hydromer, Inc. It is generated, after dip coating, via polymerization of isocyanate groups upon exposure to moisture and heat. For clinical use of coated medical devices, sterilization is required, and ETO treatment is the most commonly used method of sterilizing ETTs. Coatings prepared with CSA-131(NDSA) gave a stable coating (13 ± 2 μm) that showed no detectable adduct formation (< 1%) by mass spectrometric analysis after ETO treatment.

To image the coating, coated and uncoated ETT segments were soaked (30 s) in a solution of crystal violet in ethanol. The segments were then washed with water and dried. Coated segments retained the dye, while uncoated segments remained unstained (Figure 6-2). The stained coating proved uniform with a thickness of approximately 10 μm.

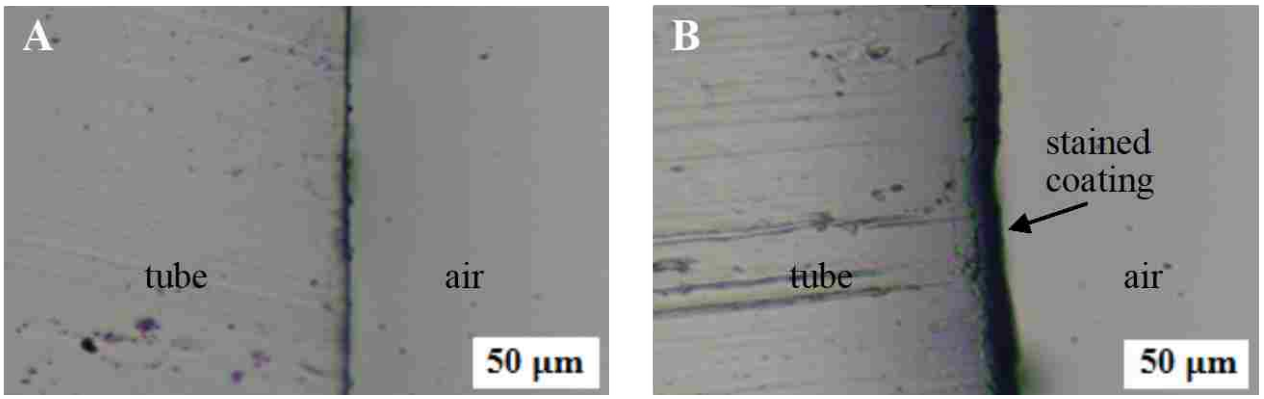

Figure 6-2: Microscopy images of the inner lumen of ETT stained with crystal violet. **A:** uncoated ETT. **B:** coated ETT.

The amount of CSA-131(NDSA) added to the coating solution was 10% (w/w) of the non-volatiles in solution. To quantify the amount of ceragenin in the coating, CSA-131 was extracted from coated ETT segments using 90% isopropanol/10% aqueous HCl (1 *M*). From these experiments, we determined that the total amount of CSA-131 was 39.4 µg/cm^2 (6.9 mg on the entire tube), as determined via mass spectrometry with a mass-labeled internal standard or via HPLC using ELSD.

CSA-131(NDSA) has limited solubility (< 20 µg/mL) in water, and for the solubility of CSA-131 to increase in water, ion exchange must occur (e.g., chloride for NDSA). This ion exchange process, as well as the structure of the polyurethane, contributes to the controlled release of the ceragenin from the coating. The rate at which CSA-131 eluted from the coating was determined using two methods. For the inner lumen, a drip flow procedure was used in which phosphate-buffered saline (PBS) was dripped through intact, coated ETTs at the rate of 1 mL/min, the rate at which fluids pass through ETTs in the trachea. For the outer lumen, coated ETTs were incubated in a larger tube of the approximate size of an adult trachea (2.5 cm diameter and 30 cm length). Rates of elution from the inner lumen (drip-flow method) are shown in Table 1; after the first hour

of elution, the concentration of CSA-131 dropped below the detection limit (0.25 µg/mL). Elution from the outer lumen was measured over 96 h, and comparable amounts eluted over each 24 h period (Table 6-1). Notably, in both the drip flow elution and elution into a static solution, the concentration of CSA-131 never exceeded 1 µg/mL.

Table 6-1: Elution of CSA-131 from the inner lumen of intact, coated ETTs measured via drip flow (1 mL/min).

Surface	Time Interval	Amount Eluted	*Elution per cm^2	Concentration of CSA-131 in Eluent
Inner lumen*	0 - 30 min	22.2 µg	0.30 µg/cm^2	0.74 µg/mL
	30 - 60 min	9.3 µg	0.12 µg/cm^2	0.31 µg/mL
	60 - 120 min	<DT**	N/A	N/A
	Totals	**31.5 µg**	**0.42 µg/cm^2**	
Outer lumen***	0 - 24 h	94.3 µg	0.95 µg/cm^2	0.79 µg/mL
	24 - 48 h	84.9 µg	0.85 µg/cm^2	0.71 µg/mL
	48 - 72 h	64.9 µg	0.65 µg/cm^2	0.54 µg/mL
	72 - 96 h	80.1 µg	0.81 µg/cm^2	0.67 µg/mL
	Totals	**324 µg**	**3.26 µg/cm^2**	

*Inner lumen elution measured via drip flow (1 mL/min) with an ETT inner lumen surface area of 74.8 cm^2

**Below Detection Limit (DT). Detection limit: 0.25 µg/mL

***Outer lumen elution measured in a static solution (120 mL) with an ETT outer lumen surface area of 99.4 cm^2

To determine the efficacy of coated ETTs in preventing microbial growth, bacterial suspensions (10^6 CFU/mL) or fungal suspensions (10^3 CFU/mL) were prepared in growth media, and segments (5 mm) of coated ETTs were immersed in the media. The suspensions were incubated at 37 °C for 24 h, and the tube segments were re-challenged every 24 h in fresh growth media. Two measures of microbial growth were quantified: (1) microbial growth in the

surrounding medium and (2) microbial biofilm formation on the tube segments. For the first measure, aliquots were removed from the growth media, serially diluted and plated; with this measure, continuous testing was possible. In contrast, to quantify biofilm growth, it was necessary to remove tube segments, gently wash them in PBS and sonicate them in neutralizing broth. Tube segments thus treated could not be returned for continued study because sonication may have altered the structure of the coating.

As anticipated, with uncoated tube segments, microbial growth was observed in the growth media and biofilms formed on the segments. In contrast, coated ETT segments prevented microbial growth in the surrounding media and prevented biofilm formation for multiple days. Quantification of microbial biofilm formation on tube segments with representative organisms is shown in Figure 6-3. Duration of activity ranged from four days with *P. aeruginosa* to 16 days with *C. albicans*. During these intervals, biofilm formation was reduced by ca. six logs, with no bacteria or fungi detected on the tube segments. Because colonization of ETTs is polymicrobial, we also quantified microbial growth from mixed species inocula (MRSA with PA01 and PA01 with *C. auris*). While the duration of prevention of biofilm formation decreased in the presence of mixed species of micro-organisms (Figure 6-4), the coated tubes continued to reduce or prevent colonization for multiple days.

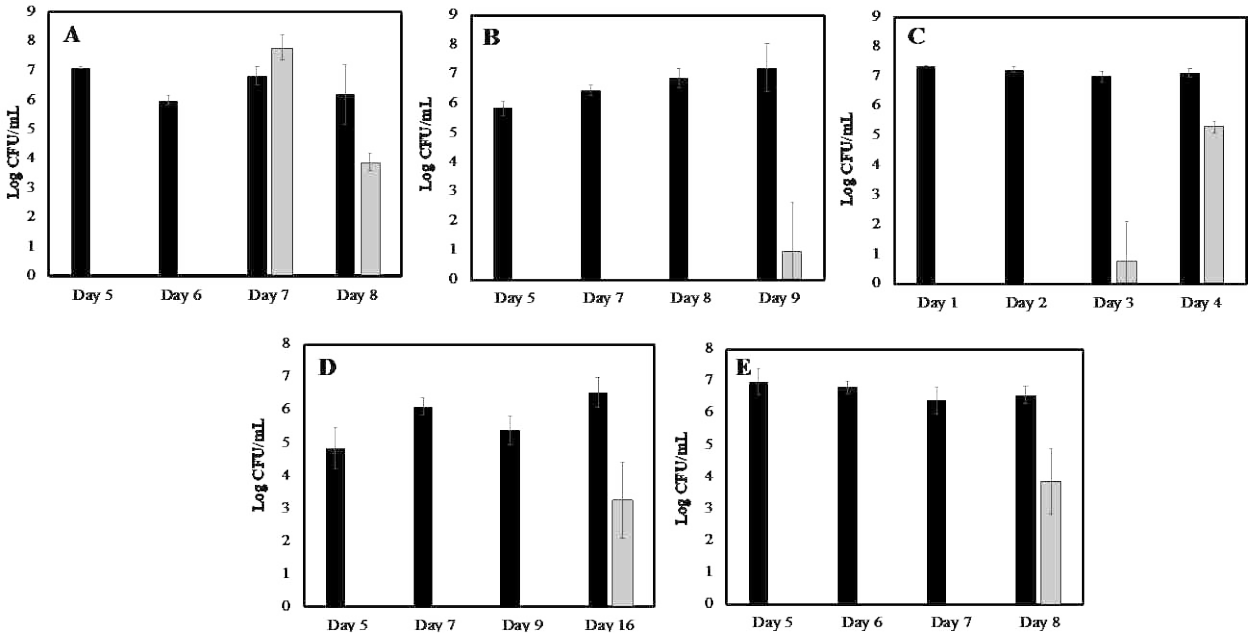

Figure 6-3: Biofilms formed on ETT segments (5 mm) after the indicated number of days of incubation (daily exchange of growth medium and re-inoculation). Measurements made in triplicate. Black bars: uncoated tube segments; gray bars: coated segments. **A:** MRSA (BAA-41, 10^6 CFU inoculation). **B:** *K. pneumoniae* (ATCC 13883, 10^6 CFU inoculation). **C:** *P. aeruginosa* (ATCC 47085, 10^6 CFU inoculation). **D:** *C. albicans* (ATCC 90028, 10^3 CFU inoculation). **E:** *C. auris* (CDC 0383, 10^3 CFU inoculation).

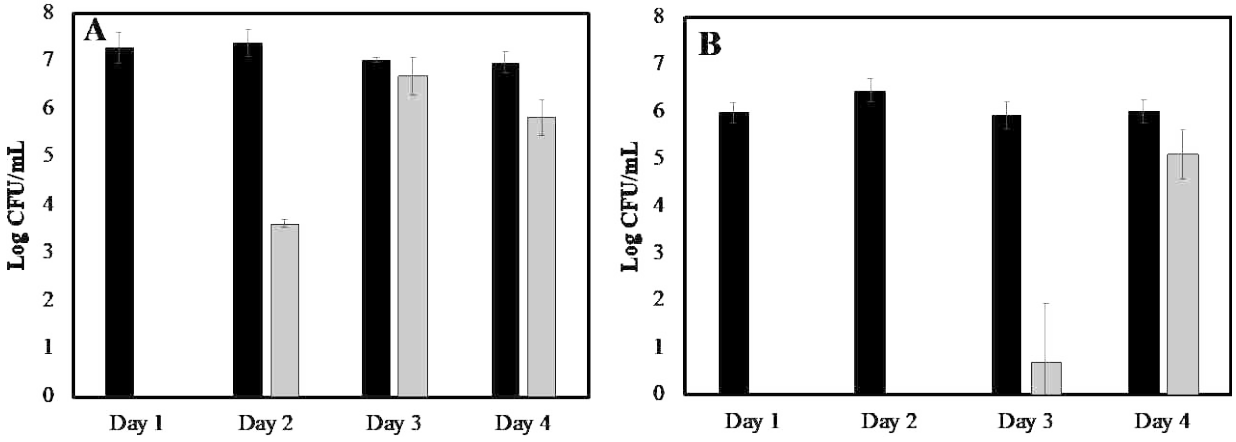

Figure 6-4: Mixed species biofilms formed on ETT segments (5 mm) after the indicated number of days of incubation (daily exchange of growth medium and re-inoculation). Measurements made in triplicate. Black bars: uncoated tube segments; gray bars: coated segments. **A:** MRSA (BAA-41, 10^6 CFU inoculation) with *P. aeruginosa* (ATCC 47085, 10^6 CFU inoculation). **B:** *P. aeruginosa* (ATCC 47085, 10^6 CFU inoculation) with *C. auris* (CDC 0383, 10^3 CFU inoculation).

To visualize biofilm formation and prevention thereof, we prepared samples for SEM. Representative images are shown in Figure 6-5. *C. auris* (CDC 383) readily formed a stable biofilm on uncoated ETT segments even though this organism has been reported to form less biofilm than *C. albicans* [272]. After 14 days of growth (with re-inoculation every 24 h), the fungal biofilm was nearly completely covered with the extra-cellular matrix (Figure 6-5A), seen as a "cotton-like mass" with *C. albicans* biofilm formation [273]. At 14 days, the coated ETT surface showed no fungal growth by SEM (Figure 6-5B). Culturing of adhered organisms indicated fungal colonization of coated tubes by day 8 (approximately a three log reduction relative to controls, Figure 6-3E); however, the populations of fungi adhered to coated tubes did not reach the levels of those adhered to uncoated tubes through 14 days. The lack of fungi observed by SEM may be due to loss of loosely adhered organisms on the coated tubes. Mixed species challenge of uncoated ETTs at 48 h with MRSA and PA01 showed biofilm formation in which both types of bacteria were readily distinguishable (Figure 6-5C), while the coated segment remained uncolonized (Figure 6-5D). Similarly, challenge of uncoated tube segments with a combination of PA01 and *C. auris* showed biofilm formation with both organisms (Figure 6-5E); extensive colonization of *Candida* biofilms by *Pseudomonas* has been observed [274]. There was no biofilm formation on the coated ETT segment (Figure 6-5F).

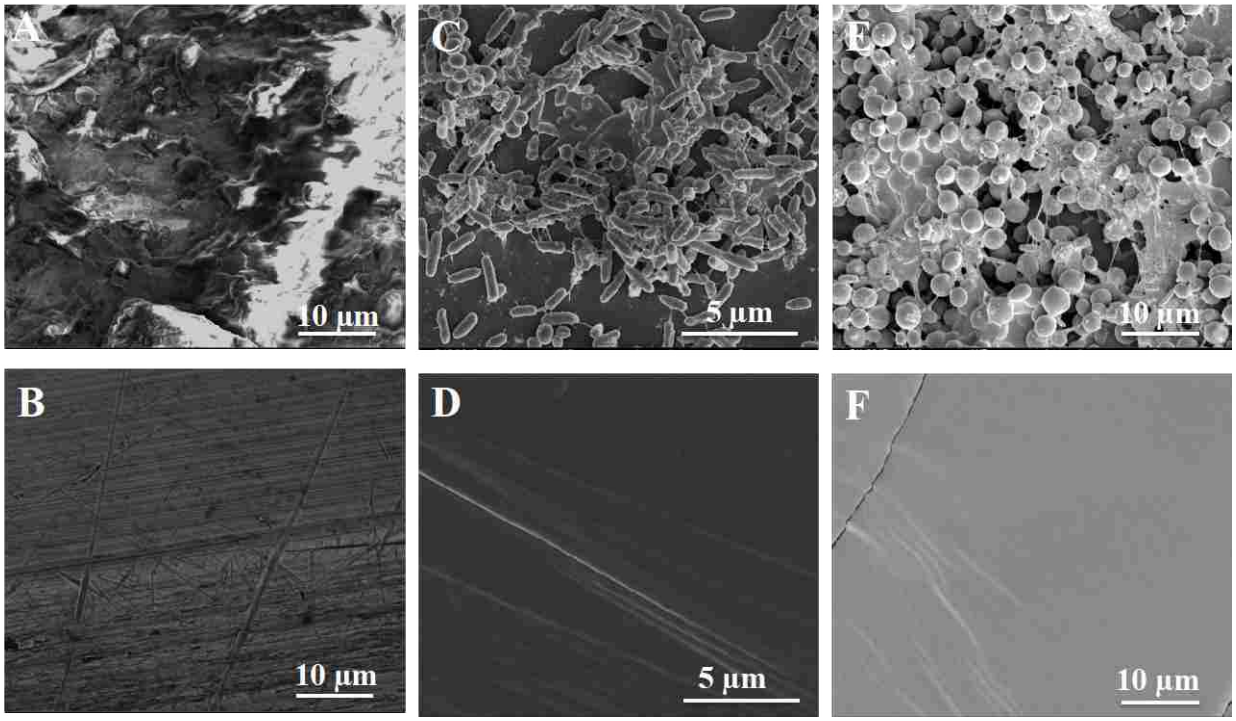

Figure 6-5: SEM images of ETT surfaces: **A:** biofilm of *C. auris* (CDC 383) on an uncoated tube after 14 days (daily inoculation). **B:** surface of a coated tube after 14 days (daily inoculation with *C. auris*). **C:** mixed species biofilm of MRSA and PA01 on an uncoated tube after 48 h. **D:** surface of a coated tube after 48 h (inoculation with MRSA and PA01). **E:** mixed species biofilm of PA01 and *C. auris* on an uncoated tube after 48 h. **F:** surface of a coated tube after 48 h (inoculation with PA01 and *C. auris*).

Inflammation, in response to endotoxin, is a primary cause of lung damage and other deleterious responses to ventilator-associated infections [254-258]. The antimicrobial effects of the ETT coating were expected to reduce the amount of endotoxin on the tubes and in the surrounding growth media. To test this hypothesis, coated and uncoated ETT segments were exposed to *P. aeruginosa* (PA01) in a nutrient medium for 24 h. To quantify endotoxin on tube surfaces, tubes were removed from culture, gently rinsed with PBS to remove planktonic bacteria and sonicated in neutralizing broth. Aliquots from the resulting broth were serially diluted and assayed for endotoxin. Endotoxin amounts in the growth medium and on the tube segments are shown in Figure 6-6. Concomitant with bacterial growth, endotoxin amounts increased in the presence of uncoated tube segments, both on the segments and in the growth medium. In contrast, with the

coated segments, endotoxin was substantially reduced in the growth medium and on the tube segments.

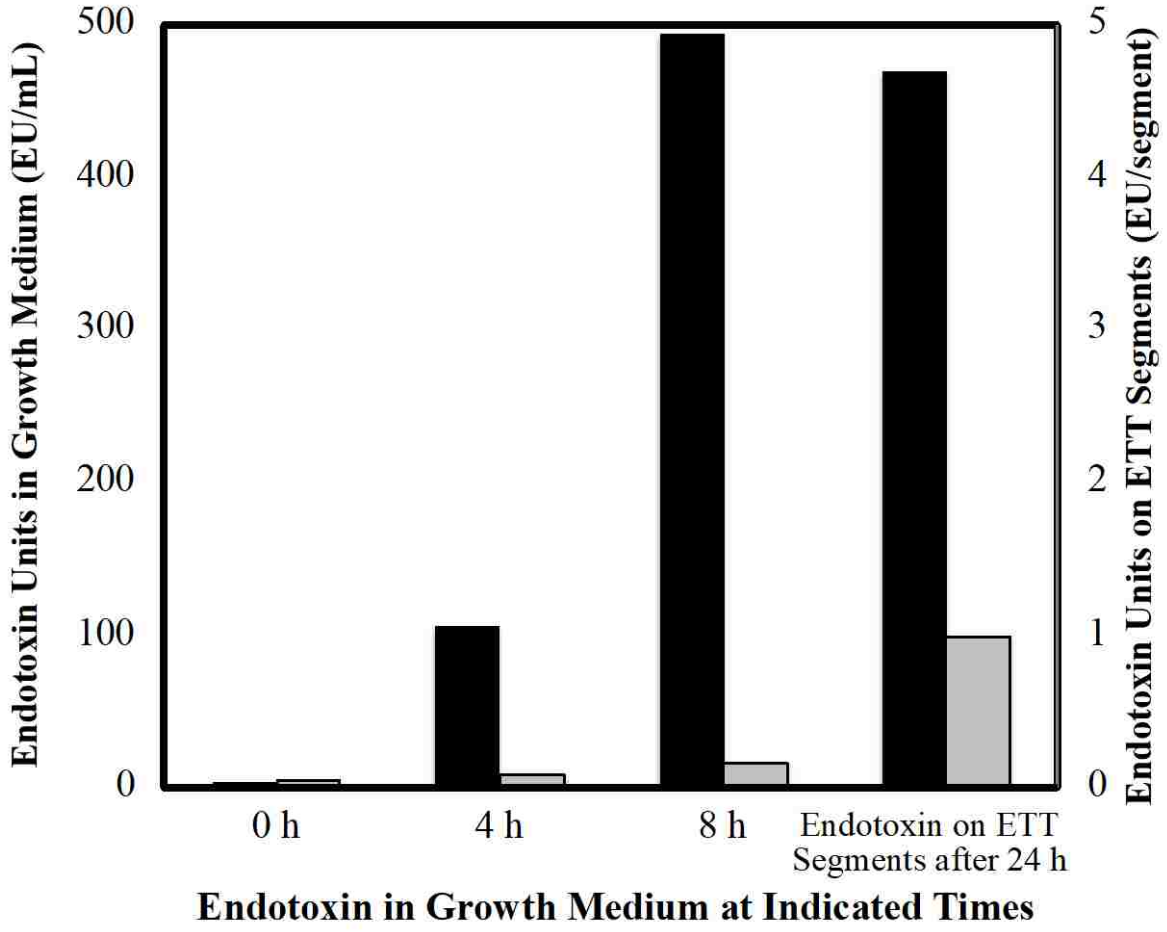

Figure 6-6: Quantification of the amounts of endotoxin in the growth medium and on ETT segments after incubation with P. aeruginosa for the indicated time periods. Black bars, uncoated tube segments. Grey bars, coated tube segments.

To demonstrate the safety of the coated ETT, a GLP study of intubation in pigs was performed. The animals were intubated and mechanically ventilated for 24 h, and to simulate a worst-case scenario, test samples were manufactured with CSA-131(NDSA) in an amount 133% of the coated ETTs described above. There was no mortality during the study, and the six treated pigs were

humanely euthanized according to protocol at their scheduled endpoints of 24 h post treatment (Table 6-2). The oropharyngeal area, trachea and lungs were grossly examined for abnormalities. There were no significant macroscopic findings in these six animals. Histological analyses were performed on lung and tracheal tissue. The test animals had no inflammation in the lungs while the control animals had minimal inflammation in some sections (data not shown). The interstitial edema seen in the lungs of both the test and control animals is considered not related to either device but to the procedure and prolonged recumbency of the animals. The test animals had increased cilia loss in the trachea compared to the control animals but it was not a significant difference. In the trachea and in the lung, under the conditions of this study and based on the Irritant Rank score, the test article was considered a non-irritant when compared to the control. To determine if intubation with coated ETTs resulted in systemic exposure to CSA-131, blood samples were taken and analyzed for CSA-131 at times between 0 and 24 h post intubation. Both the controls and the test group had no detectable CSA found in the blood (detection limit of 5 ng/mL).

Table 6-2: CSA-131(NDSA) intratracheal repeat dose GLP study design.

	Treatment (intratracheal instillation)			**In-Life Procedures** (Day 0-8)	**Terminal Procedure** (Day 9)
	Day 0	**Day 1**	**Day 2**		
1/1	Vehicle 1 mL	Vehicle 1 mL	Vehicle 1 mL	Body weight: twice daily	Complete necropsy; histopathology
1/1	CSA-131 150 mg in 1 mL	CSA-131 150 mg in 1 mL	CSA-131 75 mg in 1 mL	Qualitative food consumption: daily	
1/1	CSA-131 300 mg in 1 mL	CSA-131 300 mg in 1 mL	CSA-131 150 mg in 1 mL	Blood collection for TK and clinical pathology: pre-study and at necropsy	
1/1	CSA-131 1000 mg in 1 mL	CSA-131 300 mg in 1 mL	CSA-131 150 mg in 1 mL		

6.4 Conclusions

There is a pressing need for development of means of protecting medical devices from microbial colonization, and this need is complicated by the continuous emergence of drug-resistant pathogens. The broad-spectrum antimicrobial activities of the ceragenins, including activity against drug-resistant bacteria and fungi, qualifies them as a potential solution to this need. Use of a ceragenin to protect a medical device required optimization of coating method and composition; full characterization of the coating involved study of ceragenin elution and protection of surfaces from bacterial and fungal challenges; and demonstration of safety in a porcine intubation model. These steps have been completed and the ceragenin-coated ETTs appear well suited for use in preventing microbial colonization and reduction of inflammatory responses to bacteria and fungi in intubated patients.

Chapter 7 Antibacterial and antifungal activities of poloxamer micelles containing ceragenin CSA-131 on ciliated tissues

7.1 1. Introduction

The broad-spectrum activity of ceragenins and AMPs is due primarily to the selective association of these antimicrobials with bacterial and fungal membranes. For example, we have shown that ceragenins bind to bacterial membrane surfaces even in the presence of larger surface areas of mammalian cells [67]. This selectivity likely contributes to the antimicrobial activities of ceragenin of many tissues, without adverse effects, including the peritoneal cavity [132], in bone fractures [122], and on bone [119,120] and lung-associated [247] medical devices.

With most bacterial and fungal pathogens, ceragenins display inhibitory activity at μg/mL concentrations ; however, higher concentrations may be necessary to fully eradicate biofilm forms of these organisms [93,275]. In biofilm form, microorganisms enter a sessile state in which some cells, including persister cells [276], remain viable even after most other cells have been eradicated by applied antimicrobials. Biofilms contribute to multiple diseases [277]. For example, infections associated with cystic fibrosis (CF) show substantial contributions from bacteria in biofilm form [278,279]. Substantial doses of antibiotics, including tobramycin, are used in an effort to suppress bacterial growth, yet biofilms persist [278,280].

In the lungs of CF patients, bacterial biofilms accumulate along with DNA, F-actin, and mucins. These compounds deactivate innate immune defenses, including AMPs, while ceragenins remain active in their presence [63,103]. Consequently, ceragenins appear well suited for use in reducing the biofilm burden in the CF lung. The presence of endogenous AMPs in the lungs [281] suggests that tissues in the lungs are tolerant of these antimicrobials, and the fact that a ceragenin-

releasing endotracheal tube is well tolerated *in vivo* [247] suggests that the lung epithelium may also be unaffected by ceragenins. However, while epithelial cells may remain viable, the cilia on these cells, which play a critical role in maintaining lung health, are fragile and can be damaged by antibiotics and mechanical insults. Consequently, evaluation of the potential use of ceragenins for the eradication of biofilms must include observation of the impact of these antimicrobials on cilia function. In initial experiments, we observed that the exposure of lungs and tracheal explants to high concentrations of a ceragenin, CSA-131, led to decreases in cilia function. We therefore sought methods to decrease the impact of this ceragenin on cilia, allowing the use of concentrations of CSA-131 sufficient to eradicate biofilms without interfering with the essential role that these cilia play.

Various poloxamers have been developed for use as drug carriers. The poloxamer Pluronic® F127 (hereafter referred to as pluronic) has been especially well studied due to its abilities to form well-defined micelles and sequester drugs for delivery to specific tissues [282]. In two previous studies, it was observed that combinations of this non-ionic surfactant and ceragenins decreased host cell cytotoxicity without substantially impairing antibacterial activities [80,108]. The mechanism of decreased toxicity is most likely due to transient encapsulation of ceragenins in micelles formed by the pluronic. While ensconced in micelles, ceragenins are less prone to associate with host membranes, yet the higher affinity of ceragenins for microbial membranes [67] and the dynamic nature of micelles allow ceragenins to affect antimicrobial activities. In this manner, pluronic micelles may act to amplify the membrane selectivity of ceragenins.

To observe the impact of pluronic micelles on ceragenins activity and to optimize ceragenin formulation for use in treating biofilm-based infections in the lung, we studied the impact of a lead ceragenin, CSA-131, with and without pluronic on cilia beating and the inhibition of bacterial and

fungal growth *in vitro* and in tracheal and lung tissue explants. We found that the use of pluronic with relatively high concentrations of CSA-131 leaves cilia beating intact, and the pluronic has no impact on the antimicrobial activities of CSA-131. These results suggest that the formulation of ceragenin CSA-131 in pluronic micelles may allow use of high concentrations of this antimicrobial, sufficient to eliminate biofilms without negatively impacting cilia function.

7.2 Material and methods

Pluronic® F127, 2,3-bis-(2-methoxy-4-nitro-5-sulfophenyl)-2H-tetrazolium-5-carboxanilide and menadione were obtained from Sigma-Aldrich (St. Louis, MO, USA) and used as received.

7.2.1 Microbial cultures

S. aureus (ATCC 25923) and *P. aeruginosa* (ATCC 47085 (PA01)) were grown from fresh colonies in trypticase soy broth (TSB) and incubated overnight at 37 °C. Fungal cultures, *Candida albicans* (ATCC 90028) and *Candida auris* (CDC 0382, 0384, 0387, and 0389), were grown overnight in sabouraud dextrose broth (SDB) or Roswell Park Memorial Institute medium (RPMI). Cultures of bacteria and fungi were centrifuged, and pellets were washed three times with phosphate buffered saline (PBS) and further resuspended in fresh PBS. Bacterial cultures were diluted in TSB and fungal cultures were diluted in SDB or RPMI to 10^3 or 10^6 CFU/mL (optical density (OD) readings at 600 nm).

7.2.2 Susceptibility testing in the presence or absence of pluronic

7.2.2.1 MIC

MICs were measured using the broth microdilution protocol described by the Clinical and Laboratory Standards Institute [150]. Briefly, two-fold dilutions of CSA-131 were dispensed in

separate wells of a 96-well plate. Aliquots (100 µL) of a prepared inoculum (10^6 CFU/mL for bacteria and 10^3 CFU/mL for fungi) were added, and plates were incubated at 37 °C for 18–20 h. Bacterial or fungal growth was visually observed to determine the MICs. Negative and positive controls were included for each set of MIC measurements. For studies with pluronic, the surfactant was added at 4% and 5% to the initial inocula in each experiment. Measurements were performed in triplicate for all susceptibility tests.

7.2.2.2 Determination of antifungal and antibacterial susceptibilities of biofilms by XTT assay

Biofilm formation by selected bacterial and fungal strains was quantified by measuring metabolic activity within biofilms using 2,3-bis-(2-methoxy-4-nitro-5-sulfophenyl)-2H-tetrazolium-5-carboxanilide (XTT) [236]. Biofilms were formed in 96-well plates and incubated for 48 h at 37 °C. After three washes with PBS to remove planktonic cells, CSA-131 (100 µg/mL) in the presence or absence of 4% or 5% pluronic was added to the wells and incubated for 24 h. After incubation, the wells were carefully washed with PBS. A solution of 10 mM menadione in 100% acetone was added to an XTT solution (0.5 mg/mL) and mixed. An aliquot of the XTT/menadione solution (100 µL) was added to each well. Each plate was then wrapped in aluminum foil and incubated for 2–3 h at 37 °C. To prepare to read the optical density, aliquots of the supernatant (70 µL) were removed from each well. Using a microtiter plate reader, colorimetric changes were measured at 490 nm. The percent of biofilm survival for each well containing CSA-131 with or without pluronic was calculated in comparison to the biofilm formed in the absence of the ceragenin (control).

7.2.2.3 Determination of minimum biofilm eradication concentrations (MBEC)

Inocula (10^6 CFU/mL) of bacterial and fungal strains (*P. aeruginosa*, *S. aureus*, *C. albicans*, and *C. auris*) were incubated at 37 °C for 48 h in 1 mL of TSB or SDB in 96-well plates. Following

incubation, the growth medium was gently removed, and wells were washed three times with sterile PBS. CSA-131 (100 µg/mL), in TSB or SDB and in the presence or absence of pluronic (4% or 5%), was added to the wells at concentrations ranging from 1 to 256 µg/mL, and each plate was incubated at 37 °C for 24 h. Wells, including well edges, were scraped thoroughly with a plastic spatula. Well contents were removed in 1 mL of neutralizing broth (Dey-Engley, Sigma–Aldrich) and placed in a sonicating water bath (Fisher Scientific FS60, 42 kHz, 100 W, Pittsburg, PA, USA) to disrupt biofilms. After 15 min, the resulting samples were serially diluted, and bacterial samples were plated on TSA while fungal samples were plated on SDA. After 24 h or 48 h of incubation at 37 °C, colonies were counted and MBECs were determined. The MBEC was defined as the lowest concentration of antibiotic that prevented bacterial regrowth [283].

7.2.2.4 Measurement of kinetics of bactericidal and fungicidal activity

Cultures of *S. aureus*, *P. aeruginosa*, and *C. albicans* were prepared as described for MIC measurements and placed in 96-well plates (10^6 CFU for bacteria and 10^3 CFU for fungi) with or without CSA-131 (100 µg/mL), with or without pluronic (4%), in TSB (with bacteria) or SDB (with fungi). Cultures were incubated at 37 °C. At 5, 15, 30, 60, and 120 min, aliquots were removed from each well and added to neutralizing buffer to ensure that no further antibacterial activity occurred. These samples were then serially diluted and plated on TSA or SDA. Cultures were incubated at 37 °C for 24 h or 48 h, and colonies were counted and recorded.

7.2.3 Preparation of tracheal explants

Normal healthy porcine trachea and lung tissue was excised very fresh from slaughter. After aseptic collection, whole tissues were transported in a 1:1 mixture of Dulbecco's modified Eagle's medium (DMEM) and RPMI, which was pre-warmed and supplemented with penicillin-

streptomycin-glutamine 100X (Hyclone, Logan, UT, USA). Explants were washed by tissue immersion three to four times in warm, fresh DMEM/RPMI media. Explants were maintained by continuous immersion in DMEM/RPMI media in a 5% CO_2–95% air mixture in a humidified incubator at 37 °C. Ethics statement: Trachea and lung materials were obtained from a local butcher (Circle V meat Co., Spanish Fork, UT, USA) and were sourced from animals slaughtered for human consumption; hence, ethical approval was not required for this research.

7.2.4 Latex bead clearance assay

Tracheas were washed and extra exterior tissues to the cartilage were removed. Tracheas were opened and cut into approximately 2 × 1 cm explants consisting of the respiratory mucosa and underlying cartilage. Explants were then immersed in different concentrations of CSA-131, with and without pluronic, in the DMEM/RPMI mixture in 24-well plates for 1 h in a humidified incubator at 37 °C with 5% CO_2. Explants were then placed on small circular filter papers, which were placed on top of 1% agarose gel plugs bathed in medium in 6-well plates. To determine cilia activity on explants, epithelial surfaces were tested via a bead clearance assay 1 h post treatment with CSA-131 (100 µg/mL), with or without pluronic (1%, 2%, 3%, 4%, and 5%). Five microliters of a suspension of 1 µm diameter polystyrene microsphere beads (Polysciences, Inc., Warrington, PA, USA) were pipetted on one edge of epithelial surfaces and evaluated for their complete clearance (movement) across the surface with categorization of clearance in under 10 min, between 10 and 20 min, between 20 and 30 min, and no clearance (>30 min). Independent replicates were completed for each time point. Outcomes were then counted and a percentage of clearance was determined [284].

7.2.5 SEM of cilia on porcine trachea

Explants (5 mm^3) were washed gently in Sorensen buffer (0.1 M, pH 7.2) to remove mucus and secretions. The fixative compounds were all diluted in the Sorensen buffer. The trachea pieces were incubated for 24 h with 2% of glutaraldehyde (Electron Microscopy Sciences, Hatfield, PA, USA) at 4 °C and then rinsed five times in Sorensen buffer. Additional post-fixation was performed using 1% of OsO_4 (Electron Microscopy Sciences, Hatfield, PA, USA) for 1.5 h under the hood at room temperature. After fixation, OsO_4 was removed by rinsing the explants at least seven times in Sorensen buffer and then explants were dehydrated in increasing concentrations of ethanol: 10, 30, and 50, each step for 15–20 min. The process was completed inside critical dryer baskets with 70% and 95% ethanol finishing with twice in 100% for 15–20 min. Samples were then submerged in 100% ethanol in the critical point dryer at the critical point of carbon dioxide. Prepared samples were mounted on aluminum stands and then sputter-coated with 5–10 nm of a gold-palladium alloy and observed with SEM (FEI Helios NanoLab 600 SEM/FIB, Hillsboro, OR, USA) at 5 kV.

7.2.6 *Ex Vivo* efficacy evaluation

Using 5 mm^3 explant cubes of porcine trachea and lung, *ex vivo* antifungal efficacy experiments were conducted. Cubes were dissected using a sterile razor blade form the ventral surface of the left caudal lobe of three sets of porcine lungs [285]. After trimming excess tissues away from the explants to produce uniform of size (5 mm), explants were incubated at 37 °C in DMEM/RPMI inoculated with 10^6 CFU/explant of *C. auris* (CDC 0384) or *C. albicans* (ATCC 90028) in a 48-well plate. Explants were treated after 2 h of incubation with CSA-131 in the presence or absence of pluronic. Treated explants were incubated for 24 h at 37 °C. After incubation, tissues were suspended in 250 µL of neutralizing broth and vortex on the highest

setting for 4 min. Samples were then serially diluted in PBS, plated on 5% sheep blood TSA plates, and incubated at 37 °C for 48 h [235].

7.3 Results and discussion

We initially determined the impact of pluronic, at 4% and 5% of the growth medium, on the antibacterial and antifungal activity of ceragenin CSA-131. The amphiphilic nature of the ceragenin makes it likely that it associates well with pluronic micelles. At issue is whether the ceragenin can effectively escape micelles to exert antimicrobial effects. Earlier reports with bacteria [80,108] demonstrated that pluronic did not substantially affect antibacterial activity. The MICs and MBECs of CSA-131 alone and in the presence of pluronic at 4% and 5% are given in Table 7-1. MBECs are the concentrations required to eliminate biofilms, including persister cells, to detection limits. With both *S. aureus* and *P. aeruginosa*, MICs were unchanged in the presence of pluronic, as observed previously. Notably, *Candida* spp., MICs were also unaffected by pluronic, even though these are eukaryotic organisms. Notably, MBECs with both bacteria and fungi were unchanged in the presence of pluronic. Results from studies given in Table 7-1 and a previous study by Nagant et al. [93,108] suggest that a concentration of ceragenin of 100 μg/mL is sufficient to eradicate established bacterial and fungal biofilms. Consequently, we used this concentration as a target for antibacterial and antifungal activity, as well as in tolerability studies with trachea and lung explants. A key preliminary question in these studies is whether the pluronic alone has any effect on bacteria and fungi. To answer this question, the target concentration of CSA-131 (100 μg/mL) was prepared with and without pluronic, and antibiofilm activity was measured (Figure 7-1).

Table 7-1: MICs of CSA-131 with bacteria and fungi in the absence or presence of pluronic.

	MIC [MBEC] (µg/mL)		
Strains	**CSA-131**	**CSA-131 + 4% pluronic**	**CSA-131 + 5% pluronic**
S. aureus ATCC 25923	1 [100]	1 [100]	1 [100]
P. aeruginosa ATCC 47085	2 [100]	2 [100]	2 [100]
C. auris CDC 382	0.5 [82]	0.5 [82]	0.5 [82]
C. auris CDC 384	0.5 [48]	0.5 [48]	0.5 [48]
C. auris CDC 387	0.5 [64]	0.5 [64]	0.5 [48]
C. auris CDC 389	0.5 [48]	0.5 [48]	0.5 [48]
C. albicans ATCC 90028	0.5 [48]	0.5 [48]	0.5 [48]

In addition, established biofilms were exposed to pluronic alone.In these assays, biofilms were generated over 48 h, and after treatment, bacterial and fungal counts were determined by plating organisms freed from biofilms and counting colonies. Detection limits for the experiments were two logs. At 100 µg/mL, with and without pluronic, CSA-131 lowered bacterial and fungal counts to the detection limit (>four-log reduction (99.99% reduction)). Pluronic alone did not significantly influence microbial counts from the biofilms.

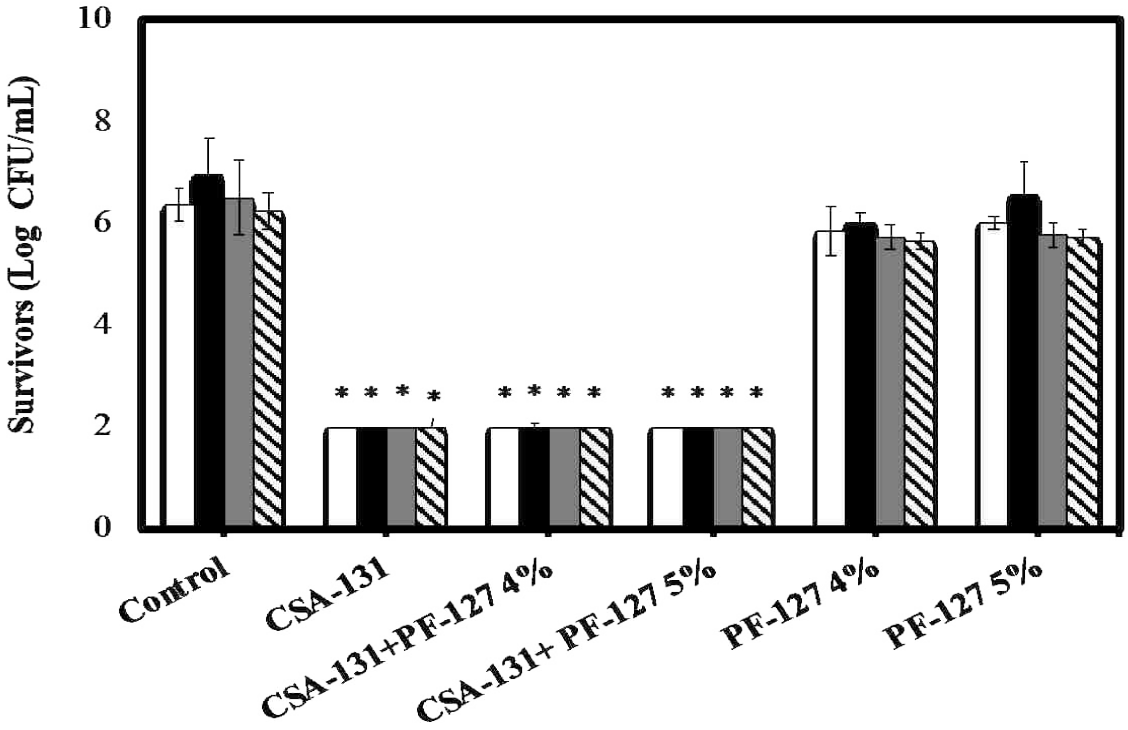

Figure 7-1: Antibiofilm results determined through the plating of microorganisms freed from biofilms, culturing, and plate counting. White bars: *S. aureus* (ATCC 25923); black bars: *P. aeruginosa* (ATCC 47085); gray bars: *C. albicans* (ATCC 90028); hashed bars: *C. auris* (CDC 384). Detection limit: 2 logs. * indicates $p < 0.05$ relative to controls and to pluronic alone.

To corroborate the antibiofilm data from counting bacterial and fungal colonies, a colorimetric assay was performed to quantify biofilms remaining on surfaces after treatment. Results were normalized to untreated controls (Figure 7-2). Significant decreases in biofilm were observed, but differences between CSA-131 alone and with pluronic were not significant.

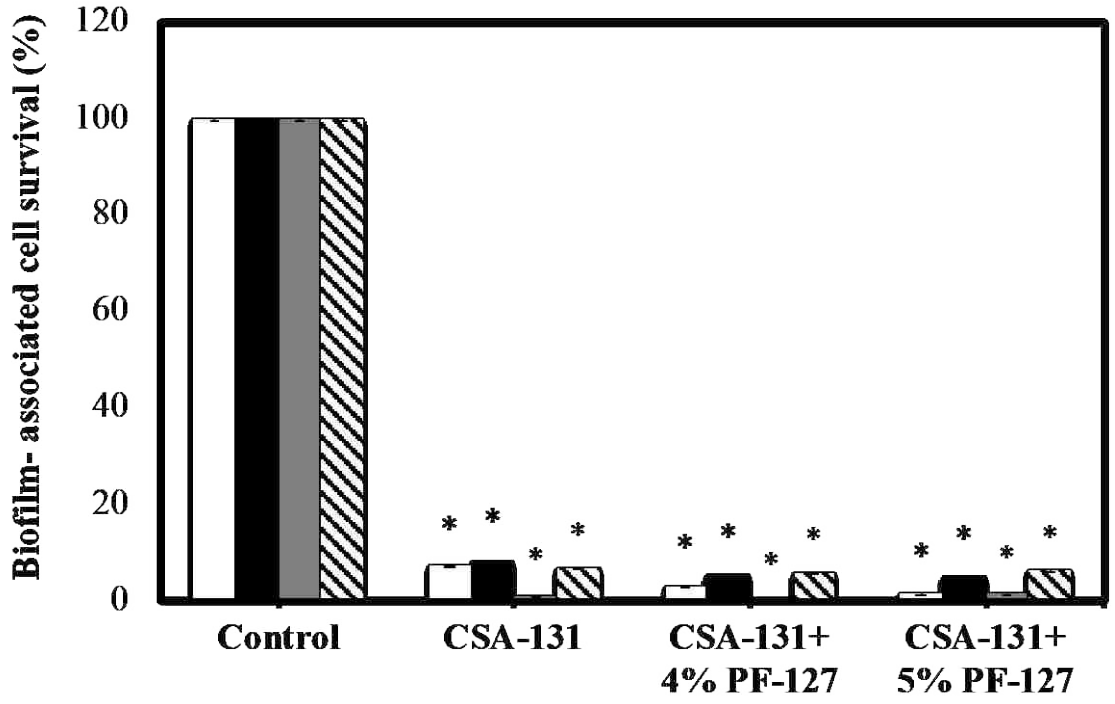

Figure 7-2: Antibiofilm results determined through colorimetric (XTT) assay represented as percent survival. White bars: *S. aureus* (ATCC 25923); black bars: *P. aeruginosa* (ATCC 47085); gray bars: *C. albicans* (ATCC 90028); hashed bars: *C. auris* (CDC 384). * indicates $p < 0.05$ relative to controls.

A possible consequence of the association of CSA-131 with pluronic micelles would be the slowing of the kinetic antimicrobial activities of this ceragenin relative to the ceragenin alone. We measured bacterial and fungal counts over time with CSA-131 (100 µg/mL) and CSA-131 with pluronic (4%). Results from an experiment with *P. aeruginosa* (ATCC 47085) are shown in Figure 7-3. Inocula of just over 10^6 CFU/mL were reduced to the detection limit within 15 min. At 5 min, there was a small difference in bacterial counts with CSA-131 alone and CSA-131 with pluronic. With *S. aureus* and with *C. albicans*, no significant differences between kinetic activity of the ceragenin alone and with pluronic were observed Figure 7-3.

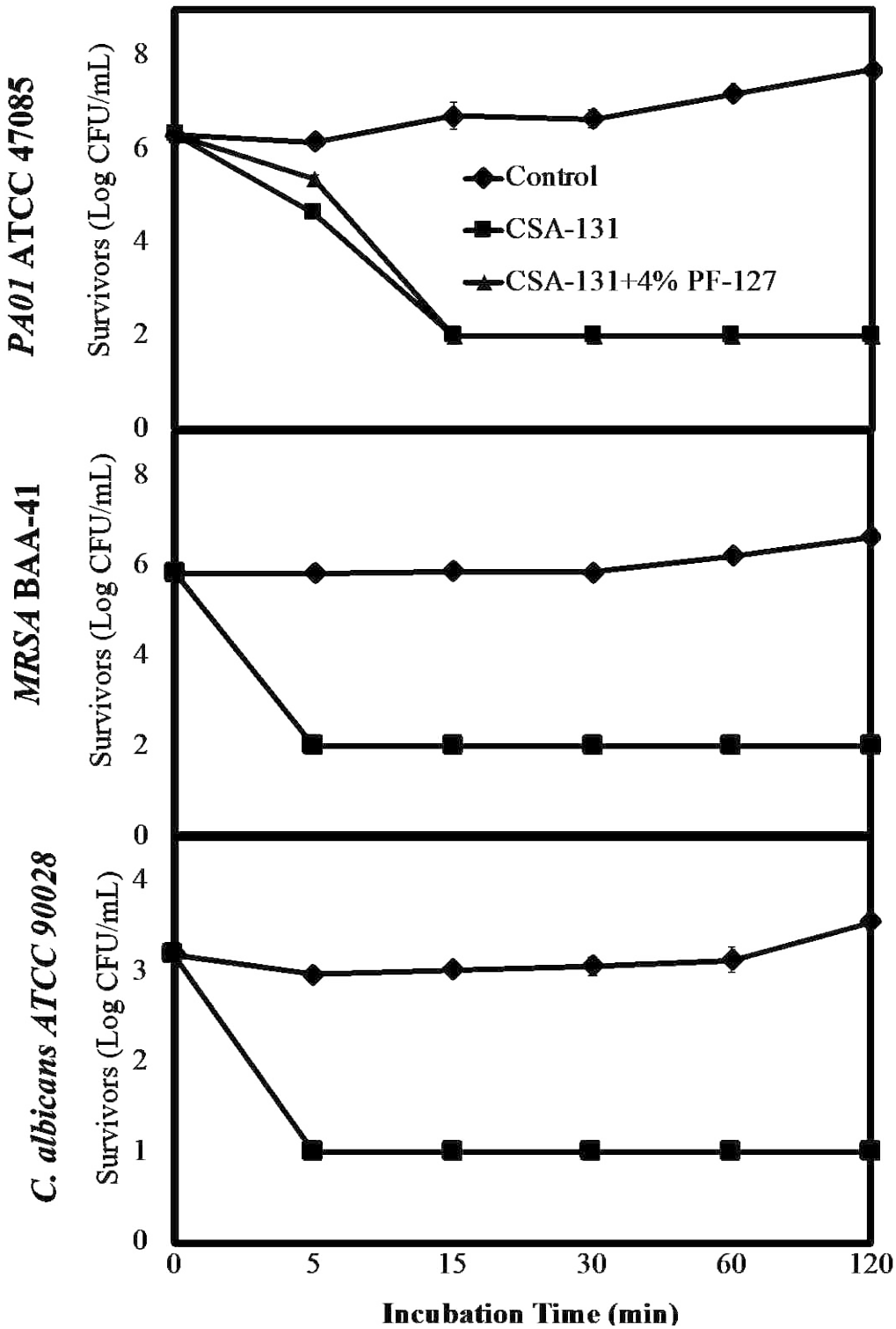

Figure 7-3: Kinetic antibacterial activity against *P. aeruginosa*, MRSA, and *C. albicans* of CSA-131 (100 _g/mL) (black squares), CSA-131 (100 _g/mL) with pluronic (4%) (black triangles); untreated control (black diamonds). Detection limit was two logs.

Having established the antibiofilm activity of CSA-131 in the presence of pluronic, we determined the impact of formulations of CSA-131 on ciliated tissue explants from porcine tracheas. The cilia on these tissues play a critical role in removing particulate matter from the lung and trachea; consequently, it was important to establish that CSA-131 can exert antibacterial and antifungal activity without damaging cilia. Furthermore, the presence of undamaged cilia is an indication that the underlying epithelial and goblet cells are unaffected by ceragenin treatment. An *ex vivo* assay was used to evaluate pluronic-containing formulations. In this assay the beating of cilia can be actively observed. These observations were used to determine the concentration of pluronic, with CSA-131 (100 μg/mL), that would prevent an impact on cilia function, and by extension leave the underlying epithelial and goblet cells undamaged [285]. This method involves sectioning porcine trachea which is supported in a nutrient medium, placing small beads on one side of the explant, and measuring the transfer (clearance) of the beads to the other side of the explants (Figure 7-4). In our hands, we could reproducibly measure bead clearance one hour after sectioning and treatment. Twelve explants were used for each test condition, and the results are reported as the number clearing beads in a given amount of time.

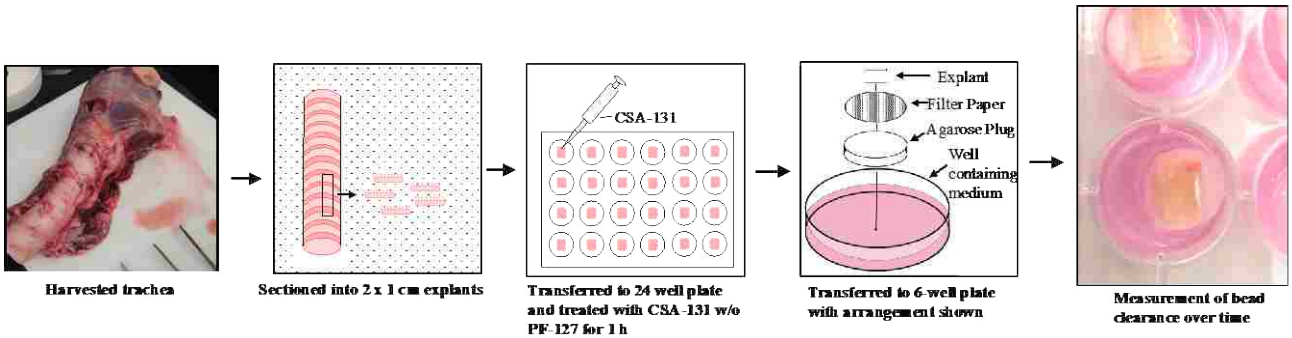

Figure 7-4: Description of methods used in harvesting and testing porcine trachea explants.

With no treatment with CSA-131, all 12 explants cleared the applied beads within 20 min, and 10 of the explants cleared the beads in less than 10 min (Table 7-1). Treatment of the explants with CSA-131 at 100 µg/mL for one hour caused a majority (six of 12) to lose the ability to clear the beads. Increasing amounts of pluronic (from 1 to 5%) restored the ability of the cilia to clear the beads, and at 5% pluronic, bead clearance was the same as the control.

Table 7-2: Number of explants (out of 12) clearing beads during the indicated amount of time after incubation with CSA-131 (100 µg/mL) for 1 h. The control was not treated with CSA-131. Indicated amounts of pluronic were used with ceragenin.

	Time Required for Bead Clearance			
Pluronic	**<10 min**	**<20 min**	**<30 min**	**No Clearance**
Control	10/12	2/12	-	-
0%	3/12	2/12	1/12	6/12
1%	4/12	2/12	1/12	5/12
2%	7/12	3/12	2/12	-
3%	7/12	4/12	1/12	-
4%	8/12	4/12	-	-
5%	10/12	2/12	-	-

To visualize the impacts of treatment of CSA-131, with and without pluronic, on cilia, we obtained scanning electron microscope (SEM) images of explants that had been treated with CSA-131 (100 µg/mL) alone and with pluronic (4%) (Figure 7-5). With the untreated explant, intact cilia were observed without exposure of the underlying goblet or epithelial cells. In the image of the explant treated with CSA-131 alone, exposed goblet cells were observed, suggesting that some loss of cilia had occurred. This loss correlated with decreased cilia function in the bead clearance assay. In contrast, with the explant treated with CSA-131 with pluronic (4%), a fully intact cilia

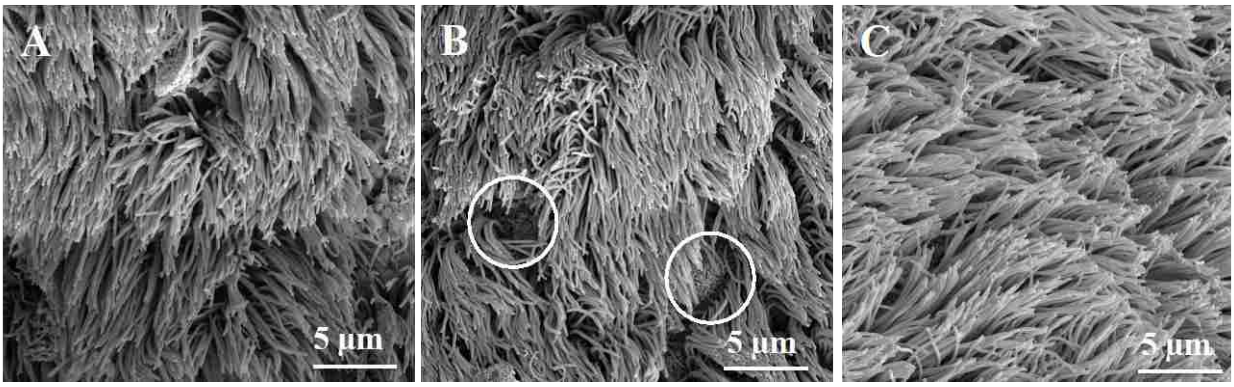

Figure 7-5: SEM images of cilia on porcine trachea explants **A**: untreated, **B**: treated with CSA-131 at 100 µg/mL, and **C**: treated with CSA-131 at 100 µg/mL with 4% pluronic. Exposed goblet cells are circled in the image from treatment with CSA-131 without pluronic.

bed was observed with no exposure of goblet or epithelial cells. This treatment did not influence bead clearance, and it did not appear to influence the cilia bed. Dias et al. observed a similar loss of cilia and concomitant exposure of goblet cells in canine trachea from intubated dogs [286].

We next verified that CSA-131, formulated with pluronic, was able to eradicate microorganisms in tissue from the trachea and lung. For these studies, explants were infected with either *C. albicans* or *C. auris* then treated with CSA-131 alone or with pluronic (4% or 5%). In control explants, fungal counts were over six logs in both tissue types (Figure 7-6). From treated explants, fungal counts were one and a half to two logs less (a decrease of up to 99%). Differences from controls were statistically significant ($p < 0.05$), but small differences between results with CSA-131 alone and CSA-131 with pluronic (4% or 5%) were not significant. Interestingly, there was no significant difference of fungal growth in the tracheal and lung explants.

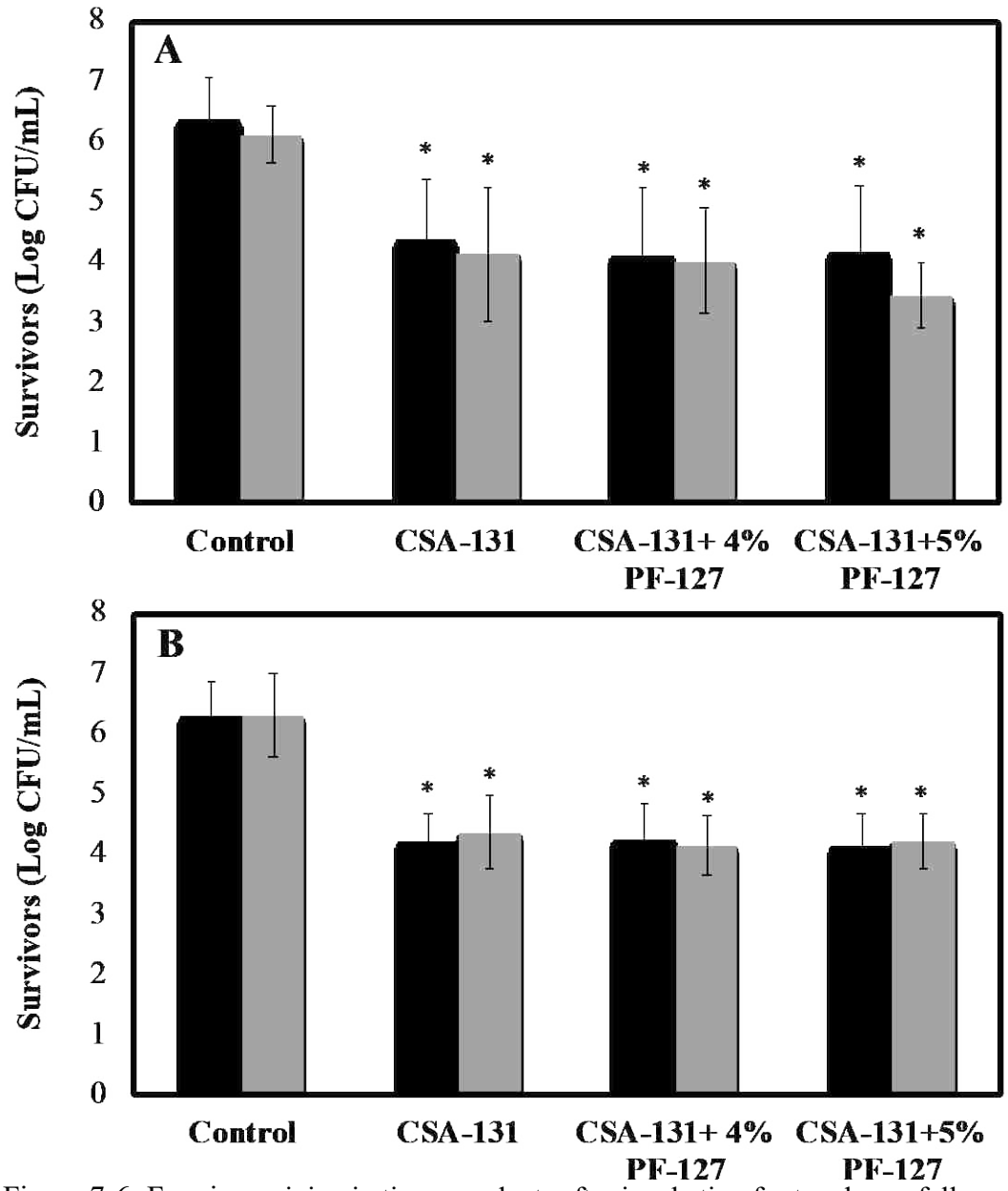

Figure 7-6: Fungi remaining in tissue explants after incubation for two hours followed by treatment with CSA-131 (with and without pluronic (4% or 5%) for one hour. Black bars: *C. albicans* (ATCC 90028); gray bars: *C. auris* (CDC 384). **A**: trachea explants; **B**: lung

7.4 Conclusions

Bacteria and fungi are both important pathogens in the trachea and lung, and infections are increasingly recognized as polymicrobial. Consequently, effective development of new therapies

should target a broad spectrum of bacteria and fungi. In addition, persistent infections, including those associated with CF, involve biofilm components, which adds an antibiofilm component to therapy development. AMPs play important roles in controlling microbial growth in these tissues; however, it is evident that in some situations these innate immune defenses fail to fully protect the trachea and lung. Considerations of means of augmenting the activities of AMPs are complicated by the susceptibility of cilia to damage, and since they play vital roles in these tissues, potential treatments must take into account impacts on cilia. Ceragenins have been shown to have potent activity against pathogens associated with the trachea and lung, including the ability to eradicate established biofilms. Nevertheless, concentrations of ceragenin CSA-131 necessary to eliminate biofilms cause cilia damage. To mitigate these effects on cilia, we employed the poloxamer Pluronic® F-127. The association of CSA-131 with micelles formed by this surfactant does not alter antimicrobial activity against planktonic or biofilm forms of targeted microorganisms. However, with pluronic, the impact of CSA-131 on cilia is abolished. *Ex vivo* studies of CSA-131 with pluronic demonstrate the ability of this ceragenin to substantially reduce numbers of pathogenic strains of fungi in tissue. As a mimic of AMPs and with the protective effects of pluronic, ceragenin CSA-131 appears to be well suited for the treatment of polymicrobial and biofilm-related infections.

Bibliography

1 Migliavacca, R. & Sambri, V. Antimicrobial resistance global emergence: healthcare facilities or environmental microbiota as the most important reservoir of antibiotic resistant microorganisms? *Microbiologia Medica* **31** (2016).

2 Simpkin, V. L., Renwick, M. J., Kelly, R. & Mossialos, E. Incentivising innovation in antibiotic drug discovery and development: progress, challenges and next steps. *The Journal of Antibiotics* (2017).

3 Theuretzbacher, U. J. C. M. & Infection. Antibiotic innovation for future public health needs. **23**, 713-717 (2017).

4 Simpkin, V. L., Renwick, M. J., Kelly, R. & Mossialos, E. J. T. J. o. a. Incentivising innovation in antibiotic drug discovery and development: Progress, challenges and next steps. **70**, 1087 (2017).

5 Padiyara, P., Inoue, H. & Sprenger, M. Global governance mechanisms to address antimicrobial resistance. *Infectious Diseases: Research and Treatment* **11**, 1178633718767887 (2018).

6 Simpkin, V. L., Renwick, M. J., Kelly, R. & Mossialos, E. Incentivising innovation in antibiotic drug discovery and development: progress, challenges and next steps. *The Journal of antibiotics* **70**, 1087 (2017).

7 Imler, J.-L. & Bulet, P. in *Mechanisms of epithelial defense* Vol. 86 1-21 (Karger Publishers, 2005).

8 Ebenhan, T., Gheysens, O., Kruger, H. G., Zeevaart, J. R. & Sathekge, M. M. Antimicrobial peptides: their role as infection-selective tracers for molecular imaging. *BioMed research international* **2014** (2014).

9 Ganz, T. The Role of Antimicrobial Peptides in Innate Immunity1. *Integr. Comp. Biol.* **43**, 300-304, doi:10.1093/icb/43.2.300 (2003).

10 Zasloff, M. Antimicrobial peptides of multicellular organisms. *nature* **415**, 389 (2002).

11 Peschel, A. & Sahl, H.-G. The co-evolution of host cationic antimicrobial peptides and microbial resistance. *Nature Reviews Microbiology* **4**, 529-536 (2006).

12 Mangoni, M. L., McDermott, A. M. & Zasloff, M. Antimicrobial peptides and wound healing: biological and therapeutic considerations. *Experimental dermatology* (2016).

13 Nang, S. C. *et al.* Fitness cost of mcr-1-mediated polymyxin resistance in Klebsiella pneumoniae. *Journal of Antimicrobial Chemotherapy* (2018).

14 Hashemi, M. M., Holden, B. S., Durnaś, B., Bucki, R. & Savage, P. B. Ceragenins as Mimics of Endogenous Antimicrobial Peptides. *Journal of Antimicrobial Agents* **3**, 141 (2017).

15 Diggins, F. W. The true history of the discovery of penicillin, with refutation of the misinformation in the literature. *Br. J. Biomed. Sci.* **56**, 83 (1999).

16 Hashemi, M. M., Aminlari, M. & Moosavinasab, M. Preparation of and studies on the functional properties and bactericidal activity of the lysozyme–xanthan gum conjugate. *LWT - Food Science and Technology* **57**, 594-602, doi:http://dx.doi.org/10.1016/j.lwt.2014.01.040 (2014).

17 Aminlari, L., Hashemi, M. M. & Aminlari, M. Modified lysozymes as novel broad spectrum natural antimicrobial agents in foods. *J. Food Sci.* **79**, R1077-1090, doi:10.1111/1750-3841.12460 (2014).

18 Hashemi, M. M. *et al.* Production and Application of Lysozyme-Gum Arabic Conjugate in Mayonnaise as a Natural Preservative and Emulsifier. *Polish journal of food and nutrition sciences*, DOI: 10.1515/pjfns-2017-0011 (2017).
19 Zhang, L.-j. & Gallo, R. L. Antimicrobial peptides. *Curr. Biol.* **26**, R14-R19 (2016).
20 Jung, Y.-J. & Kang, K.-K. Application of antimicrobial peptides for disease control in plants. *Plant Breeding and Biotechnology* **2**, 1-13 (2014).
21 Soyeurt, H. *et al.* Genetic variability of lactoferrin content estimated by mid-infrared spectrometry in bovine milk. *Journal of dairy science* **90**, 4443-4450 (2007).
22 Giacometti, A. *et al.* Comparative activities of cecropin A, melittin, and cecropin A–melittin peptide CA(1–7)M(2–9)NH2 against multidrug-resistant nosocomial isolates of Acinetobacter baumannii. *Peptides* **24**, 1315-1318, doi:http://dx.doi.org/10.1016/j.peptides.2003.08.003 (2003).
23 Bahar, A. A. & Ren, D. Antimicrobial Peptides. *Pharmaceuticals* **6**, 1543-1575, doi:10.3390/ph6121543 (2013).
24 Zasloff, M. Magainins, a class of antimicrobial peptides from Xenopus skin: isolation, characterization of two active forms, and partial cDNA sequence of a precursor. *Proceedings of the National Academy of Sciences* **84**, 5449-5453 (1987).
25 Choi, S.-K. *et al.* Identification of a polymyxin synthetase gene cluster of Paenibacillus polymyxa and heterologous expression of the gene in Bacillus subtilis. *Journal of bacteriology* **191**, 3350-3358 (2009).
26 Xu, L. *et al.* Complete genome sequence and comparative genomic analyses of the vancomycin-producing Amycolatopsis orientalis. *BMC Genomics* **15**, 363 (2014).
27 Daphny, C. S., Bibiana, M. A., Vengatesan, R., Selvamani, P. & Latha, S. Antimicrobial peptides-A milestone for developing antibiotics against drug resistant infectious pathogens. *J. Pharm. Sci. Res.* **7**, 226-230 (2015).
28 Wang, G. in *Computational Peptidology* 43-66 (Springer, 2015).
29 Johansson, J., Gudmundsson, G. H., Rottenberg, M. n. E., Berndt, K. D. & Agerberth, B. Conformation-dependent antibacterial activity of the naturally occurring human peptide LL-37. *Journal of Biological Chemistry* **273**, 3718-3724 (1998).
30 Patch, J. A. & Barron, A. E. Helical peptoid mimics of magainin-2 amide. *Journal of the American Chemical Society* **125**, 12092-12093 (2003).
31 Lehrer, R. I., Bevins, C. L. & Ganz, T. in *Mucosal Immunology, Two-Volume Set* (Elsevier Inc., 2005).
32 Mojsoska, B. & Jenssen, H. Peptides and peptidomimetics for antimicrobial drug design. *Pharmaceuticals* **8**, 366-415 (2015).
33 Hartmann, M. *et al.* Damage of the Bacterial Cell Envelope by Antimicrobial Peptides Gramicidin S and PGLa as Revealed by Transmission and Scanning Electron Microscopy. *Antimicrobial Agents and Chemotherapy* **54**, 3132-3142, doi:10.1128/aac.00124-10 (2010).
34 Rosenfeld, Y. & Shai, Y. Lipopolysaccharide (Endotoxin)-host defense antibacterial peptides interactions: role in bacterial resistance and prevention of sepsis. *Biochimica et Biophysica Acta (BBA)-Biomembranes* **1758**, 1513-1522 (2006).
35 Ding, B. *et al.* Correlation of the Antibacterial Activities of Cationic Peptide Antibiotics and Cationic Steroid Antibiotics. *Journal of Medicinal Chemistry* **45**, 663-669, doi:10.1021/jm0105070 (2002).

36 Sato, H. & Feix, J. B. Peptide–membrane interactions and mechanisms of membrane destruction by amphipathic α-helical antimicrobial peptides. *Biochimica et Biophysica Acta (BBA)-Biomembranes* **1758**, 1245-1256 (2006).
37 Ganz, T. & Lehrer, R. I. Antimicrobial peptides of vertebrates. *Curr. Opin. Immunol.* **10**, 41-44 (1998).
38 Loeffler, J. M., Nelson, D. & Fischetti, V. A. Rapid killing of Streptococcus pneumoniae with a bacteriophage cell wall hydrolase. *Science* **294**, 2170-2172 (2001).
39 Jenssen, H., Hamill, P. & Hancock, R. E. W. Peptide Antimicrobial Agents. *Clinical Microbiology Reviews* **19**, 491-511, doi:10.1128/cmr.00056-05 (2006).
40 Sun, Y. & Shang, D. J. M. o. i. Inhibitory effects of antimicrobial peptides on lipopolysaccharide-induced inflammation. **2015** (2015).
41 Mangoni, M. L., McDermott, A. M. & Zasloff, M. Antimicrobial peptides and wound healing: biological and therapeutic considerations. *Experimental dermatology* **25**, 167-173 (2016).
42 Olekson, M., You, T., Savage, P. B. & Leung, K. P. Ceragenin peptide-mimics inhibit biofilms and affect mammalian cell viability and migration in vitro. *FEBS Open Bio* (2017).
43 Heilborn, J. D. *et al.* The cathelicidin anti-microbial peptide LL-37 is involved in re-epithelialization of human skin wounds and is lacking in chronic ulcer epithelium. *Journal of Investigative Dermatology* **120**, 379-389 (2003).
44 Epand, R. M., Epand, R. F. & Savage, P. B. Ceragenins (cationic steroid compounds), a novel class of antimicrobial agents. *Drug News Perspect* **21**, 307-311 (2008).
45 Guan, Q. *et al.* Preparation and characterization of cholic acid-derived antimicrobial agents with controlled stabilities. *Organic letters* **2**, 2837-2840 (2000).
46 Savage, P. B. & Li, C. Cholic acid derivatives: novel antimicrobials. *Expert opinion on investigational drugs* **9**, 263-272 (2000).
47 Li, C. *et al.* Antimicrobial activities of amine-and guanidine-functionalized cholic acid derivatives. *Antimicrobial agents and chemotherapy* **43**, 1347-1349 (1999).
48 Isogai, E., Isogai, H., Takahashi, K., Okumura, K. & Savage, P. B. Ceragenin CSA-13 exhibits antimicrobial activity against cariogenic and periodontopathic bacteria. *Oral Microbiology and Immunology* **24**, 170-172, doi:10.1111/j.1399-302X.2008.00464.x (2009).
49 Surel, U., Niemirowicz, K., Marzec, M., Savage, P. B. & Bucki, R. Ceragenins–a new weapon to fight multidrug resistant bacterial infections. *Studia Medyczne* **30**, 207-213 (2014).
50 Li, C., Peters, A. S., Meredith, E. L., Allman, G. W. & Savage, P. B. Design and Synthesis of Potent Sensitizers of Gram-Negative Bacteria Based on a Cholic Acid Scaffolding. *Journal of the American Chemical Society* **120**, 2961-2962, doi:10.1021/ja973881r (1998).
51 Ding, B., Taotofa, U., Orsak, T., Chadwell, M. & Savage, P. B. Synthesis and Characterization of Peptide− Cationic Steroid Antibiotic Conjugates. *Organic letters* **6**, 3433-3436 (2004).
52 Savage, P. B., Li, C., Taotafa, U., Ding, B. & Guan, Q. Antibacterial properties of cationic steroid antibiotics. *FEMS microbiology letters* **217**, 1-7 (2002).
53 Li, C., Dalley, N. K. & Savage, P. B. Short syntheses of triamine derivatives of cholic acid. *Tetrahedron Lett.* **40**, 1861-1864 (1999).
54 Lai, X.-Z. *et al.* Ceragenins: cholic acid-based mimics of antimicrobial peptides. *Accounts of chemical research* **41**, 1233-1240 (2008).

55 Schmidt, E. J. *et al.* Activities of cholic acid-derived antimicrobial agents against multidrug-resistant bacteria. *Journal of Antimicrobial Chemotherapy* **47**, 671-674 (2001).
56 Lai, X. Z. *et al.* Ceragenins: cholic acid-based mimics of antimicrobial peptides. *Acc Chem Res* **41**, doi:10.1021/ar700270t (2008).
57 Zhou, X.-T., Rehman, A.-u., Li, C. & Savage, P. B. Preparation of a protected triamino analogue of cholic acid and sequential incorporation of amino acids in solution and on a solid support. *Organic letters* **2**, 3015-3018 (2000).
58 Taotafa, U., McMullin, D. B., Lee, S. C., Hansen, L. D. & Savage, P. B. Anionic facial amphiphiles from cholic acid. *Organic letters* **2**, 4117-4120 (2000).
59 Savage, P. B. Cationic steroid antibiotics. *Current Medicinal Chemistry-Anti-Infective Agents* **1**, 293-304 (2002).
60 Savage, P. B. Multidrug-resistant bacteria: overcoming antibiotic permeability barriers of gram-negative bacteria. *Annals of medicine* **33**, 167-171 (2001).
61 Wimley, W. C. Describing the mechanism of antimicrobial peptide action with the interfacial activity model. *ACS chemical biology* **5**, 905 (2010).
62 Bucki, R. *et al.* Inactivation of Endotoxin by Human Plasma Gelsolin. *Biochemistry* **44**, 9590-9597, doi:10.1021/bi0503504 (2005).
63 Bucki, R., Sostarecz, A. G., Byfield, F. J., Savage, P. B. & Janmey, P. A. Resistance of the antibacterial agent ceragenin CSA-13 to inactivation by DNA or F-actin and its activity in cystic fibrosis sputum. *Journal of Antimicrobial Chemotherapy* **60**, 535-545, doi:10.1093/jac/dkm218 (2007).
64 Chileveru, H. R. *et al.* Visualizing Attack of Escherichia coli by the Antimicrobial Peptide Human Defensin 5. *Biochemistry* **54**, 1767-1777, doi:10.1021/bi501483q (2015).
65 Choi, H., Rangarajan, N. & Weisshaar, J. C. Lights, camera, action! Antimicrobial peptide mechanisms imaged in space and time. *Trends in microbiology* **24**, 111-122 (2016).
66 Meincken, M., Holroyd, D. L. & Rautenbach, M. Atomic Force Microscopy Study of the Effect of Antimicrobial Peptides on the Cell Envelope of Escherichia coli. *Antimicrobial Agents and Chemotherapy* **49**, 4085-4092, doi:10.1128/aac.49.10.4085-4092.2005 (2005).
67 Ding, B. *et al.* Origins of cell selectivity of cationic steroid antibiotics. *Journal of the American Chemical Society* **126**, 13642-13648 (2004).
68 Pogoda, K. *et al.* Stiffening of bacteria cells as a first manifestation of bactericidal attack. *Micron* **101**, 95-102 (2017).
69 Kichler, A., Leborgne, C., Savage, P. B. & Danos, O. Cationic steroid antibiotics demonstrate DNA delivery properties. *Journal of controlled release* **107**, 174-182 (2005).
70 Howell, M. D. *et al.* Ceragenins: a class of antiviral compounds to treat orthopox infections. *J Invest Dermatol* **129**, doi:10.1038/jid.2009.120 (2009).
71 Wnorowska, U. *et al.* Bactericidal Activities of Cathelicidin LL-37 and Select Cationic Lipids against the Hypervirulent Pseudomonas aeruginosa Strain LESB58. *Antimicrobial Agents and Chemotherapy* **59**, 3808-3815, doi:10.1128/aac.00421-15 (2015).
72 Chin, J. N., Jones, R. N., Sader, H. S., Savage, P. B. & Rybak, M. J. Potential synergy activity of the novel ceragenin, CSA-13, against clinical isolates of Pseudomonas aeruginosa, including multidrug-resistant P. aeruginosa. *Journal of antimicrobial chemotherapy* **61**, 365-370 (2008).
73 Chin, J. N., Rybak, M. J., Cheung, C. M. & Savage, P. B. Antimicrobial activities of ceragenins against clinical isolates of resistant Staphylococcus aureus. *Antimicrobial agents and chemotherapy* **51**, 1268-1273 (2007).

74 Bozkurt-Guzel, C., Savage, P. B., Akcali, A. & Ozbek-Celik, B. Potential synergy activity of the novel ceragenin, CSA-13, against carbapenem-resistant Acinetobacter baumannii strains isolated from bacteremia patients. *BioMed research international* **2014** (2014).
75 Leszczyńska, K. *et al.* Antibacterial activity of the human host defence peptide LL-37 and selected synthetic cationic lipids against bacteria associated with oral and upper respiratory tract infections. *Journal of Antimicrobial Chemotherapy* **68**, 610-618 (2013).
76 Saha, S., Savage, P. & Bal, M. Enhancement of the efficacy of erythromycin in multiple antibiotic‐resistant gram‐negative bacterial pathogens. *Journal of applied microbiology* **105**, 822-828 (2008).
77 Li, C., Budge, L. P., Street, S. E. & Savage, P. B. Preparation of amino acid-appended cholic acid derivatives as sensitizers of Gram-negative bacteria. *Tetrahedron Lett.* **40**, 1865-1868 (1999).
78 Bozkurt-Guzel, C., Savage, P. B. & Gerceker, A. A. In vitro activities of the novel ceragenin CSA-13, alone or in combination with colistin, tobramycin, and ciprofloxacin, against Pseudomonas aeruginosa strains isolated from cystic fibrosis patients. *Chemotherapy* **57**, 505-510 (2012).
79 Jones, J. W., Shaffer, S. A., Ernst, R. K., Goodlett, D. R. & Tureček, F. Determination of pyrophosphorylated forms of lipid A in Gram-negative bacteria using a multivaried mass spectrometric approach. *Proceedings of the National Academy of Sciences* **105**, 12742-12747, doi:10.1073/pnas.0800445105 (2008).
80 Leszczyńska, K. *et al.* Potential of ceragenin CSA-13 and its mixture with pluronic F-127 as treatment of topical bacterial infections. *J Appl Microbiol* **110**, doi:10.1111/j.1365-2672.2010.04874.x (2011).
81 Zhang, M. *et al.* Floricolin C elicits intracellular ROS accumulation and disrupts mitochondria to exert fungicidal action. *FEMS Yeast Res.* (2018).
82 Durnaś, B. *et al.* Candidacidal Activity of Selected Ceragenins and Human Cathelicidin LL-37 in Experimental Settings Mimicking Infection Sites. *PloS one* **11**, e0157242 (2016).
83 Tsai, P.-W., Cheng, Y.-L., Hsieh, W.-P. & Lan, C.-Y. Responses of Candida albicans to the human antimicrobial peptide LL-37. *Journal of microbiology* **52**, 581-589 (2014).
84 Lee, H., Hwang, J.-S. & Lee, D. G. Scolopendin, an antimicrobial peptide from centipede, attenuates mitochondrial functions and triggers apoptosis in Candida albicans. *Biochemical Journal* **474**, 635-645 (2017).
85 Lee, J. & Lee, D. G. Melittin triggers apoptosis in Candida albicans through the reactive oxygen species-mediated mitochondria/caspase-dependent pathway. *FEMS microbiology letters* **355**, 36-42 (2014).
86 Wong, J. H. *et al.* Antifungal action of human cathelicidin fragment (LL13–37) on Candida albicans. *Peptides* **32**, 1996-2002 (2011).
87 Niemirowicz, K. *et al.* Formulation and candidacidal activity of magnetic nanoparticles coated with cathelicidin LL-37 and ceragenin CSA-13. *Scientific Reports* **7** (2017).
88 Davey, M. E. & O'toole, G. A. Microbial biofilms: from ecology to molecular genetics. *Microbiology and molecular biology reviews* **64**, 847-867 (2000).
89 Percival, S. L., Suleman, L., Vuotto, C. & Donelli, G. Healthcare-associated infections, medical devices and biofilms: risk, tolerance and control. *J. Med. Microbiol.* **64**, 323-334 (2015).
90 Kohanski, M. A., Dwyer, D. J. & Collins, J. J. How antibiotics kill bacteria: from targets to networks. *Nature Reviews Microbiology* **8**, 423 (2010).

91 Pollard, J. *et al.* Activities of ceragenin CSA-13 against established biofilms in an in vitro model of catheter decolonization. *Anti-Infective Agents in Medicinal Chemistry (Formerly Current Medicinal Chemistry-Anti-Infective Agents)* **8**, 290-294 (2009).
92 Nagant, C. *et al.* Effect of a low concentration of a cationic steroid antibiotic (CSA‐13) on the formation of a biofilm by Pseudomonas aeruginosa. *Journal of applied microbiology* **111**, 763-772 (2011).
93 Nagant, C. *et al.* Study of the effect of antimicrobial peptide mimic, CSA‐13, on an established biofilm formed by Pseudomonas aeruginosa. *Microbiologyopen* **2**, 318-325 (2013).
94 Piktel, E., Pogoda, K., Savage, P. B. & Bucki, R. (Future Medicine, 2017).
95 Tan, I. S. & Ramamurthi, K. S. Spore formation in Bacillus subtilis. *Environmental microbiology reports* **6**, 212-225 (2014).
96 Piktel, E. *et al.* Sporicidal activity of ceragenin CSA-13 against Bacillus subtilis. *Scientific Reports* **7**, 44452 (2017).
97 Yasin, B. *et al.* θ Defensins protect cells from infection by herpes simplex virus by inhibiting viral adhesion and entry. *J. Virol.* **78**, 5147-5156 (2004).
98 Park, Y., Jang, S. H., Lee, D. G. & Hahm, K. S. Antinematodal effect of antimicrobial peptide, PMAP‐23, isolated from porcine myeloid against Caenorhabditis elegans. *Journal of Peptide Science* **10**, 304-311 (2004).
99 Lara, D., Feng, Y., Bader, J., Savage, P. B. & Maldonado, R. A. Anti-trypanosomatid activity of ceragenins. *Journal of Parasitology* **96**, 638-642 (2010).
100 Niederkorn, J. Y., Alizadeh, H., Leher, H. & McCulley, J. P. The pathogenesis of Acanthamoeba keratitis. *Microbes and Infection* **1**, 437-443 (1999).
101 Polat, Z. A., Savage, P. B. & Genberg, C. In vitro amoebicidal activity of a ceragenin, cationic steroid antibiotic-13, against Acanthamoeba castellanii and its cytotoxic potential. *Journal of Ocular Pharmacology and Therapeutics* **27**, 1-5 (2011).
102 Polat, Z. A., Cetin, A. & Savage, P. B. Evaluation of the in vitro activity of ceragenins against Trichomonas vaginalis. *Acta Parasitologica* **61**, 376-381 (2016).
103 Bucki, R., Namiot, D. B., Namiot, Z., Savage, P. B. & Janmey, P. A. Salivary mucins inhibit antibacterial activity of the cathelicidin-derived LL-37 peptide but not the cationic steroid CSA-13. *Journal of Antimicrobial Chemotherapy* **62**, 329-335, doi:10.1093/jac/dkn176 (2008).
104 Bucki, R. *et al.* Targeting polyelectrolyte networks in purulent body fluids to modulate bactericidal properties of some antibiotics. *Infection and drug resistance* **11**, 77-86 (2018).
105 Moscoso, M., Esteban-Torres, M., Menéndez, M. & García, E. In Vitro Bactericidal and Bacteriolytic Activity of Ceragenin CSA-13 against Planktonic Cultures and Biofilms of Streptococcus pneumoniae and Other Pathogenic Streptococci. *PLoS ONE* **9**, e101037, doi:10.1371/journal.pone.0101037 (2014).
106 Nagant, C. *et al.* Interaction between tobramycin and CSA-13 on clinical isolates of Pseudomonas aeruginosa in a model of young and mature biofilms. *Applied microbiology and biotechnology* **88**, 251-263 (2010).
107 Escobar-Chávez, J. J. *et al.* Applications of thermo-reversible pluronic F-127 gels in pharmaceutical formulations. *J. Pharm. Pharm. Sci.* **9**, 339-358 (2006).
108 Nagant, C., Savage, P. & Dehaye, J.-P. Effect of pluronic acid F‐127 on the toxicity towards eukaryotic cells of CSA‐13, a cationic steroid analogue of antimicrobial peptides. *Journal of applied microbiology* **112**, 1173-1183 (2012).

109 Hoppens, M. A. *et al.* Ceragenin Mediated Selectivity of Antimicrobial Silver Nanoparticles. *ACS Applied Materials & Interfaces* **6**, 13900-13908, doi:10.1021/am504640f (2014).
110 Niemirowicz, K. *et al.* Bactericidal activity and biocompatibility of ceragenin-coated magnetic nanoparticles. *Journal of Nanobiotechnology* **13**, 1-11, doi:10.1186/s12951-015-0093-5 (2015).
111 Niemirowicz, K. *et al.* Core–shell magnetic nanoparticles display synergistic antibacterial effects against Pseudomonas aeruginosa and Staphylococcus aureus when combined with cathelicidin LL-37 or selected ceragenins. *International Journal of Nanomedicine* **11**, 5443-5455, doi:10.2147/IJN.S113706 (2016).
112 Durnaś, B. *et al.* Anaerobic bacteria growth in the presence of cathelicidin LL-37 and selected ceragenins delivered as magnetic nanoparticles cargo. *BMC Microbiol.* **17**, 167 (2017).
113 Szczotka-Flynn, L. B., Pearlman, E. & Ghannoum, M. Microbial contamination of contact lenses, lens care solutions, and their accessories: a literature review. *Eye & contact lens* **36**, 116 (2010).
114 Gu, X. *et al.* Optimization of ceragenins for prevention of bacterial colonization of hydrogel contact lensesceragenins for contact lenses. *Investigative ophthalmology & visual science* **54**, 6217-6223 (2013).
115 Darouiche, R. O. Treatment of infections associated with surgical implants. *New England Journal of Medicine* **350**, 1422-1429 (2004).
116 Hetrick, E. M. & Schoenfisch, M. H. Reducing implant-related infections: active release strategies. *Chemical Society Reviews* **35**, 780-789 (2006).
117 Costerton, J. W. Biofilm theory can guide the treatment of device-related orthopaedic infections. *Clinical Orthopaedics and Related Research®* **437**, 7-11 (2005).
118 Williams, D. L., Sinclair, K. D., Jeyapalina, S. & Bloebaum, R. D. Characterization of a novel active release coating to prevent biofilm implant ‐ related infections. *Journal of Biomedical Materials Research Part B: Applied Biomaterials* **101**, 1078-1089 (2013).
119 Williams, D. L. *et al.* In vivo efficacy of a silicone–cationic steroid antimicrobial coating to prevent implant-related infection. *Biomaterials* **33**, 8641-8656, doi:http://dx.doi.org/10.1016/j.biomaterials.2012.08.003 (2012).
120 Sinclair, K. D. *et al.* Model development for determining the efficacy of a combination coating for the prevention of perioperative device related infections: a pilot study. *Journal of Biomedical Materials Research Part B: Applied Biomaterials* **101**, 1143-1153 (2013).
121 Scott, M. G., Davidson, D. J., Gold, M. R., Bowdish, D. & Hancock, R. E. The human antimicrobial peptide LL-37 is a multifunctional modulator of innate immune responses. *The Journal of Immunology* **169**, 3883-3891 (2002).
122 Schindeler, A. *et al.* Local delivery of the cationic steroid antibiotic CSA-90 enables osseous union in a rat open fracture model of Staphylococcus aureus infection. *J Bone Joint Surg Am* **97**, 302-309 (2015).
123 Epand, R. F., Savage, P. B. & Epand, R. M. Bacterial lipid composition and the antimicrobial efficacy of cationic steroid compounds (Ceragenins). *Biochimica et Biophysica Acta (BBA)-Biomembranes* **1768**, 2500-2509 (2007).
124 Nibbering, P. *et al.* Radiolabelled antimicrobial peptides for imaging of infections: A review. *Nuclear medicine communications* **19**, 1117-1122 (1998).

125 Hoppens, M. A. *et al.* Maghemite, silver, ceragenin conjugate particles for selective binding and contrast of bacteria. *J Colloid Interface Sci* **413**, doi:10.1016/j.jcis.2013.09.016 (2014).
126 Roohi, S. *et al.* Preparation, quality control and biological evaluation of 99mTc-labelled cationic steroid antibiotic (CSA-13). *Radiochimica Acta International journal for chemical aspects of nuclear science and technology* **97**, 57-62 (2009).
127 Zahoor, R. *et al.* Synthesis of 99mTc-cationic steroid antimicrobial-107 and in vitro evaluation. *Journal of Radioanalytical and Nuclear Chemistry* **295**, 841-844 (2013).
128 Leszczynska, K. *et al.* Bactericidal activities of the cationic steroid CSA-13 and the cathelicidin peptide LL-37 against Helicobacter pylori in simulated gastric juice. *BMC Microbiol* **9**, 187, doi:10.1186/1471-2180-9-187 (2009).
129 Trainor, E. A., Horton, K. E., Savage, P. B., Testerman, T. L. & McGee, D. J. Role of the HefC Efflux Pump in Helicobacter pylori Cholesterol-Dependent Resistance to Ceragenins and Bile Salts. *Infection and Immunity* **79**, 88-97, doi:10.1128/iai.00974-09 (2011).
130 Wang, J. *et al.* Ceragenin CSA13 Reduces Clostridium difficile Infection in Mice by Modulating the Intestinal Microbiome and Metabolites. *Gastroenterology* (2018).
131 Pfalzgraff, A. *et al.* Antimicrobial endotoxin‐neutralizing peptides promote keratinocyte migration via P2X7 receptor activation and accelerate wound healing in vivo. *Br. J. Pharmacol.* (2018).
132 Bucki, R. *et al.* Bactericidal Activity of Ceragenin CSA-13 in Cell Culture and in an Animal Model of Peritoneal Infection. *Antimicrobial agents and chemotherapy* **59**, 6274-6282 (2015).
133 Rojas, L. J. *et al.* Colistin Resistance in Carbapenem-Resistant Klebsiella pneumoniae: Laboratory Detection and Impact on Mortality. *Clinical Infectious Diseases*, ciw805 (2016).
134 McGann, P. *et al.* Escherichia coli Harboring mcr-1 and blaCTX-M on a Novel IncF Plasmid: First Report of mcr-1 in the United States. *Antimicrobial Agents and Chemotherapy* **60**, 4420-4421, doi:10.1128/aac.01103-16 (2016).
135 Schwarz, S. & Johnson, A. P. Transferable resistance to colistin: a new but old threat. *Journal of Antimicrobial Chemotherapy*, doi:10.1093/jac/dkw274 (2016).
136 Cheng, Y. H. *et al.* Colistin resistance mechanisms in Klebsiella pneumoniae strains from Taiwan. *Antimicrob Agents Chemother* **59**, 2909-2913, doi:10.1128/AAC.04763-14 (2015).
137 Lim, L. M. *et al.* Resurgence of Colistin: A Review of Resistance, Toxicity, Pharmacodynamics, and Dosing. *Pharmacotherapy* **30**, 1279-1291, doi:10.1592/phco.30.12.1279 (2010).
138 Gao, R. *et al.* Dissemination and Mechanism for the MCR-1 Colistin Resistance. *PLoS pathogens* **12**, e1005957 (2016).
139 Castanheira, M. *et al.* Detection of mcr-1 among Escherichia coli clinical isolates collected worldwide as part of the SENTRY Antimicrobial Surveillance Program during 2014-2015. *Antimicrobial Agents and Chemotherapy*, doi:10.1128/aac.01267-16 (2016).
140 Chen, H.-L. *et al.* Identification of a novel antimicrobial peptide from human hepatitis B virus core protein arginine-rich domain (ARD). *PLoS Pathog* **9**, e1003425 (2013).
141 Peters, B. M., Shirtliff, M. E. & Jabra-Rizk, M. A. Antimicrobial peptides: primeval molecules or future drugs? *PLoS Pathog* **6**, e1001067 (2010).

142 Epand, R. F., Pollard, J. E., Wright, J. O., Savage, P. B. & Epand, R. M. Depolarization, Bacterial Membrane Composition, and the Antimicrobial Action of Ceragenins. *Antimicrobial Agents and Chemotherapy* **54**, 3708-3713, doi:10.1128/aac.00380-10 (2010).
143 Deslouches, B. *et al.* Engineered Cationic Antimicrobial Peptides To Overcome Multidrug Resistance by ESKAPE Pathogens. *Antimicrobial agents and chemotherapy* **59**, 1329-1333 (2015).
144 Ouhara, K. *et al.* Susceptibilities of periodontopathogenic and cariogenic bacteria to antibacterial peptides, β-defensins and LL37, produced by human epithelial cells. *Journal of Antimicrobial Chemotherapy* **55**, 888-896 (2005).
145 Hashemi, M. M., Aminlari, M. & Moosavinasab, M. Preparation of and studies on the functional properties and bactericidal activity of the lysozyme–xanthan gum conjugate. *LWT-Food Science and Technology* **57**, 594-602 (2014).
146 Raetz, C. R., Reynolds, C. M., Trent, M. S. & Bishop, R. E. Lipid A modification systems in gram-negative bacteria. *Annual review of biochemistry* **76**, 295 (2007).
147 Gunn, J. S. Bacterial modification of LPS and resistance to antimicrobial peptides. *Journal of endotoxin research* **7**, 57-62 (2001).
148 Richter, S. N. *et al.* Transfer of KPC-2 Carbapenemase from Klebsiella pneumoniae to Escherichia coli in a Patient: First Case in Europe. *Journal of Clinical Microbiology* **49**, 2040-2042, doi:10.1128/jcm.00133-11 (2011).
149 Goren, M. G. *et al.* Transfer of Carbapenem-Resistant Plasmid from Klebsiella pneumoniae ST258 to Escherichia coli in Patient. *Emerging Infectious Diseases* **16**, 1014-1017, doi:10.3201/eid1606.091671 (2010).
150 Wikler, M. A. *Methods for dilution antimicrobial susceptibility tests for bacteria that grow aerobically: approved standard*. (Clinical and Laboratory Standards Institute, 2006).
151 Pollard, J. E. *et al.* In vitro evaluation of the potential for resistance development to ceragenin CSA-13. *J Antimicrob Chemother* **67**, 2665-2672, doi:10.1093/jac/dks276 (2012).
152 Olajuyigbe, O. O. & Afolayan, A. J. In Vitro Antibacterial and Time-Kill Evaluation of the Erythrina caffra Thunb. Extract against Bacteria Associated with Diarrhoea. *The Scientific World Journal* **2012**, 738314, doi:10.1100/2012/738314 (2012).
153 Eugene, C. Y. & Hackett, M. Rapid isolation method for lipopolysaccharide and lipid A from gram-negative bacteria. *Analyst* **125**, 651-656 (2000).
154 Arroyo, L. A. *et al.* The pmrCAB operon mediates polymyxin resistance in Acinetobacter baumannii ATCC 17978 and clinical isolates through phosphoethanolamine modification of Lipid A. *Antimicrobial agents and chemotherapy*, AAC. 00256-00211 (2011).
155 Clements, A. *et al.* Secondary acylation of Klebsiella pneumoniae lipopolysaccharide contributes to sensitivity to antibacterial peptides. *Journal of Biological Chemistry* **282**, 15569-15577 (2007).
156 Llobet, E. *et al.* Deciphering tissue-induced Klebsiella pneumoniae lipid A structure. *Proceedings of the National Academy of Sciences of the United States of America* **112**, E6369-6378, doi:10.1073/pnas.1508820112 (2015).
157 Hood, M. I., Becker, K. W., Roux, C. M., Dunman, P. M. & Skaar, E. P. Genetic Determinants of Intrinsic Colistin Tolerance in Acinetobacter baumannii. *Infection and Immunity* **81**, 542-551, doi:10.1128/iai.00704-12 (2013).
158 Moskowitz, S. M., Ernst, R. K. & Miller, S. I. PmrAB, a Two-Component Regulatory System of Pseudomonas aeruginosa That Modulates Resistance to Cationic Antimicrobial

Peptides and Addition of Aminoarabinose to Lipid A. *Journal of Bacteriology* **186**, 575-579, doi:10.1128/jb.186.2.575-579.2004 (2004).

159 De Majumdar, S. *et al.* Elucidation of the RamA Regulon in Klebsiella pneumoniae Reveals a Role in LPS Regulation. *PLoS Pathogens* **11**, e1004627, doi:10.1371/journal.ppat.1004627 (2015).

160 Raetz, C. R. H., Reynolds, C. M., Trent, M. S. & Bishop, R. E. LIPID A MODIFICATION SYSTEMS IN GRAM-NEGATIVE BACTERIA. *Annual review of biochemistry* **76**, 295-329, doi:10.1146/annurev.biochem.76.010307.145803 (2007).

161 Matamouros, S. & Miller, S. I. S. Typhimurium strategies to resist killing by cationic antimicrobial peptides. *Biochimica et Biophysica Acta (BBA) - Biomembranes* **1848**, 3021-3025, doi:http://dx.doi.org/10.1016/j.bbamem.2015.01.013 (2015).

162 Girardello, R. *et al.* Diversity of polymyxin resistance mechanisms among Acinetobacter baumannii clinical isolates. *Diagnostic Microbiology and Infectious Disease* (2016).

163 Poirel, L. *et al.* The mgrB gene as a key target for acquired resistance to colistin in Klebsiella pneumoniae. *J Antimicrob Chemother* **70**, 75-80, doi:10.1093/jac/dku323 (2015).

164 Lee, J.-Y. & Ko, K. S. Mutations and expression of PmrAB and PhoPQ related with colistin resistance in Pseudomonas aeruginosa clinical isolates. *Diagnostic Microbiology and Infectious Disease* **78**, 271-276, doi:http://dx.doi.org/10.1016/j.diagmicrobio.2013.11.027 (2014).

165 Davies, G. *et al.* 1: 6 - DI - 4 ′ - CHLOROPHENYLDIGUANIDOHEXANE (" HIBITANE " *). LABORATORY INVESTIGATION OF A NEW ANTIBACTERIAL AGENT OF HIGH POTENCY. **9**, 192-196 (1954).

166 Kampf, G. J. J. o. H. I. Acquired resistance to chlorhexidine–is it time to establish an 'antiseptic stewardship'initiative? **94**, 213-227 (2016).

167 Lim, K., Kam, P. J. A. & care, i. Chlorhexidine--pharmacology and clinical applications. **36**, 502-512 (2008).

168 Smith, K. & Hunter, I. S. J. J. o. m. m. Efficacy of common hospital biocides with biofilms of multi-drug resistant clinical isolates. **57**, 966-973 (2008).

169 Bock, L., Wand, M. & Sutton, J. J. J. o. H. I. Varying activity of chlorhexidine-based disinfectants against Klebsiella pneumoniae clinical isolates and adapted strains. **93**, 42-48 (2016).

170 Wand, M. E., Bock, L. J., Bonney, L. C., Sutton, J. M. J. A. a. & chemotherapy. Mechanisms of increased resistance to chlorhexidine and cross-resistance to colistin following exposure of Klebsiella pneumoniae clinical isolates to chlorhexidine. **61**, e01162-01116 (2017).

171 Denny, J. & Munro, C. L. J. B. r. f. n. Chlorhexidine bathing effects on health-care-associated infections. **19**, 123-136 (2017).

172 Bhardwaj, P. *et al.* Reduced chlorhexidine and daptomycin susceptibility in vancomycin-resistant Enterococcus faecium after serial chlorhexidine exposure. **62**, e01235-01217 (2018).

173 Wright, M. S. *et al.* Genomic and transcriptomic analyses of colistin-resistant clinical isolates of Klebsiella pneumoniae reveal multiple pathways of resistance. **59**, 536-543 (2015).

174 Hammerl, J. A., Grobbel, M., Tenhagen, B.-A., Kaesbohrer, A. J. J. o. P. H. & Emergency. Impact of mcr-1 harbouring bacteria in clinical settings and the public health sector: how can we act against this novel threat? **1** (2017).
175 Curiao, T. *et al.* Multiple adaptive routes of Salmonella enterica Typhimurium to biocide and antibiotic exposure. **17**, 491 (2016).
176 Hashemi, M. M., Holden, B. S. & Savage, P. B. Ceragenins as non-peptide mimics of endogenous antimicrobial peptides. 139-169 (2018).
177 Hashemi, M. M. *et al.* Susceptibility of colistin-resistant, Gram-negative bacteria to antimicrobial peptides and ceragenins. *Antimicrobial Agents and Chemotherapy*, AAC. 00292-00217 (2017).
178 Mukherjee, S., Moustafa, D., Smith, C. D., Goldberg, J. B. & Bassler, B. L. The RhlR quorum-sensing receptor controls Pseudomonas aeruginosa pathogenesis and biofilm development independently of its canonical homoserine lactone autoinducer. *PLoS pathogens* **13**, e1006504 (2017).
179 Wiśniewski, J. R., Zougman, A., Nagaraj, N. & Mann, M. J. N. m. Universal sample preparation method for proteome analysis. **6**, 359 (2009).
180 Peng, J., Cao, J., Ng, F. M. & Hill, J. J. J. o. p. Pseudomonas aeruginosa develops Ciprofloxacin resistance from low to high level with distinctive proteome changes. **152**, 75-87 (2017).
181 Tattawasart, U., Maillard, J.-Y., Furr, J. & Russell, A. J. I. j. o. a. a. Outer membrane changes in Pseudomonas stutzeri resistant to chlorhexidine diacetate and cetylpyridinium chloride. **16**, 233-238 (2000).
182 Limoli, D. H., Jones, C. J. & Wozniak, D. J. J. M. s. Bacterial extracellular polysaccharides in biofilm formation and function. **3** (2015).
183 Karatzas, K. A. *et al.* Phenotypic and proteomic characterization of multiply antibiotic-resistant variants of Salmonella enterica serovar Typhimurium selected following exposure to disinfectants. *Applied and Environmental Microbiology* **74**, 1508-1516 (2008).
184 Formosa, C., Herold, M., Vidaillac, C., Duval, R. & Dague, E. J. J. o. A. C. Unravelling of a mechanism of resistance to colistin in Klebsiella pneumoniae using atomic force microscopy. **70**, 2261-2270 (2015).
185 Walsh, F. & Duffy, B. J. P. o. The culturable soil antibiotic resistome: a community of multi-drug resistant bacteria. **8**, e65567 (2013).
186 Kim, S. J. & Ko, K. S. J. I. j. o. a. a. Diverse genetic alterations responsible for post-exposure colistin resistance in populations of the same strain of Klebsiella pneumoniae. **52**, 425-429 (2018).
187 Fernández‐Reyes, M. *et al.* The cost of resistance to colistin in Acinetobacter baumannii: a proteomic perspective. **9**, 1632-1645 (2009).
188 Southey-Pillig, C. J., Davies, D. G. & Sauer, K. J. J. o. b. Characterization of temporal protein production in Pseudomonas aeruginosa biofilms. **187**, 8114-8126 (2005).
189 Peng, J., Cao, J., Ng, F. M. & Hill, J. Pseudomonas aeruginosa develops Ciprofloxacin resistance from low to high level with distinctive proteome changes. *J. Proteomics* **152**, 75-87, doi:https://doi.org/10.1016/j.jprot.2016.10.005 (2017).
190 Condell, O. *et al.* Comparative analysis of Salmonella susceptibility and tolerance to the biocide chlorhexidine identifies a complex cellular defense network. *Frontiers in microbiology* **5**, 373 (2014).

191 Hancock, R. E. & Brinkman, F. S. J. A. R. i. M. Function of Pseudomonas porins in uptake and efflux. **56**, 17-38 (2002).
192 Li, X. *et al.* The outer membrane protein OprF and the sigma factor SigX regulate antibiotic production in Pseudomonas fluorescens 2P24. **206**, 159-167 (2018).
193 Maccarini, M. *et al.* Functional characterization of cell-free expressed OprF porin from Pseudomonas aeruginosa stably incorporated in tethered lipid bilayers. **33**, 9988-9996 (2017).
194 Fito-Boncompte, L. *et al.* Full virulence of Pseudomonas aeruginosa requires OprF. **79**, 1176-1186 (2011).
195 Balibar, C. J., Grabowicz, M. J. A. a. & chemotherapy. Mutant alleles of lptD increase the permeability of Pseudomonas aeruginosa and define determinants of intrinsic resistance to antibiotics. **60**, 845-854 (2016).
196 Derouiche, R., Benedetti, H., Lazzaroni, J.-C., Lazdunski, C. & Lloubes, R. J. J. o. B. C. Protein complex within Escherichia coli inner membrane. TolA N-terminal domain interacts with TolQ and TolR proteins. **270**, 11078-11084 (1995).
197 Dennis, J. J., Lafontaine, E. R. & Sokol, P. A. J. J. o. b. Identification and characterization of the tolQRA genes of Pseudomonas aeruginosa. **178**, 7059-7068 (1996).
198 Gaspar, J. A., Thomas, J. A., Marolda, C. L. & Valvano, M. A. J. M. m. Surface expression of O ‐ specific lipopolysaccharide in Escherichia coli requires the function of the TolA protein. **38**, 262-275 (2000).
199 Heilpern, A. J. & Waldor, M. K. J. J. o. b. CTXφ infection of Vibrio cholerae requires the tolQRA gene products. **182**, 1739-1747 (2000).
200 Nikolaidis, I., Favini ‐ Stabile, S. & Dessen, A. J. P. s. Resistance to antibiotics targeted to the bacterial cell wall. **23**, 243-259 (2014).
201 Olaitan, A. O., Morand, S. & Rolain, J.-M. J. F. i. m. Mechanisms of polymyxin resistance: acquired and intrinsic resistance in bacteria. **5**, 643 (2014).
202 Park, S. Y. & Groisman, E. A. J. M. m. Signal ‐ specific temporal response by the S almonella PhoP/PhoQ regulatory system. **91**, 135-144 (2014).
203 Zhang, Y. F. *et al.* Probing the sRNA regulatory landscape of P. aeruginosa: post ‐ transcriptional control of determinants of pathogenicity and antibiotic susceptibility. **106**, 919-937 (2017).
204 De Majumdar, S. *et al.* Elucidation of the RamA regulon in Klebsiella pneumoniae reveals a role in LPS regulation. **11**, e1004627 (2015).
205 Tao, K., Narita, S.-i. & Tokuda, H. Defective lipoprotein sorting induces lolA expression through the Rcs stress response phosphorelay system. *Journal of bacteriology* **194**, 3643-3650 (2012).
206 Lourdault, K., Cerqueira, G. M., Wunder, E. A. & Picardeau, M. Inactivation of clpB in the pathogen Leptospira interrogans reduces virulence and resistance to stress conditions. *Infection and immunity* **79**, 3711-3717 (2011).
207 Rema, T. *et al.* Proteomic analyses of chlorhexidine tolerance mechanisms in delftia acidovorans biofilms. *mSphere* **1**, e00017-00015 (2016).
208 Kohanski, M. A., Dwyer, D. J., Wierzbowski, J., Cottarel, G. & Collins, J. J. Mistranslation of membrane proteins and two-component system activation trigger antibiotic-mediated cell death. *Cell* **135**, 679-690 (2008).

209 Liu, Y., Dong, Y., Chen, Y.-Y. M. & Burne, R. A. Environmental and growth phase regulation of the Streptococcus gordonii arginine deiminase genes. *Applied and environmental microbiology* **74**, 5023-5030 (2008).
210 Nde, C. W., Jang, H.-J., Toghrol, F., Bentley, W. E. J. E. s. & technology. Global transcriptomic response of Pseudomonas aeruginosa to chlorhexidine diacetate. **43**, 8406-8415 (2009).
211 Wand, M. E., Bock, L. J., Bonney, L. C. & Sutton, J. M. Mechanisms of Increased Resistance to Chlorhexidine and Cross-Resistance to Colistin following Exposure of Klebsiella pneumoniae Clinical Isolates to Chlorhexidine. *Antimicrobial Agents and Chemotherapy* **61**, doi:10.1128/aac.01162-16 (2017).
212 Gilbert, P. & Moore, L. Cationic antiseptics: diversity of action under a common epithet. *Journal of applied microbiology* **99**, 703-715 (2005).
213 Martínez, J. L. & Rojo, F. Metabolic regulation of antibiotic resistance. *FEMS microbiology reviews* **35**, 768-789 (2011).
214 Fernández‐Reyes, M. *et al.* The cost of resistance to colistin in Acinetobacter baumannii: a proteomic perspective. *Proteomics* **9**, 1632-1645 (2009).
215 Tomaras, A. P., Dorsey, C. W., Edelmann, R. E. & Actis, L. A. Attachment to and biofilm formation on abiotic surfaces by Acinetobacter baumannii: involvement of a novel chaperone-usher pili assembly system. *Microbiology* **149**, 3473-3484 (2003).
216 O'toole, G. A. & Kolter, R. Flagellar and twitching motility are necessary for Pseudomonas aeruginosa biofilm development. *Molecular microbiology* **30**, 295-304 (1998).
217 Kim, W. & Surette, M. G. Swarming populations of Salmonella represent a unique physiological state coupled to multiple mechanisms of antibiotic resistance. *Biol. Proced. Online* **5**, 189 (2003).
218 Butler, M. T., Wang, Q. & Harshey, R. M. Cell density and mobility protect swarming bacteria against antibiotics. *Proceedings of the National Academy of Sciences* **107**, 3776-3781 (2010).
219 Whitchurch, C. B. *et al.* Characterization of a complex chemosensory signal transduction system which controls twitching motility in Pseudomonas aeruginosa. *Molecular microbiology* **52**, 873-893 (2004).
220 Laverty, G., Gorman, S. P. & Gilmore, B. F. Biomolecular mechanisms of Pseudomonas aeruginosa and Escherichia coli biofilm formation. *Pathogens* **3**, 596-632 (2014).
221 Pasquale, T., Tomada, J. R., Ghannoun, M., Dipersio, J. & Bonilla, H. Emergence of Candida tropicalis resistant to caspofungin. *Journal of Antimicrobial Chemotherapy* **61**, 219-219, doi:10.1093/jac/dkm453 (2008).
222 Forsberg, K. *et al.* Candida auris: The recent emergence of a multidrug-resistant fungal pathogen. *Med. Mycol.* (2018).
223 Fayemiwo, S. & Makanjuola, O. Candida auris infection: How prepared is Nigeria for this emerging fungal agent? *African Journal of Clinical and Experimental Microbiology* **19**, 58-63 (2018).
224 Mohsin, J. *et al.* The first cases of Candida auris candidaemia in Oman. *Mycoses* **60**, 569-575, doi:10.1111/myc.12647 (2017).
225 Rudramurthy, S. M. *et al.* Candida auris candidaemia in Indian ICUs: analysis of risk factors. *Journal of Antimicrobial Chemotherapy* **72**, 1794-1801, doi:10.1093/jac/dkx034 (2017).

226 Lockhart, S. R. *et al.* Simultaneous Emergence of Multidrug-Resistant Candida auris on 3 Continents Confirmed by Whole-Genome Sequencing and Epidemiological Analyses. *Clinical Infectious Diseases* **64**, 134-140, doi:10.1093/cid/ciw691 (2017).
227 Sarma, S. & Upadhyay, S. Current perspective on emergence, diagnosis and drug resistance in Candida auris. *Infection and Drug Resistance* **10**, 155 (2017).
228 Tsay, S. *et al.* Notes from the Field: Ongoing Transmission of Candida auris in Health Care Facilities-United States, June 2016-May 2017. *MMWR. Morbidity and mortality weekly report* **66**, 514-515 (2017).
229 McCarthy, M. W. & Walsh, T. J. Drug development challenges and strategies to address emerging and resistant fungal pathogens. *Expert review of anti-infective therapy* **15**, 577-584 (2017).
230 Swidergall, M. & Ernst, J. F. Interplay between Candida albicans and the antimicrobial peptide armory. *Eukaryot. Cell*, EC. 00093-00014 (2014).
231 Duncan, V. M. & O'Neil, D. A. Commercialization of antifungal peptides. *Fungal Biol. Rev.* **26**, 156-165 (2013).
232 Kodedová, M. & Sychrová, H. Synthetic antimicrobial peptides of the halictines family disturb the membrane integrity of Candida cells. *Biochimica et Biophysica Acta (BBA)-Biomembranes* (2017).
233 Park, C. & Lee, D. G. Melittin induces apoptotic features in Candida albicans. *Biochem. Biophys. Res. Commun.* **394**, 170-172 (2010).
234 Sóczó, G. *et al.* Correlation of posaconazole minimum fungicidal concentration and time–kill test against nine Candida species. *Journal of Antimicrobial Chemotherapy* **60**, 1004-1009, doi:10.1093/jac/dkm350 (2007).
235 Anderson, M. J., Parks, P. J. & Peterson, M. L. A mucosal model to study microbial biofilm development and anti-biofilm therapeutics. *Journal of microbiological methods* **92**, 201-208 (2013).
236 Moss, B. J., Kim, Y., Nandakumar, M. & Marten, M. R. Quantifying metabolic activity of filamentous fungi using a colorimetric XTT assay. *Biotechnology progress* **24**, 780-783 (2008).
237 Wayne, P. J. C. d. M.-A. & S, S. Clinical and Laboratory Standards Institute: Reference method for broth dilution antifungal susceptibility testing of yeasts; approved standard. **3** (2008).
238 De Seta, F., Schmidt, M., Vu, B., Essmann, M. & Larsen, B. Antifungal mechanisms supporting boric acid therapy of Candida vaginitis. *Journal of Antimicrobial Chemotherapy* **63**, 325-336, doi:10.1093/jac/dkn486 (2009).
239 Mangoni, M. L., Luca, V. & McDermott, A. M. Fighting microbial infections: a lesson from amphibian skin-derived esculentin-1 peptides. *Peptides* **71**, 286-295 (2015).
240 Bruzual, I., Riggle, P., Hadley, S. & Kumamoto, C. A. Biofilm formation by fluconazole-resistant Candida albicans strains is inhibited by fluconazole. *Journal of Antimicrobial Chemotherapy* **59**, 441-450, doi:10.1093/jac/dkl521 (2007).
241 Kagan, S. *et al.* Anti-Candida albicans biofilm effect of novel heterocyclic compounds. *Journal of Antimicrobial Chemotherapy* **69**, 416-427, doi:10.1093/jac/dkt365 (2014).
242 Khan, M. S. A. & Ahmad, I. Antibiofilm activity of certain phytocompounds and their synergy with fluconazole against Candida albicans biofilms. *Journal of Antimicrobial Chemotherapy* **67**, 618-621, doi:10.1093/jac/dkr512 (2012).

243 Lazzell, A. L. *et al.* Treatment and prevention of Candida albicans biofilms with caspofungin in a novel central venous catheter murine model of candidiasis. *Journal of Antimicrobial Chemotherapy* **64**, 567-570, doi:10.1093/jac/dkp242 (2009).
244 Larkin, E. *et al.* The Emerging Pathogen Candida auris: Growth Phenotype, Virulence Factors, Activity of Antifungals, and Effect of SCY-078, a Novel Glucan Synthesis Inhibitor, on Growth Morphology and Biofilm Formation. *Antimicrobial Agents and Chemotherapy* **61**, e02396-02316, doi:10.1128/AAC.02396-16 (2017).
245 Oh, B. J. *et al.* Biofilm formation and genotyping of Candida haemulonii, Candida pseudohaemulonii, and a proposed new species (Candida auris) isolates from Korea. *Med. Mycol.* **49**, 98-102 (2011).
246 Larkin, E. *et al.* The Emerging Candida auris: Characterization of Growth Phenotype, Virulence Factors, Antifungal Activity, and Effect of SCY-078, a Novel Glucan Synthesis Inhibitor, on Growth Morphology and Biofilm Formation. *Antimicrobial agents and chemotherapy* **61** (2017).
247 Hashemi, M. M. *et al.* Preclinical testing of a broad-spectrum antimicrobial endotracheal tube coated with an innate immune synthetic mimic. *Journal of Antimicrobial Chemotherapy* **73**, 143-150, doi:10.1093/jac/dkx347 (2018).
248 Tecle, T., Tripathi, S. & Hartshorn, K. L. Defensins and cathelicidins in lung immunity. *Innate Immun.* **16**, 151-159 (2010).
249 Lecaille, F., Lalmanach, G. & Andrault, P.-M. Antimicrobial proteins and peptides in human lung diseases: A friend and foe partnership with host proteases. *Biochimie* **122**, 151-168 (2016).
250 Hotterbeekx, A. *et al.* The endotracheal tube microbiome associated with Pseudomonas aeruginosa or Staphylococcus epidermidis. *Scientific reports* **6**, 36507 (2016).
251 Cairns, S. *et al.* Molecular analysis of microbial communities in endotracheal tube biofilms. *PLoS One* **6**, e14759 (2011).
252 Haas, C. F., Eakin, R. M., Konkle, M. A. & Blank, R. Endotracheal Tubes: Old and NewDiscussion. *Respir. Care* **59**, 933-955 (2014).
253 Mehta, A. & Bhagat, R. Preventing ventilator-associated infections. *Clin. Chest Med.* **37**, 683-692 (2016).
254 Yang, Y.-W., Jiang, Y.-Z., Hsu, C.-M. & Chen, L.-W. Pseudomonas aeruginosa ventilator-associated pneumonia induces lung injury through TNF-α/c-Jun NH2-terminal kinase pathways. *PloS one* **12**, e0169267 (2017).
255 Nathe, K. E. *et al.* Innate immune activation in neonatal tracheal aspirates suggests endotoxin-driven inflammation. *Pediatr. Res.* **72**, 203 (2012).
256 Chiesa, C. *et al.* Fetal and early neonatal interleukin-6 response. *Cytokine* **76**, 1-12 (2015).
257 Pelekanou, A. *et al.* Decrease of CD4-lymphocytes and apoptosis of CD14-monocytes are characteristic alterations in sepsis caused by ventilator-associated pneumonia: results from an observational study. *Critical care* **13**, R172 (2009).
258 Ely, E. W. *et al.* Delirium as a predictor of mortality in mechanically ventilated patients in the intensive care unit. *JAMA* **291**, 1753-1762 (2004).
259 Rodrigues, M. E. *et al.* Polymicrobial ventilator-associated pneumonia: fighting in vitro Candida albicans-Pseudomonas aeruginosa biofilms with antifungal-antibacterial combination therapy. *PloS one* **12**, e0170433 (2017).
260 Flemming, H.-C. *et al.* Biofilms: an emergent form of bacterial life. *Nature Reviews Microbiology* **14**, 563 (2016).

261 Burmølle, M., Ren, D., Bjarnsholt, T. & Sørensen, S. J. Interactions in multispecies biofilms: do they actually matter? *Trends in microbiology* **22**, 84-91 (2014).
262 Li, J. *et al.* Heteroresistance to colistin in multidrug-resistant Acinetobacter baumannii. *Antimicrobial agents and chemotherapy* **50**, 2946-2950 (2006).
263 Cheng, Y.-H. *et al.* Colistin-resistant mechanisms of Klebsiella pneumoniae in Taiwan. *Antimicrobial agents and chemotherapy*, AAC. 04763-04714 (2015).
264 Castanheira, M. *et al.* Detection of mcr-1 among Escherichia coli clinical isolates collected worldwide as part of the SENTRY antimicrobial surveillance program during 2014-2015. *Antimicrobial agents and chemotherapy*, AAC. 01267-01216 (2016).
265 Larkin, E. *et al.* The emerging Candida auris: characterization of growth phenotype, virulence factors, antifungal activity, and effect of SCY-078, a novel glucan synthesis inhibitor, on growth morphology and biofilm formation. *Antimicrobial Agents and Chemotherapy*, AAC. 02396-02316 (2017).
266 Stulik, L., Hudcova, J., Craven, D. E., Nagy, G. & Nagy, E. Low efficacy of antibiotics against Staphylococcus aureus airway colonization in ventilated patients. *Clinical Infectious Diseases* **64**, 1081-1088 (2017).
267 Burnham, J. P. & Kollef, M. H. (Oxford University Press US, 2017).
268 Griffin, M. *et al.* Antifungal use in immunocompetent, critically ill patients with pneumonia does not improve clinical outcomes. *Heart & Lung: The Journal of Acute and Critical Care* **45**, 538-543 (2016).
269 Tokmaji, G. *et al.* Silver‐coated endotracheal tubes for prevention of ventilator‐associated pneumonia in critically ill patients. *Cochrane Database of Systematic Reviews* (2015).
270 Politano, A. D., Campbell, K. T., Rosenberger, L. H. & Sawyer, R. G. Use of silver in the prevention and treatment of infections: silver review. *Surg. Infect. (Larchmt.)* **14**, 8-20 (2013).
271 Luo, Y. *et al.* The naturally occurring host defense peptide, LL-37, and its truncated mimetics KE-18 and KR-12 have selected biocidal and antibiofilm activities against Candida albicans, Staphylococcus aureus, and Escherichia coli in vitro. *Frontiers in microbiology* **8**, 544 (2017).
272 Beyth, N., Bahir, R., Matalon, S., Domb, A. J. & Weiss, E. I. Streptococcus mutans biofilm changes surface-topography of resin composites. *Dent. Mater.* **24**, 732-736 (2008).
273 Sherry, L. *et al.* Biofilm-forming capability of highly virulent, multidrug-resistant Candida auris. *Emerging infectious diseases* **23**, 328 (2017).
274 El-Baky, R. M. A., El Ela, D. & Gad, G. F. M. N-acetylcysteine inhibits and eradicates Candida albicans biofilms. *American Journal of Infectious Diseases and Microbiology* **2**, 122-130 (2014).
275 Hashemi, M. M. R., J.; Holden, B.S.; Taylor, M.F.; Weber, S.; Wilson, J.; Hilton, B.; Zaugg, A.L.; Ellis, S.W.; Yost, C.D & FINNEGAN, P. M. K., C.K.; BERKOW,E.L.; DENG,S.; LOCKHART,S.R.; PETERSON,M.; SAVAGE, P.B. Ceragenins are active against drug-resistant Candida auris clinical isolates in planktonic and

biofilm forms. *J. Antimicrob. Chemother* (2018).
276 Lynch, A. S. & Robertson, G. T. Bacterial and Fungal Biofilm Infections. *Annu. Rev. Med.* **59**, 415-428, doi:10.1146/annurev.med.59.110106.132000 (2008).
277 Lewis, K. Persister cells. *Annu. Rev. Microbiol.* **64**, 357-372 (2010).

278 Høiby, N. Understanding bacterial biofilms in patients with cystic fibrosis: current and innovative approaches to potential therapies. *Journal of Cystic Fibrosis* **1**, 249-254 (2002).
279 Smith, W. D. *et al.* Current and future therapies for Pseudomonas aeruginosa infection in patients with cystic fibrosis. *FEMS microbiology letters* **364** (2017).
280 Waters, V. & Smyth, A. Cystic fibrosis microbiology: advances in antimicrobial therapy. *Journal of Cystic Fibrosis* **14**, 551-560 (2015).
281 Seiler, F., Moritz Lepper, P., Bals, R. & Beisswenger, C. Regulation and function of antimicrobial peptides in immunity and diseases of the lung. *Protein and peptide letters* **21**, 341-351 (2014).
282 Pitto-Barry, A. & Barry, N. P. Pluronic® block-copolymers in medicine: from chemical and biological versatility to rationalisation and clinical advances. *Polymer Chemistry* **5**, 3291-3297 (2014).
283 Mataraci, E. & Dosler, S. In Vitro Activities of Antibiotics and Antimicrobial Cationic Peptides Alone and in Combination against Methicillin-Resistant Staphylococcus aureus Biofilms. *Antimicrobial Agents and Chemotherapy* **56**, 6366-6371, doi:10.1128/AAC.01180-12 (2012).
284 Nunes, S. F. *et al.* An ex vivo swine tracheal organ culture for the study of influenza infection. *Influenza Other Respi. Viruses* **4**, 7-15 (2010).
285 Harrison, F., Muruli, A., Higgins, S. & Diggle, S. P. Development of an ex vivo porcine lung model for studying growth, virulence, and signaling of Pseudomonas aeruginosa. *Infection and immunity* **82**, 3312-3323 (2014).
286 Dias, N. H., Braz, J. R. C., Defaveri, J., Carvalho, L. R. & Martins, R. H. G. Morphological findings in the tracheal epithelium of dogs exposed to the inhalation of poorly conditioned gases under use of an endotracheal tube or laryngeal mask airway. *Acta Cir. Bras.* **26**, 357-364 (2011).